Multi-century records of snow water equivalent and streamflow drought from energy-limited tree rings in south coastal British Columbia

by

Bethany Coulthard
B.A., Mount Allison University, 2007
M.Sc., University of Victoria, 2009

A Dissertation Submitted in Partial Fulfillment
of the Requirements for the Degree of

DOCTOR OF PHILOSOPHY

in the Department of Geography

Supervisory Committee

Multi-century records of snow water equivalent and streamflow drought from energy-limited tree rings in south coastal British Columbia

by

Bethany Coulthard

B.A., Mount Allison University, 2007

M.Sc., University of Victoria, 2009

Supervisory Committee

Dr. Dan J. Smith (Department of Geography)

Supervisor

Dr. David Atkinson (Department of Geography)

Departmental Member

Dr. Brian Starzomski (School of Environmental Studies)

Outside Member

Abstract

Supervisory Committee

Dr. Dan J. Smith (Department of Geography)

Supervisor

Dr. David Atkinson (Department of Geography)

Co-Supervisor or Departmental Member

Dr. Brian Starzomski (School of Environmental Studies)

Outside Member

Anthropogenic climate change has triggered widespread shifts in the global hydrological cycle. In south coastal British Columbia, these changes have led to more winter precipitation falling as rain rather than snow, more rain on snow events, and generally reduced snowpacks. Since snowmelt is a primary source of summer surface runoff and groundwater, snowpack declines have caused severe seasonal streamflow droughts in recent decades. For accurate water supply forecasting under future climate change, it is crucial to know if snowpack and runoff declines are unprecedented in the last several hundred years. This research focused on developing multi-century, annually-resolved records of snow water equivalent and streamflow drought to determine if recent conditions deviate from long-term norms. The research targeted small temperate watersheds that are not usually conducive to application of dendrohydrological methodologies.

Traditional dendrohydrology relies on moisture-limited tree-ring records from arid settings. This dissertation presents a new method for developing tree-ring based reconstructions from energy-limited trees. Tree-ring records from high-elevation mountain hemlock (*Tsuga mertensiana* (Bong.) Carrière) and amabilis fir (*Amabilis* (Dougl.) Forbes) stands were collected at sites in south coastal British Columbia. Ring-width measurements were used to develop multi-century dendrohydrological models of snow water equivalent and streamflow drought. A

322-year reconstruction of May 1 snow water equivalent for Vancouver Island explains 56% of the instrumental SWE data variance and suggests snowpacks in 2015 were lower than in any year since 1675. A 477-year reconstruction of summer streamflow for Tsable River explains 63% of gauged streamflow variance and indicates that since 1520 twenty-one droughts occurred that were more extreme than recent "severe" droughts. Finally, a reconstruction of regionally synchronous streamflow among four south coastal rivers explains 64% of the regionalized streamflow variance. In addition to snow-sensitive tree-ring data, the latter model incorporated a paleorecord of the Palmer Drought Severity Index as a summer temperature and aridity proxy. The reconstruction suggests that since the mid-1600s sixteen regional-scale droughts occurred that were more extreme than any within the instrumental period. All three models were particularly accurate at estimating lowest snow and runoff years, and reflected the long-term influence of cool phases of the Pacific Decadal Oscillation on regional snowmelt and summer discharge trends and patterns.

The reconstructions suggest: 1) snowpack declines in 2015 were unmatched in the past ~340 years; and, 2) existing water management strategies based on hydrometric data records underestimate potential magnitudes of natural droughts. Worst-case scenario droughts compounded by land use change and climate change could result in droughts more severe than any in the past several hundred years. Energy-limited tree-ring records have strong potential as paleohydrological proxies and for expanding applications of dendrohydrology to arid settings. For some of the tree-ring chronologies examined in this study, the correlation with snow water equivalent became non-significant after the mid-1990s, possibly due to warming spring temperatures. Future studies using this type of tree-ring data must carefully evaluate the recent stability of climate-growth relationships.

Table of Contents

List of Tables

List of Figures

Abbreviations

AIC	Akaike Information Criterion
B.C.	British Columbia
DEM	Digital elevation model
D-W	Durbin-Watson
EPS	Expressed Population Signal
ENSO	El Niño Southern Oscillation
LOO	Leave-one-out
PAS	Precipitation-as-snow
PCA	Principal Components Analysis
PC1	First Principal Component
PDO	Pacific Decadal Oscillation
PDSI	Palmer Drought Severity Index
PNA	Pacific North America
RMSE	Root mean squared error
SE	Standard Error
SWE	Snow water equivalent
TR	Tree-ring
UVTRL	University of Victoria Tree-Ring Laboratory
VIF	Variance Inflation Factor

Acknowledgments

My doctoral program has been a very lucky one, surrounded by some tremendous colleagues and mentors who have gone above and beyond in supporting me, and this work. My most heartfelt thanks go to my supervisor Dan Smith. Dan, you have been a mentor in work and a mentor in life. Thank you for showing me the beautiful land you love. It has been a life-changing experience. I know many sunny glacier days and long stretches of highway lie ahead for you, and I hope I will be riding shotgun again soon. Hopefully with zero broken bones between the two of us.

To my committee members Brian Starzomski and David Atkinson, thank you so much for your time and effort in thoughtfully guiding my research program, and for your general support and enthusiasm. It has been a real pleasure working with you both. Emma Watson graciously agreed to act as my external examiner, and I could not have asked for a more exciting and thoughtful dissertation defence – thank you Emma. To Colin Laroque, Dave Meko, Malcolm Hughes, Dan Griffin, Kevin Anchukaitis, Chris Gentry, Matt Bekker, Justin DeRose, Flurin Babst, Henri Grissino-Mayer, Jim Speer, and Valerie Trouet: thank you for giving of your time to talk tree rings, and for inviting me into a wonderful research community. To my dear friends in the University of Victoria Tree-Ring Laboratory, past and present: Dan sure knows how to pick ‘em. Thank you for making ‘work’ one of the most fun (indoor) places to be. I know many more years of sciencing, adventures, and cold pops are in store for us.

Most of all to my family, friends, and Andrew: thank you for believing in me, and for your unending support. I could not have done this without you.

Dedication

For Andrew, who put as much of himself into this as I did. Thank you.

Chapter 1 Drought in south coastal British Columbia

1.1 Introduction

Anthropogenic climate warming and land-use change have caused widespread shifts in the global hydrological cycle (Huntington 2006). In many regions droughts have become longer and more severe, impacting drinking water, agriculture, industry, sanitation, human security, and the natural environment (Field 2014).

South coastal British Columbia (B.C.), Canada, is an exceptionally 'water-rich' setting that has been impacted by severe seasonal streamflow droughts as a result of atmospheric warming (Rodenhuis *et al.* 2007). Streamflow drought (hereinafter also called 'drought') refers to below-normal stream discharge, a component of hydrological drought that often also coincides with reduced groundwater availability (VanLoon and Laaha 2015). Drought is difficult to imagine in a landscape dominated by temperate rainforests, deep annual snowpacks, extensive glacial storage, and greater than 5000 mm of rain per year in some areas, especially when juxtaposed with the extreme precipitation and flooding that occurs during winter (Whitfield *et al.* 2003). However, longer, more severe, and more frequent summer streamflow droughts are affecting most watersheds in the region (Pike *et al.* 2010). As summer rainfall is minimal in this setting, summer drought is often closely linked to snow meltwater availability (Rodenhuis *et al.* 2007). This research focuses on developing long-term snow, streamflow, and drought records for south coastal B.C. to determine if recent drought conditions deviate from long-term norms.

Small and steep watersheds predominate in the mountainous landscape of south coastal B.C. (for example on Vancouver Island, Figure 1.1). In this region a large proportion of winter rainfall drains quickly to the Pacific Ocean, often during high-magnitude rainfall and flood events (Eaton and Moore 2010). The small water reservoirs typical in this setting often cannot store sufficient winter runoff to meet municipal, industrial, agricultural, and ecological water demands during dry summers. Consequently, regional water supplies rely heavily on snow meltwater during summer (Cowichan Watershed Board 2015).

Recent declines in annual snow meltwater volumes, combined with hotter and drier summers, have led to droughts in the south coastal regional that are unprecedented in the instrumental record. In 2015, some Vancouver Island snowpacks were 0% of normal and high summer temperatures were record-breaking, contributing to what was likely the most widespread and severe summer streamflow drought on record (BC River Forecast Centre 2015).

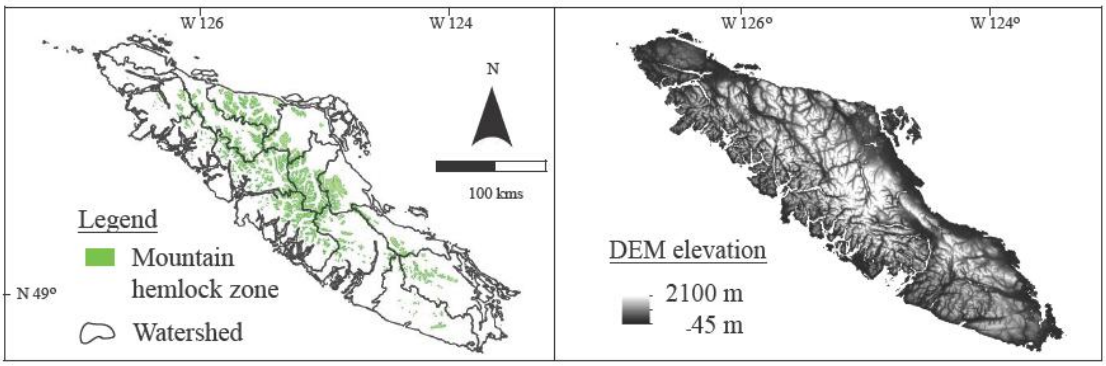

Figure 1.1: Maps of Vancouver Island showing 6th-order watersheds and area occupied by the Mountain Hemlock Biogeoclimatic Zone on the left (Pojar *et al.* 1991) and a Digital Elevation Model (DEM) on the right.

1.2 Drought drivers and impacts

Understanding natural ranges of long-term hydrological variability and the unusualness of extreme droughts is essential for effective water management (Meko and Woodhouse 2011). Hydrologists estimate probabilities and magnitudes of extreme droughts based on climatic and hydrometric data, with the accuracy of their estimates contingent on the length of climate and streamflow records (Engeland *et al.* 2004). Because these data rarely extend before the mid-20th century in south coastal B.C., worst-case scenario 'natural' low snowpacks and droughts are likely systematically underestimated (Walker 2000). Climate change will only exacerbate natural dry extremes; projections suggest recent droughts will resemble average conditions in the future (Snover *et al.* 2013).

The amplification of summer drought in south coastal B.C. is fundamentally linked to the hydroclimatological complexity of the region (Pike *et al.* 2008). Most

annual precipitation falls during winter storms that originate in the Pacific Ocean. Large amounts of snow are released orographically at high elevation and are accompanied by rain in surrounding coastal lowlands (Valentine *et al.* 1978). Historically snowpacks above 1000 m asl persist well into mid-summer and buffer runoff during the warm and dry conditions of July and August (Pojar *et al.* 1991; Kiffney *et al.* 2002). However, warmer winters have drawn down regional snowpacks, diminishing the proportion of moisture stored as snow into spring and summer (Pike *et al.* 2010). Mean winter temperatures in the B.C. coast and coast mountain regions rose 1.4°C from 1895 to 1995 and snowpacks declined by 6% per decade from 1953-2000 (B.C. Ministry of Water, Land and Air Protection 2002). The winter rain-to-snow ratio has shifted to favour rainfall rather than snow, and rain on snow events are more frequent (Pike *et al.* 2010).

Hotter and drier summer weather has exacerbated runoff declines in south coastal B.C., where mean summer temperatures have increased by 0.7°C since 1900 (B.C. Ministry of Water, Land and Air Protection 2002; Pike *et al.* 2010). Summer rainfall is nominal in this region so that drought season runoff is often more closely linked with snow meltwater contributions than summer rainfall quantities (Rodenhuis *et al.* 2007). Summer runoff from glacial meltwater is virtually absent on Vancouver Island, and on the south coast mainland where large glacial systems are present, municipal water is largely sourced from precipitation-derived groundwater (Zubel 2000; Eaton and Moore 2010). With summer precipitation totals projected to decline 13% by 2050, summer droughts are anticipated to become even more common (B.C. Ministry of Water, Land and Air Protection 2002; Pike *et al.* 2008).

The impacts of these summer droughts are far-reaching and acute. In recent years droughts have prompted the implementation of highest-level water use restrictions, leading to significant economic losses in the industrial, agricultural and hydroelectric power generation sectors (BC Ministry of Forests, Lands, and Natural Resource Operations 2015; CVRD 2015; Duffy 2015; Hume 2015). Droughts have also contributed to exceptional wildfire seasons (BC Wildfire Service 2015) and have seriously impacted stream ecosystem function imperilling the survival of Pacific salmon populations (Lill 2002).

Motivated in part by escalating concerns about drought in the south coastal region, in 2015 the B.C. government released a new *Water Sustainability Act* that identifies key provincial resource management priorities including water regulation during scarcity, and the improvement of water security, water use efficiency, and water conservation (B.C. Water Sustainability Act 2015). To address these priorities it is essential that water managers have an accurate understanding of worst-case scenario natural droughts in preparation for intensified droughts under projected climate change (Snover *et al.* 2013).

1.3 Dendrohydrology

Dendrohydrology is one of the few methods available for developing long-term, annually- and seasonally-resolved hydrological reconstuctions (Loaiciga *et al.* 1993). These records have been widely incorporated into water management and conservation, climate change adaptation, and hazard management strategies over the past 30 years (Meko and Woodhouse 2011).

Dendrohydrological methodologies have primarily been applied in arid environments using tree-ring (TR) records from moisture-limited species to reconstruct paleohistories of precipitation, snowpack, streamflow runoff, and drought (Meko and Woodhouse 2011). Notable achievements include gridded reconstructions of the Palmer Drought Severity Index across North America and China (Li *et al.* 2007), characterization of long-term drought across the Mediterranean and North Africa (Touchan *et al.* 2011), a suite of streamflow reconstructions of large watersheds in the southwest United States (Meko and Woodhouse 2005; Meko *et al.* 2011), detection of the 16th century North American megadrought (Stahle *et al.* 2000), and historical quantifications of recent North American drought and snowpack declines (Woodhouse *et al.* 2010; Pederson *et al.* 2011; Griffin and Anchukaitis 2014; Belmecheri *et al.* 2015). In Canada, moisture-limited TR records have been used to reconstruct streamflow, drought, and snowpack variations in the Prairie, Rocky Mountain Interior B.C. regions (Gedalof *et al.* 2004; Watson and Luckman 2004; Watson and Luckman 2005; Pederson *et al.* 2011; Fleming and Sauchyn 2013; Sauchyn *et al.* 2014). In these dry environments many reconstructions explain >60% of the instrumental data variance. Three small glacial and/or nival watersheds in

the rainshadow of B.C.'s Coast Mountains have been reconstructed based on negative TR-growth relationships with snow water equivalent (SWE; snow depth proxy) and positive relationships with summer temperature (icemelt and/or summer evaporation proxy) (Hart *et al.* 2010; Starheim *et al.* 2012). These models explain around 40% of the instrumental data variance. Both within and outside Canada, dendrohydrology has rarely been applied in non-arid settings or with non-moisture limited TR data. Increasing drought-susceptibility and management challenges in non-arid zones invites the application of dendrohydrology in these settings (Trenberth *et al.* 2004; Peng *et al.* 2011; van der Kamp *et al.* 2011).

1.4 Research motivation

There is considerable evidence to suggest that the radial growth of some high-elevation and high-latitude conifer trees is sensitive to annual variations in snowpack depth. This sensitivity arises from the role snowpacks play in controlling the length of the growing, or photosynthetic (energy) season (Ettl and Peterson 1995*a*, 1995*b*; Vaganov *et al.* 1999; Gedalof and Smith 2001*a*; Peterson *et al.* 2002; Case and Peterson 2007; Marcinkowski *et al.* 2015). This energy-limitation is physiologically distinct from moisture-limitation by snow, and requires substantial snowpacks like those that occur in Canada's west coast mountain ranges (Marcinkowski *et al.* 2015).

This research was based on the hypothesis that TR width records from mountain hemlock (*Tsuga mertensiana* (Bong.) Carrière) and amabilis fir (*Abies amabilis* (Dougl.) Forbes) trees, which can exhibit this form of snowpack-related energy-limitation, could be used as proxies for regional-scale snowpack variations in south coastal B.C. If this proxy relationship could be established, it would form the basis for developing TR-based paleorecords of snow, and snow-influenced streamflow.

The specific objectives of this research were to:

1. Develop a network of high elevation TR chronologies from trees located in south coastal B.C. that are energy-limited by annual snowpack depths.

2. Develop a dendrohydrological reconstruction of spring SWE on Vancouver Island and assess the relative severity of the record-low 2015 snowpack.

3. Develop a dendrohydrological reconstruction of extreme summer drought in a small, snow fed Vancouver Island watershed, and assess the abnormality of recent droughts in that watershed.

4. Develop a dendrohydrological reconstruction of regionally-synchronous extreme summer drought for the south coastal B.C. and assess the abnormality of recent droughts this region.

1.5 Organization of the thesis

Following this chapter, *Chapters 2, 3,* and *4* present the main results of the thesis. *Chapters 3 and 4* were written as manuscripts for journal submission. They are published and accepted for publication in Hydrological Processes and Journal of Hydrology, respectively.

Chapter 2 presents a reconstruction of SWE for Vancouver Island that provides historical context for the record-low snowpack in 2015. This chapter also addresses some benefits and drawbacks of energy-limited TR records as proxies for snow, including issues of signal stability over time.

Chapter 3 presents a reconstruction of June-August drought for Tsable River, B.C. In addition to contextualizing recent droughts, the reconstruction demonstrates that when a specific runoff regime and season are targeted, snow-sensitive energy-limited TR records are powerful for reconstructing runoff in a highly complex hydrological setting.

Chapter 4 presents regional-scale reconstruction of summer drought for south coastal B.C. An analysis of the influence of the El Niño Southern Oscillation (ENSO) and Pacific Decadal Oscillation (PDO) on summer runoff is included in this chapter.

Chapter 5 presents a comparison of the reconstructions from *Chapters 2*, *3*, and *4*, and a review of general connections between the instrumental snow and runoff records that were modeled in each those chapters.

The main findings and conclusion of the dissertation are presented in *Chapter 6*, along with potential future areas of research.

Chapter 2 Examining the utility of energy-limited tree-ring records for hindcasting variations in snow water equivalent: a long-term record for Vancouver Island

2.1 Article information

Chapter 2 has been prepared as a manuscript for submission to a journal.

2.2 Abstract

Snowpack meltwater is the primary source of summer surface water and groundwater runoff on Vancouver Island, British Columbia. In spring 2015 southern Vancouver Island snowpacks were a record 0% of normal, and the resulting deficient meltwater supply contributed to a record-breaking summer drought. Water supply forecasting depends in part on estimations of the likelihood of very low snowpack years, but instrumental snow data are often too short to accurately make these assessments. To address this problem a new method for developing multi-century snow water equivalent records is presented. Tree-ring records that are energy-limited by late-lying snowpacks were used to develop a 322-year dendrohydrological reconstruction of May 1 SWE for Vancouver Island. The model explained 56% of instrumental data variance, and was particularly effective at approximating the full range of instrumental data variance, especially extreme years. While SWE in 2015 was likely lower than in any year since 1675, this cannot be stated with statistical certainty since the model calibration did not include 2015. Uncertainty remains about how accurately the reconstruction estimates pre-instrumental years of similarly low SWE. A novel aspect of the research was use of energy-limited, rather than moisture limited, tree-ring records for developing a dendrohydrological reconstruction in a temperate setting. This approach could broaden the potential for tree-ring based reconstructions of snow, and snow-influenced variables including streamflow and drought.

2.3 Introduction

Melting snowpacks are the primary source of summer surface water and groundwater on Vancouver Island, B.C. (Eaton and Moore 2010). Nearly all annual precipitation is delivered during winter, with snowpacks providing natural water storage that persists until late in the year to augment streamflow during hot and dry summer conditions (Beaulieu *et al.* 2012). Because watersheds on the island are small and often steep, winter precipitation that falls as rain is quickly drained to the Pacific Ocean rather than being stored as snow. Glacial meltwater contributions are virtually absent. As a consequence, the small reservoirs that serve most municipal, agricultural, industrial, and hydroelectric water users have little summer recharge capacity apart from snowmelt.

In recent years, warmer winters in south coastal B.C. have led to more winter precipitation falling as rain rather than snow, more rain on snow events, and generally reduced snowpacks (Rodenhuis *et al.* 2007). In March 2015, snowpacks on Vancouver Island were 0% of normal, the lowest instrumental measurement on record (B.C. River Forecast Centre 2015). An inadequate supply of snow meltwater contributed to a severe and likely historic summer drought. Impacts ranged from highest-level water use restrictions that resulted in economic losses in the industrial, agricultural, and hydropower sectors, to deterioration of stream ecosystems, widespread Pacific salmon mortality, and an exceptional wildfire season (B.C. Ministry of Forests, Lands, and Natural Resource Operations 2015; B.C. Wildfire Service 2015; CVRD 2015; Duffy 2015; Hume 2015).

For accurate water supply forecasting, planning, and management strategies in anticipation of future change, it is essential to know if recent snowpack and seasonal runoff declines are unprecedented over the long-term (Pike *et al.* 2010). Unfortunately, regional snow records extend only to 1960 and they are unlikely to have recorded the lowest ‘natural’ snowpack years needed for interpreting the significance of reduced snowfall in 2015 (B.C. River Forecast Centre 2015).

TR data have been widely used to develop long-term proxy reconstructions of snow-influenced streamflow and drought (Case and MacDonald 2003; Griffin and

Anchukaitis 2014), and to a lesser extent snowpack depths and SWE (Pederson *et al.* 2011; Belmecheri *et al.* 2015). Dendrohydrology has largely been applied in arid environments where the annual radial growth of many tree species is moisture-limited and dependent on rainfall and/or spring soil moisture derived from snow meltwater (Timilsena and Piechota 2008). TR data in these settings are often strongly linearly correlated with total annual precipitation and/or previous-winter SWE records.

Annual radial tree growth in the temperate Pacific Northwest and B.C. is rarely moisture-limited (Peterson and Peterson 1994). There is ample evidence, however, that high-elevation conifer trees in this setting are limited by winter precipitation variations (Ettl and Peterson 1995*a*, 1995*b*; Vaganov *et al.* 1999; Gedalof and Smith 2001*a*; Peterson and Peterson 2001; Peterson *et al.* 2002; Case and Peterson 2007). Distinct from sensitivity to SWE or snowpack based on moisture-limitation, this climate-growth relationship results from the role late-lying snow plays in shortening the length of the growing, or photosynthetic (energy), season (Peterson and Peterson 2001).

Despite the global need for expanding dendrohydrology to temperate zones, the potential for developing dendrohydrological models based on 'energy-limited' TR records remains virtually unexplored (Larocque and Smith 2005). Vancouver Island is ideally suited for such an investigation, especially given the acute water management implications of a declining snowpack in this area. For this study, it was hypothesized that the annual radial growth of high-elevation conifer trees in the Vancouver Island Ranges is energy-limited as a function of snowpack depth. The purpose of this research was to develop TR records exhibiting energy-related snowpack sensitivity from high elevation trees on Vancouver Island and to develop a long-term proxy record of annual snowpack/SWE variability using those records.

2.4 Study area

The Vancouver Island Ranges are a subrange of the Insular Mountains, a discontinuous north-south trending band of high relief mountains flanking the Pacific coast of mainland B.C. (Figure 2.1). During summer the climate of this region is affected by persistent high-pressure systems leading to stable warm and dry weather, with cooler temperatures in alpine areas (Stahl *et al.* 2006). During winter moisture delivered by

North Pacific storms results in deep snowpacks above 1000 m asl (>5000 mm) and large quantities of rainfall at lower elevations (>4000 mm; Pojar *et al.* 1991). Interannual and decadal climate variability arising from ocean-atmosphere interactions in the Pacific Basin further regulate the regional hydroclimatology. Synoptic-scale modes described by the PDO and ENSO are particularly influential, and strongest during winter (Kiffney *et al.* 2002).

Seventy percent of annual precipitation falls as snow at high elevation on Vancouver Island, building deep snowpacks that may persist well into summer (Figure 2.2A; Pojar *et al.* 1991). Snowpack data from manual snow survey sites in south coastal B.C. indicate the maximum annual SWE measurement is typically recorded on May 1 (Water Survey of Canada sites 3B04, 3B19, 3B01, 3B02A, 3B23P; https://wateroffice.ec.gc.ca/). The snow survey data are significantly intercorrelated (p<0.01) over the full periods of record indicating that monthly and annual snowpack depth and water equivalent vary at a regional scale.

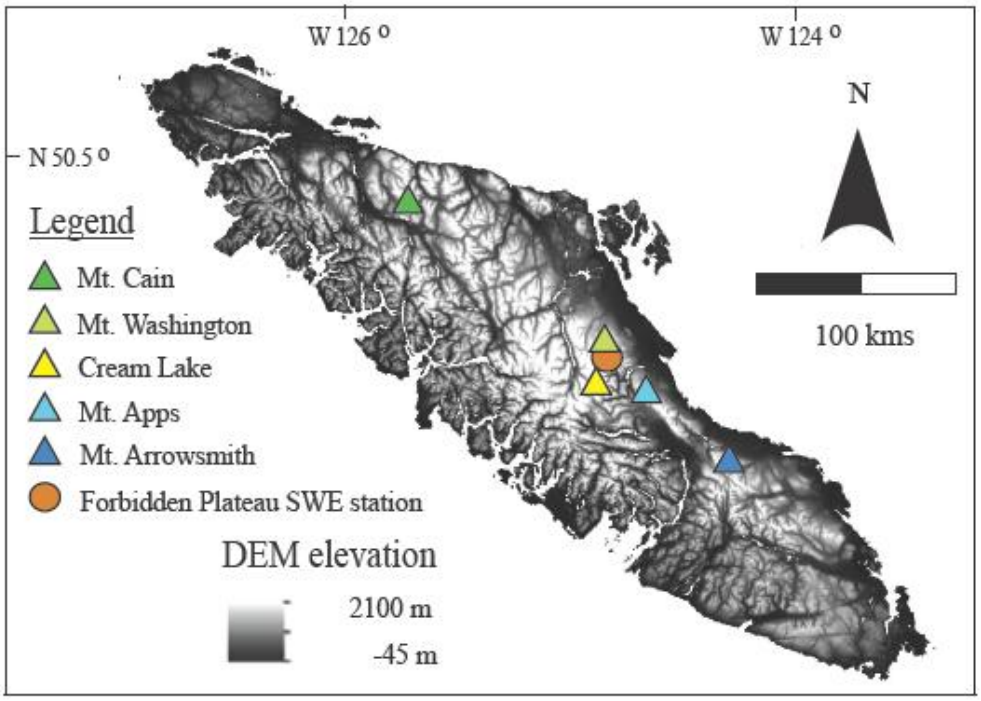

Figure 2.1: Map of the Vancouver Island study area.

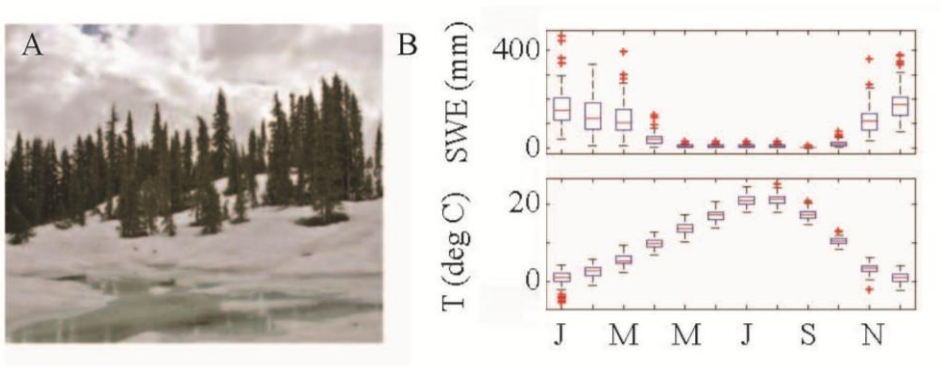

Figure 2.2: (A) Mountain hemlock and subalpine fir trees surrounded by late-lying snowpack at Kwai Lake, Forbidden Plateau (August 13, 2011). (B) Box and whisker plot of monthly SWE data from the Forbidden Plateau snow survey site, and maximum temperature data estimated on the coordinates of the Forbidden Plateau snow survey site using the program ClimateWNA ver. 4.83 (data period 1960-2011; Wang *et al.*, 2006; 2012). Climate WNA downscales PRISM (Daly *et al.* 2002) monthly data (2.5 x 2.5 arc min, reference period 1961-1990). Outliers are plotted with a red cross.

Forests above 1000 m asl are dominated by mountain hemlock trees, with amabilis fir and/or subalpine fir (*Abies lasiocarpa* (Hook.) Nutt.) trees often co-dominant. Mostly located within the Mountain Hemlock Biogeoclimatic Zone, these forests experience a typical maritime mountain climate characterized by a relatively short cool growing season, the length of which is controlled by persisting snowpacks (Klinka *et al.* 1991; Figure 2.2B).

The radial growth of treeline conifers can be energy-limited by snowpacks that maintain near-freezing conditions in the upper soil rooting zone into the spring and summer (Worrall 1983; Hansen-Bristow 1986; Peterson and Peterson 2001; Peterson *et al.* 2002). Little is known of the phenology of mountain hemlock in these environments, but field observations suggest similarities to co-occurring amabilis and subalpine fir which initiate leaf and shoot expansion shortly after snowmelt (Worrall 1983; Hansen-Bristow 1986). Annual radial growth is often also weakly influenced by current and/or previous summer temperature (Peterson and Peterson 2001; Peterson *et al.* 2002).

2.5 Data and methods

2.5.1 Climate data

SWE is strongly correlated with, and a standard estimate of, snowpack depth

(Jonas *et al.* 2009). Data from the Forbidden Plateau manual snow survey station (station code 03B01; latitude: 49.653, longitude: -125.207, elevation: 1100 m asl) were used in this study as they provide the longest SWE record (1960-2015) on Vancouver Island (Figure 2.1). Instrumental (manual) SWE data were downloaded from the Water Survey of Canada website (https://wateroffice.ec.gc.ca/) for the Forbidden Plateau snow survey site. Because manual snow survey data were only recorded in January or February though May, monthly resolution snow measurements were also used to evaluate monthly TR-climate relationships throughout the entire snow accumulation season (September through May). Monthly PAS, and minimum, mean, and maximum temperature anomaly records were estimated on the coordinates of the Forbidden Plateau snow survey site using the program ClimateWNA, ver. 4.83 (data period 1960-2011; Wang *et al.*, 2006; 2012), which downscales PRISM (Daly *et al.* 2002) monthly data (2.5 x 2.5 arc min, reference period 1961-1990). The SWE and PAS data are strongly correlated ($p<0.01$). The temperature data were examined to check for known influences of summer temperature on tree growth, which might attenuate the snow influence.

2.5.2 TR data

TR data were obtained from three sources: 1) tree cores collected in spring and summer 2015; 2) crossdated TR series from the International Tree-Ring Databank (https://www.ncdc.noaa.gov/data-access/paleoclimatology-data/datasets/tree-ring); and, 3) crossdated TR width measurements from the University of Victoria Tree-Ring Laboratory (UVTRL) archives. Sample sites were selected to maximize the sensitivity of TRs to climate and minimize any endogenous disturbance (Fritts 1976; Table 2.1). Only sample sites above 1000 m asl were analyzed, based on previous studies that report this elevation demarcates the general lower limit of snow-sensitivity in mountain hemlock trees (Peterson and Peterson 2001; Table 2.1). Older trees were sampled to provide the longest possible TR records and avoid age-related growth trends in the outermost TRs (Stokes and Smiley 1968).

Mountain hemlock chronologies from Mount Cain (sampled in 2008), Mount Washington and Mount Arrowsmith (sampled in 2015), and an amabilis fir chronology from Mount Cain (sampled in 2015) were developed for this chapter. TR data from Mt.

Apps and Cream Lake (sampled in 1997) from the UVTRL archives were combined to develop a chronology representing the Strathcona Provincial Park area (hereinafter called 'Strathcona'). TR sample site information is summarized in Table 2.1.

Table 2.1: Tree-ring sample site information.

Name	Species	Latitude, Longitude	Elev (m asl)	Site code
Mount Washington	mountain hemlock	49.44' , -125.17'	1100	W15, 97H
Mount Arrowsmith	mountain hemlock	49.14' , -124.34'	1220-1500	A15, 97A
Mount Cain	mountain hemlock	50.22' , -126.35'	1005	CN15,
Mount Cain[a]	amabilis fir	50.22' , -126.35'	1005	CANA174
Mount Apps	mountain hemlock	49°26', -124°57'	1200	97G
Cream Lake	mountain hemlock	49°29', -125°31'	1280	97CR

[a]From the ITRDB.

Two cores were extracted from each tree at standard breast height using a 5.2 mm increment borer, inserted into plastic straws for transportation. After being allowed to air-dry, the cores were glued to mounting boards and sanded to a 1200 grit finish. Ring widths from the 2015 collection were measured using the software program WinDENDRO, version 2012b (WinDENDRO 2012). Previously collected TR cores were measured using a Velmex measuring stage system and Measure J2X software. Raw ring-width measurement series were crossdated using a visual (list) method and verified statistically using the program COFECHA 3.0 (Holmes 1983; Grissino-Mayer 2001).

TR chronologies were developed using the R package dplR (Bunn 2008). Long-term trend unrelated to climate was removed from the TR width data by fitting a cubic smoothing spline with a 50% frequency response at wavelength 100 years to each series, and dividing the measured width by the corresponding value of the fitted curve (Cook and Peters 1981). As TR widths in a given year are often influenced by conditions in previous years, for each crossdated TR dataset two types of TR chronologies with different autocorrelation structures were developed. Residual chronologies that contain no statistical persistence were developed by fitting a low-order autoregressive model (Box and Jenkins 1976) to the TR data, with order identified by the Akaike Information Criterion (AIC) (Holmes 1983). ARSTAN chronologies were calculated by fitting the same autoregressive model to the data, pooling persistence common across series (one or more orders), and re-entering the pooled autocorrelation into the TR chronology (Holmes

1983). Series from individual cores were combined into single representative chronologies using a bi-weight robust mean (Mosteller and Tukey 1977). Adequacy of the sample size for capturing the hypothetical population growth signal was determined based on the expressed population signal (EPS; Wigley *et al.* 1984) statistic, and chronologies were truncated where EPS fell below 0.80.

2.5.3 Diagnostic climate correlations

The strength of linear associations between TR chronologies and climate data was summarized using the Pearson correlation coefficient. An effective sample size was used as needed to adjust for autocorrelation in testing correlations for significance for both tree-ring and climate data (Dawdy and Matalas 1964). The temporal stability of correlations was tested using a difference-of-correlations test that includes a Fisher's *Z* transformation of correlations (Snedecor and Cochrane 1989). The null hypothesis for this test was that there was no significant difference of correlations in the first and second half of the data. The first correlation tests examined associations of each TR chronology with the predictand May 1 SWE data to justify their use as model predictors. Chronologies that were significantly ($p<0.01$) negatively linearly correlated with the SWE data were added to the pool of candidate model predictors.

2.5.4 Reconstruction

The reconstruction model was estimated by forward stepwise multiple linear regression of the SWE data in year *t* on the pool of candidate predictor TR chronologies. Residual chronologies were entered in years *t*, *t*+1 and *t*+2, so that TR information in subsequent years could inform on SWE conditions in the given year (Cook and Kairiūkštis 1990). A suite of regression models were evaluated using statistics commonly employed for assessing dendroclimate reconstructions (Cook and Kairiūkštis 1990). The R^2 statistic provided a measure of model explanatory power, and analysis of the model residuals, Durbin-Watson (D-W), and variance inflation factor (VIF) statistics certified model fit and assumptions. The F-ratio provided an estimate of the statistical significance of the regression equation and the standard error of the estimate (SE) a measure of uncertainty of the predicted values of the model calibration. Given the short 37-year calibration period a leave-one-out (LOO) cross-validation procedure was employed to

validate the models against data not used in the calibrations (Michaelsen 1987). Cross-validation statistics were calculated to compare the LOO estimates with the instrumental predictand values (Cook and Kairiūkštis 1990). The best model was calibrated over the full common data period and was used to reconstruct historical SWE variability over the length of the shortest predictor dataset.

To inform an accurate interpretation of the reconstruction, climate-growth relationships of the TR model predictors were examined in detail. Monthly and seasonal correlations were calculated between the TR data and PAS, and maximum, minimum, and mean temperature data using the program Seascorr (Meko *et al.* 2011), which assesses significance of correlations by a Monte Carlo method. Tests were calculated for various monthly and seasonal periods spanning the year of TR growth and the year prior to growth. These tests provided information on the TR 'climate signal' of a monthly to seasonal resolution that could not be attained using the instrumental SWE data. This information was considered important since the TR records may be sensitive to both winter precipitation and summer temperature, and information related to each of these or other unexpected seasonal climate variables could influence the reconstruction (Peterson and Peterson 2001).

2.6 Results

2.6.1 TR data

Ten TR chronologies were developed for this study, with chronology lengths ranging from 364 to 518 years (Table 2.2). All chronologies except those from Mount Arrowsmith were most strongly significantly linearly correlated with May 1 SWE over the calibration period (1960-1997; Table 2.2). No statistically significant difference in correlations over time was detected within the calibration period (minimum/maximum *r* values = -0.75/-0.58 (early period), -0.32/-0.18 (late period); minimum/maximum *p*= 0.54/0.94; minimum/maximum n=13/18).

Table 2.2: Tree-ring chronology information.

Name	Period	Series, trees	Rbar[c]	r_1[d]	order[e]	r[f]
Mount Washington[a]	1650-2014	46, 27	0.35	-0.11	2	-0.53**
Mount Arrowsmith[a]	1675-2014	50, 26	0.31	-0.23	1	0
Mount Cain[a]	1490-2008	32, 25	0.36	0.09	2	-0.41*
Mount Cain[b]	1520-2014	50, 27	0.31	-0.08	2	-0.47**
Strathcona[a]	1600-1997	69, 47	0.29	-0.07	2	-0.55**

[a]Mountain hemlock chronology
[b]Amabilis fir chronology
[c]Mean correlation coefficient among TR series
[d]First order autocorrelation coefficient after autoregressive modeling (residual chronologies)
[e]Pooled autoregression order (ARSTAN chronologies)
[f]Correlation with May 1 SWE, *p<0.05, **p<0.01

2.6.2 Reconstruction

A model that uses the Strathcona and Mount Washington mountain hemlock residual chronologies and the Mount Cain amabilis fir ARSTAN chronology, all in time *t*, was selected for reconstructing May 1 SWE. The model equation is:

$$Y = 3642.409 + (-3224.348 * \text{Strathcona}) - (2305.371 * \text{Mount Washington}) - (981.826 * \text{Mount Cain}) \quad (1)$$

The model explains 56% of May 1 SWE variance over the calibration period and assumptions of the residuals were met. The VIF suggests no important multicollinearity among the model predictors and the F-ratio indicates a statistically significant regression equation (Table 2.3). The model is well-validated. Pearson correlation (r) and R^2 of the observed and LOO-estimated values attest to the model accuracy and the reduction of error (RE; Fritts *et al.*, 1990) value suggests good model skill (Table 2.3, Figure 2.3). The difference between the model SE and the root mean square error of cross-validation ($RMSE_v$) is only 15.3 mm; this is a practical measure of the difference in the average size of the prediction error between the model validation and calibration, in units of the predictand.

Table 2.3: Reconstruction and cross-validation statistics.

Reconstruction	R^2	D-W[a]	VIF	SE	F ratio
	0.56	2.05	1.13	391.12	14.49
Cross-validation	RE	$RMSE_v$[b]	r[c]	R^2_v[d]	
	0.55	375.84	0.74	0.55	

[a]Durbin-Watson statistic
[b]Units of SWE (mm)
[c] significant at 99% level
[d]Cross-validation R^2

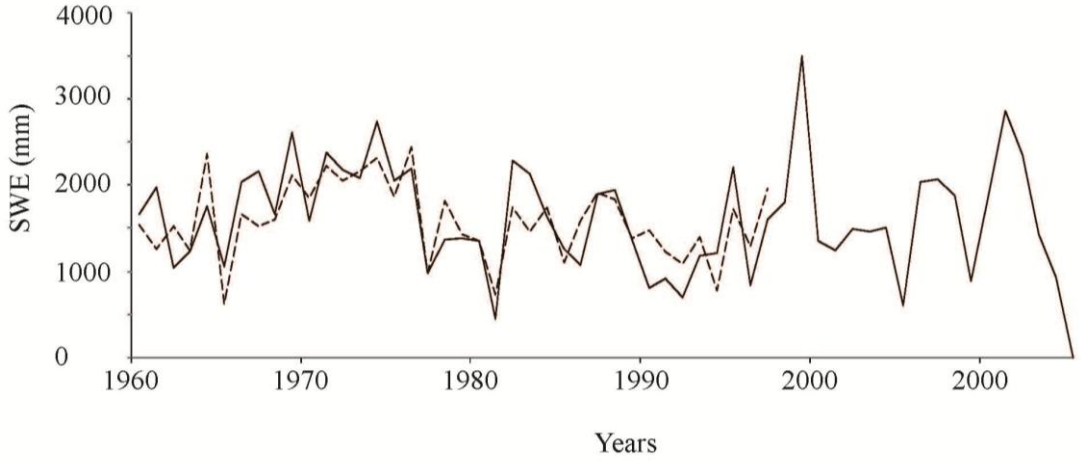

Figure 2.3: Time plot of the instrumental (solid line) and reconstructed (hatched line) SWE values over the model calibration period (both time series, 1960-1997) and to present (instrumental data only, 1998-2015).

A time plot of the reconstructed and estimated values over the calibration period provides insight on year-to-year model accuracy (Figure 2.3). The 1998-2015 SWE data are also plotted for context. Although high and low SWE values are both over- and under-estimated in some years, the direction of the model estimates is largely accurate especially in extreme years. A time plot of the full-period reconstruction is presented in Figure 2.4. A 5-year running mean of the reconstructed values highlights slightly lower frequency variability, including unusual intervals of enhanced SWE around the 1970s and reduced SWE around the late 1700s.

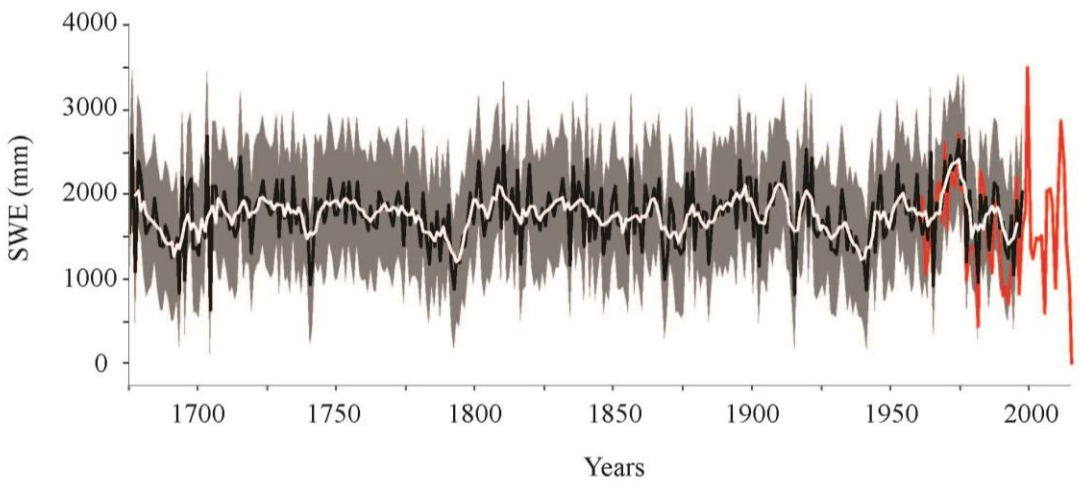

Figure 2.4: Time plot of the reconstruction (black line). The white line is a 5-year running mean of the reconstructed values, the red line is the instrumental SWE record, and the grey envelope is a running confidence interval calculated using the equation of Weisberg (1985).

2.6.3 Diagnostic climate correlations

Relationships of the predictor TR chronologies to SWE, PAS, and maximum temperature data are summarized in Figure 2.5 and Table 2.4. Winter-season PAS most strongly influences TR growth. Each chronology is also weakly positively correlated with summer temperature, either in the current year (mountain hemlock chronologies) or previous year (amabilis fir chronology).

2.7 Discussion

2.7.1 Reconstruction

The reconstruction suggests that low May 1 SWE in 2015 was unprecedented since at least 1675. The exceptional nature of annual snowfall in that year relative to the last few centuries may be related to 20th century climate shifts and/or the strong warm/dry El Niño that occurred in 2015. There is evidence that ENSO variance has strengthened in recent decades (e.g. McGregor *et al.* 2010; B.C. River Forecast Centre 2015). Though variance compression often occurs in TR-based reconstructions due to the inability of TR data to fully 'capture' ranges of climate variability, the model estimates are not

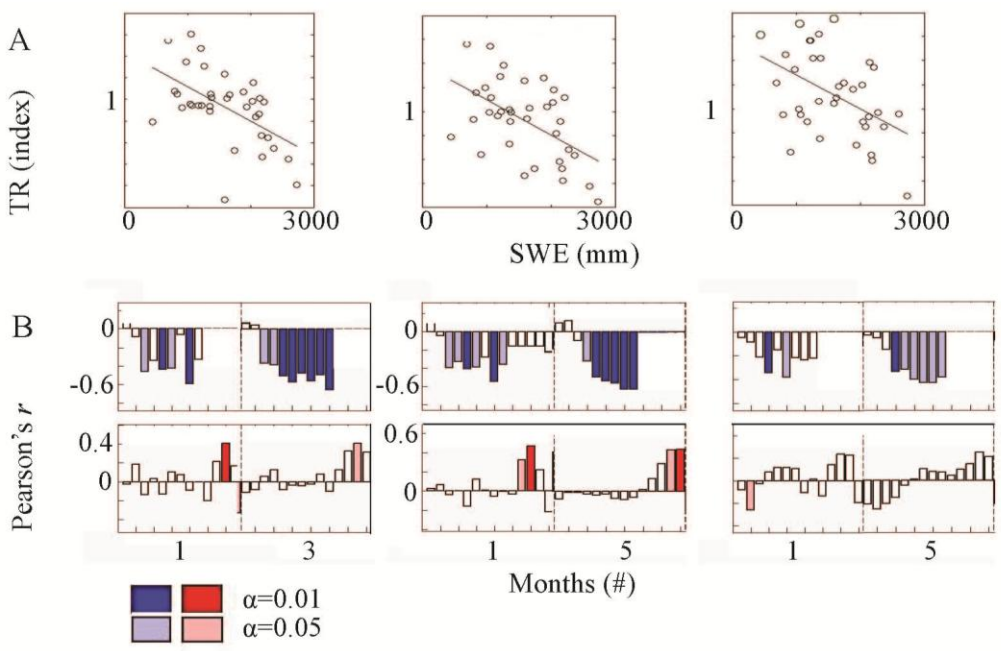

Figure 2.5: Relationships of the model predictors to snow and maximum temperature records over the calibration period (1960-1997). Strathcona (L), Mount Washington (C), Mount Cain (R). (A) Linear associations of the TR chronologies and May 1 SWE data. (B) Correlations of the TR chronologies with PAS (top) and maximum temperature (bottom) data for 1-, 3- or 5-month seasons, calculated using Seascorr (Meko *et al.* 2011). Calculated in each month of the 14-month period beginning in August of the previous year and ending in June of the current year (PAS) or August of the current year (temperature). Bars are plotted on the final month of the tested season. All PAS correlations are temporally stable (*p*-values ranged from 0.08 to 0.51, $n_1 = 19$, $n_2 = 18$).

Table 2.4: Relationships of the predictor TR chronologies with PAS and temperature data calculated over the model calibration period (1960-1997) using Seascorr (plotted in Figure 2.5). Strongest monthly or seasonal correlations are presented. Previous years are identified with capital letters. ** p <0.01, * p<0.05.

	PAS (*r*)	May 1 SWE (*r*)	Temperature (*r*)		
			Max	Min	Mean
Strathcona TSME	-0.66** Mar-May	-0.55**	0.41** July	0	0.24* July
Mount Washington TSME	-0.65** NOV-Mar	-0.53**	0.42** Jun-Aug	0	0.32* July
Mount Cain ABAM	-0.44* Jan-May	-0.47**	-0.24* SEP	0	0

compressed relative to the instrumental SWE data in the calibration period (Cook and Kairiūkštis 1990). Over- and under-estimations of instrumental SWE values in the calibration period suggest the reconstructed values may also be over- or under-estimated, but the year-to-year direction of the calibration period estimates is largely accurate and extreme values are particularly accurately estimated, with the exception of a moderately dry period in the 1990s.

While the reconstruction suggests that SWE in 2015 was unprecedented in a multi-century context, limitations of the TR data and model calibration make it impossible to state this with statistical confidence. Due to the selection of the Strathcona chronology as a predictor in the model (data period 1600-1997) the regression equation could not be calibrated on the period of highest instrumental SWE variance (1998-2015). As a result, the ability of the reconstruction to estimate the magnitudes of the most extreme instrumental SWE years, including 2015, is unknown.

The performance of the model in capturing the magnitude of the low SWE year in 1981 provides a meaningful indication of the reliability of the reconstruction for estimating similar years. The 1981 SWE value is the lowest SWE measurement on record prior to 2015, and the calibration period time plot shows the reconstructed value very closely approximates the instrumental value in that year. Using 1981 as a baseline for 'very low' snowpack, the reconstruction suggests there have been ten years prior the instrumental period when SWE was lower than at any time in the historical data record (from lowest to highest: 1704, 1674, 1660, 1665, 1661, 1915, 1693, 1671, 1941, and 1792). The accuracy of the reconstruction estimate in 1981 suggests the model would be able to estimate SWE as low as that in 2015 if such values occurred in the pre-instrumental period.

The reconstruction uses an ARSTAN chronology with first and second order autocorrelation retained (r_1=0.353, r_2=0.230), emphasizing that the influence of snow on TR growth may persist for multiple years. ARSTAN chronologies are particularly useful for dendroclimatological modeling since the persistence that is common among trees (*e.g.*, information that is likely climate-related) is retained (Holmes 1983). The diagnostic climate correlation analyses showed that variance in the predictor TR chronologies is principally related to year-to-year spring snowpack depths. However, summer

temperature also influences TR widths, albeit weakly (Table 2.4). Relatively wide confidence intervals on the model estimates may be partly due to the incorporation of summer temperature information in the reconstruction. Other sources of error could include stand level noise in the TR data (e.g. due to windthrow) and error in the SWE data measurements.

Energy-limited snow-sensitive TR records may present an additional challenge for estimating the magnitudes of lowest snowpack years. Unlike typical dendrohydrological models that are based on positive associations of tree growth with moisture, the relationship of energy-limited TRs to SWE is negative. Lowest SWE years, therefore, correspond with largest ring widths. In old, large-circumference trees such as those that were used in this study, there is an upper limit to the size of annual ring widths in the most recent growth years as a result of the distribution of the annual increment over a larger area. Even if ring width size is assessed relative to nearby ring widths (*e.g.* crossdating principal; Wigley *et al.* 1987), TRs may be unable to achieve ring widths large enough to 'capture' lowest SWE measurement magnitudes. Because the most recent portion of the TR record is used in model calibrations, this problem could generally weaken model calibration strength.

Reduced SWE in the 1790s and early 1940s corresponds with warm reconstructed annual air temperatures for Vancouver, B.C. (Ware and Thomson 2000; derived from TR data independent from this study) and positive phase PDO conditions as described by separate paleoreconstructions (Biondi *et al.* 2001, Gedalof and Smith 2001*b*, MacDonald and Case 2005). Positive phases of the PDO typically correspond with a deepening Aleutian Low, a strengthening of the Pacific North America pattern, and less winter precipitation in coastal B.C. (Fleming *et al.* 2007). Some paleorecords of ENSO also identify a relatively large number of El Niño events during these low SWE periods (McGregor *et al.* 2010). The reconstruction highlights the unusualness of a period of enhanced SWE in the early 1970s, which coincided with cool phase PDO conditions and two of the strongest 20th century La Niña events in the instrumental record (Wolter and Timlin 1993; Kiffney *et al.* 2002).

2.7.2 Non time-stable SWE sensitivity

Marcinkowski *et al.* (2015) reported non-significant correlation of mountain hemlock TR widths and SWE after about 2000 in the North Cascade Range in Washington State, United States. The accuracy of paleoenvironmental models depends upon the assumption that the climate-proxy relationships upon which a model is calibrated also existed in the past. While the sensitivity of TRs to a limiting climate variable may weaken periodically, for example due to extreme environmental conditions or disturbance, there is growing evidence of more prolonged decoupling of the TR-climate relationship beginning around the 1960s in energy-limited forests (D'Arrigo *et al.* 2008). This pattern has been documented mainly in the high-latitudes, with some examples at high-elevation forests at lower-latitudes, and is thought to be related to unprecedented 20th century atmospheric warming (Coppola *et al.* 2012). Recognition of 'divergence' has prompted more careful testing of the stability of dendroclimatic relationships in all settings (Esper and Frank 2009).

There was no statistically significant evidence of temporal instability in the relationship of the model predictors to SWE over the calibration period. However, *r* values for the difference-of-correlations test were notably lower in the later period than in the early period, and *p*-values approached $p<0.05$.

As a follow up, the two chronologies that extend beyond 2000 were used to test the stability of TR-SWE correlations in 2000 to 2015, the period of reduced SWE sensitivity identified by Marcinkowski *et al.* (2015). The previously described difference-of-correlations test indicated the Mount Washington mountain hemlock chronology exhibits a more stable correlation with May 1 SWE over 1997-2014 than over the shorter calibration period (early period $r = -0.59$, late period $r = -0.26$, $n_1=27$, $n_2=26$, $p=0.15$); but the correlation of the Mount Cain amabilis fir chronology with SWE becomes non-significant outside of the model calibration period (early period $r = -0.70$, late period $r = -0.02$, $n_1=22$, $n_2=22$, $p=0.01$). Twenty-year moving correlation tests indicate the relationship of both chronologies with SWE becomes non-significant in 20-year periods ending after the mid-1990s (Figure 2.6; significance calculated using a stationary bootstrapping method (Politis *et al.* 2004). Interestingly, the loss of SWE sensitivity is coincident with the onset of correlations with maximum spring (March) temperature in

the mountain hemlock record (Figure 2.6; significant at p=0.95 level). This finding supports the hypothesis that, as a result of less snow and earlier warmer springs, snowpack depth is being replaced by spring temperature as the dominant control on growing season length in some locations (Marcinkowski *et al.* 2015).

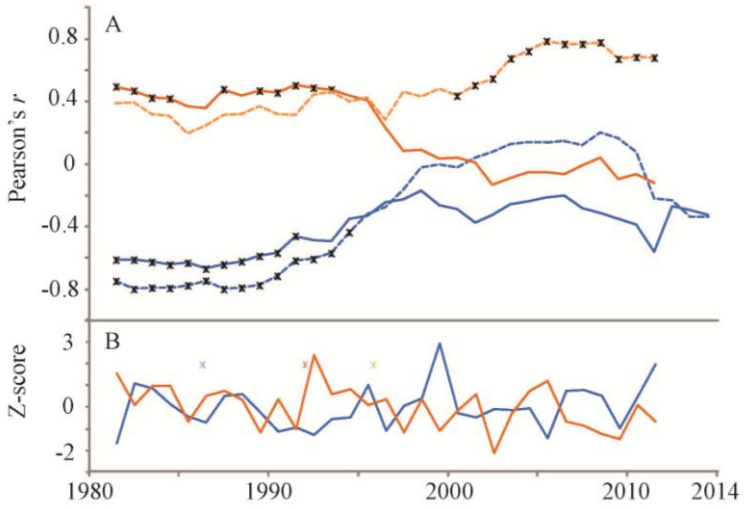

Figure 2.6: (A) Time plot of *r*-values for twenty-year moving correlations of the Mount Washington mountain hemlock chronology (solid lines) and Mount Cain amabilis fir chronology (dashed lines) with maximum March temperature (orange) and May 1 SWE (blue) data. The values are plotted on the last year of the 20-year moving correlation window. (B) Time plot of March temperature (orange) and May 1 SWE (blue) data (z-scores).

The short data interval makes it difficult to quantitatively identify a change in spring conditions since the mid-1990s that could have triggered a change in growth-limiting factors. Trend tests did not suggest statistically significant increases or decreases in either the May 1 SWE or spring maximum temperature data over the last 10-20 years, but in both cases trend may be obscured by one extreme outlier year. Visual inspection of the time plot in Figure 2.6 reveals a markedly negative association between spring temperature and SWE beginning around 2000 that suggests a stronger influence of spring temperature on melting snowpacks over the last ~15 years.

These findings support those of Marcinkowski *et al.* (2015) who reported that mountain hemlock TR data from the past 10 to 15 years may be unreliable for reconstructing SWE. SWE-growth relationships for all tree species in the study region

should be carefully evaluated and, if necessary, the recent part of the record should be omitted from model calibrations. This limitation may prevent calibration of the model on the most interesting (extreme) years and inhibit comparison of extreme years with past conditions, as was the case in this study. Overall, the findings support continued use of mountain hemlock TRs as a proxy for SWE, as their relationship to SWE is consistent through time prior to ~1995 on both Vancouver Island and in the Cascade Range (Marcinkowski *et al.* 2015).

2.8 Conclusion

This research affirms that the annual radial growth of some high-elevation conifer trees in the Vancouver Island Ranges may be energy-limited as a function of snowpack depth, and demonstrates that this climate-growth relationship can form the basis for dendrohydrological reconstructions of SWE. A reconstruction model explains 56% of instrumental May 1 SWE variance, which is comparable with the robustness of traditional arid-region dendrohydrological models. The reconstruction is remarkably effective at approximating the full range of instrumental SWE variance, especially extreme years.

The reconstruction suggests that record low SWE measurements in 2015 were lower than in any year since 1675. However, limitations of the data preclude making this conclusion with a high degree of confidence. The model could not be calibrated on the most recent SWE data, which is the period of highest variance and includes the 2015 value. As a result, it is not known whether the model would estimate a pre-instrumental SWE value as low as in 2015 accurately. The reconstruction very closely approximates the next-lowest instrumental SWE value in 1981, however, and suggests there have been ten years when SWE was lower than in 1981.

A suite of detailed correlation analyses confirmed that mountain hemlock and amabilis fir TR records act as proxies for SWE, and also showed that some temperature-related information in the TR records may be a source of model error. Correlation analyses also indicated that on Vancouver Island, the relationship of some TRs to SWE becomes non-significant in 20-year periods ending after the mid-1990s. For the mountain hemlock record that was tested, the loss of SWE sensitivity is coincident with the onset of

correlations with maximum spring temperature. These findings offer additional support to the hypothesis that less snow and earlier, warmer, springs have led to snowpack depth being replaced by spring temperature as the main control on growing season length (Marcinkowski *et al.* 2015). TR data from the past 10 to 15 years should be carefully evaluated for time stabile relationships with SWE, but the relationship does appear consistent through time prior to ~1995 on both Vancouver Island and in the Cascade Mountains. Overall, the findings presented here suggest TR records that are energy-limited by late lying snowpacks are promising for expanding dendrohydrological research to temperate environments. This approach is effective for reconstructing annual SWE, and could likely be expanded to snow-influenced streamflow and drought.

Chapter 3 A 477-year dendrohydrological assessment of drought severity for Tsable River, Vancouver Island, British Columbia, Canada

3.1 Article information

Chapter 3 consists of a manuscript published in Hydrological Processes (December 2015). The text and figures are taken directly from the published paper but have been renumbered and reformatted for consistency within this thesis. Citation style has also been reformatted for consistency.

3.1.1 Authors' names and affiliations

B. L. Coulthard[1]*, D. J. Smith[2]

[1] B. L. Coulthard, University of Victoria Tree-Ring Laboratory, Department of Geography, University of Victoria, PO Box 3060 STN CSC, Victoria, British Columbia, Canada, V8W 3R4

[2] D. J. Smith, University of Victoria Tree-Ring Laboratory, Department of Geography, University of Victoria, PO Box 3060 STN CSC, Victoria, British Columbia, Canada, V8W 3R4

*Corresponding author Email: coulthard.bethany@gmail.com, Telephone: +12504724733

3.1.2 Author's and coauthors'contributions

Coulthard developed the study and hypothesis, conducted laboratory work and statistical testing, wrote the manuscript, and produced all of the tables and figures. Smith provided tree-ring samples and measurement data archived at the University of Victoria Tree-Ring Laboratory, and reviewed and edited the manuscript

3.2 Abstract

Summer droughts are becoming more severe in many watersheds on Vancouver Island, British Columbia, as a result of climate warming. Small coastal basins that are the primary water source for most communities and essential to Pacific salmon populations have been particularly affected. Because the most extreme naturally occurring droughts

are rarely captured within short instrumental records water managers likely underestimate, and are unprepared for, worst-case scenario low flows. To provide a long-term perspective on recent droughts on Vancouver Island, we developed a 477-year long dendrohydrological reconstruction of summer streamflow for Tsable River based on a network of annual tree-ring width data. A novel aspect of our study is the use of conifer trees that are energy-limited by spring snowpack depths. Explaining 63% of the instrumental streamflow variability, to our knowledge the reconstruction is the longest of its kind in British Columbia. We demonstrate that targeting the summer streamflow component derived from snowmelt is powerful for determining drought-season discharge in hybrid runoff regimes, and we suggest this approach may be applied to small watersheds in temperate environments that are not usually conducive to dendrohydrology. Our findings suggest that since 1520, 21 droughts occurred that were more extreme than recent 'severe' events like those in 2003 and 2009. Recent droughts are therefore not anomalous relative to the ~400 year pre-instrumental record, and should be anticipated within water management strategies. In coming decades, worst-case scenario natural droughts compounded by land use change and climate change could result in droughts more sever than any since 1520. The influence of the Pacific Decadal Oscillation on instrumental and modeled Tsable River summer streamflow is likely linked to the enhanced role of snowmelt in determining summer discharge during cool phases.

3.3 Introduction

British Columbia's (B.C.) temperate rainforest coast is considered water-rich, but seasonal water scarcity and drought often occur during summer when demand for water is highest and storage is limited (Stephens *et al.* 1992). In 2014 and 2015 many streams experienced droughts that were more severe than any on record (B.C. Ministry of Forests, Lands and Natural Resource Operations 2014; B.C. River Forecast Centre 2015). Climate warming has triggered earlier, lower, longer, and more frequent low-flows throughout the coastal region (Rodenhuis *et al.* 2007), and the impact of worsening droughts on human water use, stream ecology, and the survival of Pacific salmon is recognized by the provincial government as a critical environmental management challenge (B.C. Ministry of Environment 2013).

"Hybrid" runoff regimes are the primary water source for most towns, municipalities, and First Nations communities on Vancouver Island, B.C., and are also the most vulnerable to summer water shortages (Rodenhuis *et al.* 2007). Both snowmelt and rainfall contribute substantially to annual streamflow in hybrid watersheds (Eaton and Moore 2010). The likelihood of protracted drought under future climate conditions makes an accurate understanding of worst-case scenario droughts, based on long-term natural variability, crucial for effective water management in these basins (Pike *et al.* 2010).

The purpose of our research was to develop a multi-century summer discharge (Q) record for a small hybrid watershed on southeastern Vancouver Island, and to interpret the severity of recent droughts within the context of that record. We used a dendrohydrological approach, where climate-sensitive tree-ring (TR) width records serve as proxies for climate in a paleohydrological model (Loaiciga *et al.* 1993). Detection of recent environmental change often requires these long-term records because natural climatic patterns, such as the Pacific Decadal Oscillation (PDO), persist over multiple decades and can obscure climate change effects (Moore *et al.* 2007).

While streamflow reconstructions based on TR data have been developed for drought-sensitive regions world-wide, applying traditional dendrohydrological approaches to a small hybrid watershed in a temperate environment is problematic. First, very flashy rainfall-driven runoff is often a major contributor to total annual streamflow

in coastal B.C. (Eaton and Moore 2010). Dendrohydrological models usually target annual discharge in large watersheds where both runoff and annual radial tree growth are relatively unresponsive to "flashy" rainfall events (Pederson *et al.* 2001; Boninsegna *et al.* 2009; Yang *et al.* 2010; Margolis *et al.* 2011; Meko and Woodhouse 2011; Sauchyn *et al.* 2014). Second, trees on Vancouver Island are rarely moisture-stressed, although the radial growth of some species is sensitive to winter precipitation as a result of the energy-limiting role of deep snowpacks (Marcinkowski *et al.* 2015). Dendrohydrological studies are usually conducted in arid environments using trees whose radial growth is limited by rainfall or snowmelt-derived soil moisture, which directly influence runoff (Woodhouse *et al.* 2006). We circumvent these problems by targeting low-flow season streamflow in our reconstruction, a time of year when runoff is significantly less flashy, is primarily driven by snowmelt, and is most important for drought management (Smith and Laroque 1998).

We hypothesized that summer discharge in a small hybrid basin on Vancouver Island is driven by regional snowmelt variations to the extent that TR records that are energy-limited by snow could serve as proxies for climate in a dendrohydrological reconstruction of streamflow. To date, paleohydrological efforts in B.C. have explored the utility of annual TR width and density records as proxies for winter and summer temperature and snow water equivalent (SWE) for reconstructing summer-season and mean water year runoff in nival and glacial watersheds (Gedalof *et al.* 2004; Watson and Luckman 2005; Hart *et al.* 2010; Starheim *et al.* 2013). No prior attempt has been made to develop seasonal reconstructions of the hybrid streams that are most susceptible to drought in coming decades.

We use the term "drought" to mean streamflow drought, or below-normal stream discharge, a component of hydrological drought that often also coincides with reduced groundwater availability (VanLoon and Laaha 2015). Consistent with B.C. government management practices, "drought" refers to below-normal stream runoff persisting over a period of consecutive months (B.C. Ministry of Environment 2013).

3.4 Research Background

Large precipitation and temperature gradients characterize most watersheds on Vancouver Island. Winter storms originating in the North Pacific Ocean bring moisture to the west coast of the island, where orographic lift results in deep snowpacks at high elevation and large quantities of rain in lowland areas (Stahl *et al.* 2006). Rain shadow effects on the east side of Vancouver Island result in drier conditions in lowland coastal regions (Rodenhuis *et al.* 2007). Summers are warm and dry, and dominated by persistent high-pressure systems (Rodenhuis *et al.* 2007). Seasonal hydroclimatic patterns are moderated by synoptic-scale inter-annual and decadal modes of climate variability stemming from ocean-atmosphere interactions in the Pacific Basin, of which the PDO, the El Niño Southern Oscillation (ENSO), and the Pacific North America (PNA) pattern have a particular influence on regional streamflow (Kiffney *et al.* 2002).

Hybrid streams on Vancouver Island are found primarily in mid-elevation coastal and near-coastal areas where mean watershed elevations are not high enough to be fully nival (Eaton and Moore 2010). Hybrid streams experience highest mean monthly flows during winter rains, followed by a significant pulse of runoff from snowmelt in spring. Lowest monthly flows occur during summer when discharge is governed by snow meltwater inputs, nominal summer precipitation inputs, and losses related to summer air temperatures and evaporation (Eaton and Moore 2010). Snowmelt can significantly recharge deep groundwater flow pathways to augment summer baseflow in the study region, even if only a small snow fed headwater is present (Moore *et al.* 2007; Beaulieu *et al.* 2012). Above average minimum summer discharge is, therefore, often coincident with deep snowpacks that develop during cool and wet La Niña years, especially when enhanced by cold phases of the PDO (Fleming *et al.* 2007). The proportion of rainfall-derived versus snowmelt-derived runoff varies from year to year in accordance with fluctuations in winter temperature, so that annual flows in hybrid regimes can be ‘more pluvial’ or ‘more nival’ in any given year (Moore *et al.* 2007). A high between-year range in monthly flow totals is typical (Moore *et al.* 2007).

In the south coastal region of B.C., annual minimum streamflow has decreased in hybrid watersheds over the last 30 years, with low-flow magnitudes projected to decline by up to 50% by the end of the century as a result of seasonal climate trends (Rodenhuis

et al. 2007; Mantua *et al.* 2010). Winters have become milder and wetter, with less winter precipitation falling as snow and more as rain, and more frequent rain-on-snow events. As a result, less snow meltwater is available to buffer low stream discharge during the dry summer months (Pike *et al.* 2010). Projections suggest that nival flow contributions will weaken or become non-existent, eventually shifting many hybrid systems to more pluvial regimes (Eaton and Moore 2010). Summers have become warmer and drier additionally drawing-down summer flows (Pike *et al.* 2010).

3.5 Study Site

The Tsable River watershed is a small (113 km^2) hybrid basin located on the eastern slopes of the Beaufort Range on central Vancouver Island, in the rainshadow of the Vancouver Island Ranges (Figure 3.1). With a maximum basin elevation of around 1500 m asl, a significant portion of precipitation within the watershed falls as snow above 1000 m asl (Eaton and Moore 2010). Tsable Lake (~1 km^2) and several smaller lakes are located with the basin. Draining east to the Strait of Georgia, the lower reaches of the watershed are located within the dry Coastal Douglas Fir Zone, transitioning from the Coastal Western Hemlock Zone, to the Mountain Hemlock Zone and Alpine Tundra Zone with increasing elevation (Klinka *et al.* 1991). At high elevation (1000-1500 m asl) the growing season is short and cool, with very deep snowpacks often persisting into the spring and summer. Mountain hemlock (*Tsuga mertensiana* (Bong.) Carrière) trees are dominant, with subalpine fir (*Abies lasiocarpa* (Hook.) Nutt.) and amabilis fir *(Abies amabilis* (Dougl.) Forbes) trees occasionally co-dominant. Industrial logging is the main land use in the watershed.

Highest total monthly discharge in Tsable River occurs from November through January, with spring snowmelt causing a distinct pulse of runoff in May (Figure 3.2; Eaton and Moore 2010). Analysis of annual hydrographs provides a comparison between years dominated by winter rainfall- versus summer snowmelt-derived runoff (Figure 3.2). Lowest flows occur in July through September (Figure 3.2). In recent years, Tsable River summer baseflow has been far below optimum for the river's populations of chum, coho, and pink salmon, and resident and anadromous steelhead and cutthroat trout (B.C. Conservation Foundation 2006). Despite conservation efforts, low-flows have degraded

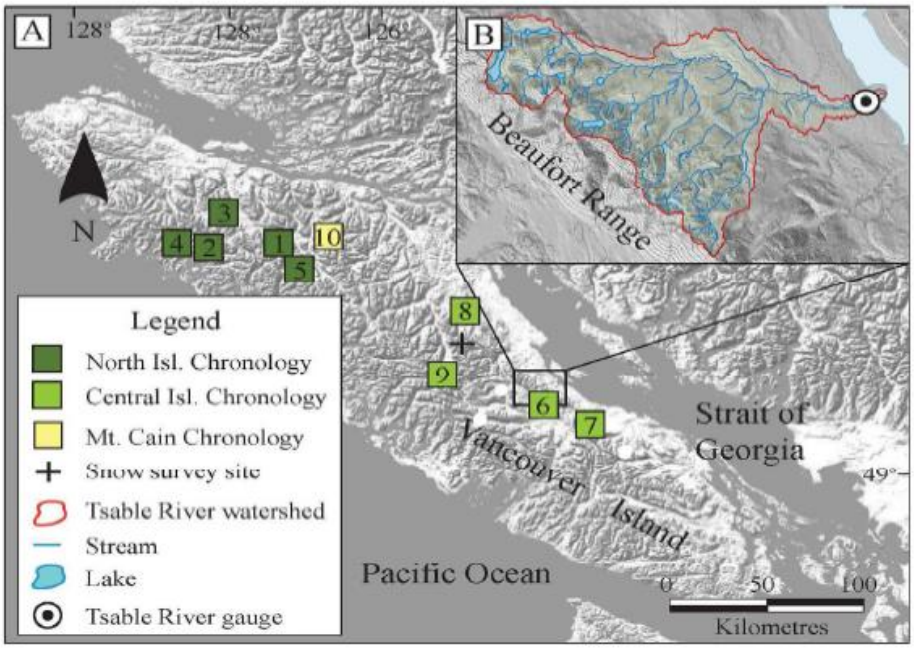

Figure 3.1: Map of the study area. (A) Vancouver Island. (B) Tsable River watershed.

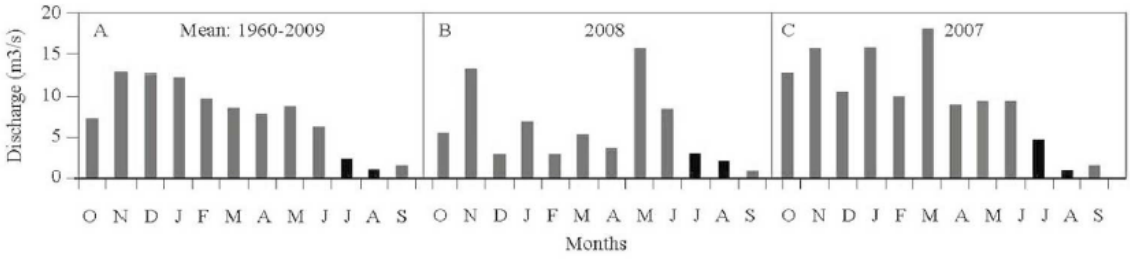

Figure 3.2: Tsable River water-year hydrographs. Dark bars indicate the reconstruction season (July-August). (A) Gauged mean monthly discharge over the length of record used (1960-2009); (B) Mean monthly discharge in a 'more nival' year when runoff during spring snowmelt outweighed rain-derived runoff during winter; (C) Mean monthly discharge in a 'more pluvial' year when runoff from winter rains outweighed runoff from spring snowmelt.

stream habitat to the extent that the wild steelhead stock has likely been extirpated since the early 2000s (Lill 2002; Silvestri 2004).

3.6 Data and Methods

3.6.1 Hydrometric and climate data

Only three hybrid streams on Vancouver Island have >50 years of natural and continuous instrumental data. Tsable River was selected for this study because it is the hybrid stream with the longest continuous natural hydrometric record (1960-2009), and the watershed does not contain large natural water storage features such as lakes and wetlands. We downloaded monthly discharge data for Tsable River from the Water Survey of Canada (http://www.wsc.ec.gc.ca/applications/H2O/index-eng.cfm). Missing values (1% of the data) were replaced with long-term monthly means (station code 08HB024; gauge location latitude: 49.517, longitude: -124.841, elevation: 1 m asl). We used the average flow from July-August for our reconstruction because the regional hydrological literature suggests stream discharge is significantly correlated with previous winter SWE during that season (Rodenhuis *et al.* 2007; Eaton and Moore 2010). The July-August streamflow data, hereinafter "summer streamflow" data, span the interval 1960-2009 and were normalized using a log10 transformation.

May 1 SWE records collected at the Forbidden Plateau manual snow survey site (data period February-May 1958-2014; station code 03B01; latitude: 49.653, longitude: -125.207, elevation: 1100 m asl) were retrieved from the Water Survey of Canada (http://a100.gov.bc.ca/pub/mss/stationdata.do?station= 3B01). May 1 is generally the maximum annual SWE measurement in the Forbidden Plateau dataset. We estimated monthly maximum temperature and total precipitation anomaly records on the coordinates of the Tsable River hydrometric gauge site using the program ClimateWNA, ver. 4.83 (Wang *et al.* 2006; 2012). The program downscales PRISM (Daly *et al.* 2002) monthly data (2.5 x 2.5 arc min) based on the reference period 1961-1990. We compared the gauged and reconstructed streamflow records with NOAA Multivariate ENSO Index ranks (http://www.esrl.noaa.gov/psd/enso/mei/) and standardized values of the PDO index downloaded from the NOAA Earth System Research Laboratory website (http://www.esrl.noaa.gov/psd/data/ climate indices/list/). Winter (averaged October-March) PDO data were used because year-to-year variability in the index is most energetic during those months (Mantua 2002).

3.6.2 Tree-ring data

Mountain hemlock and amabilis fir TR width data were used for this study. In the northwestern United States and Canada, the annual radial growth of high-elevation conifer trees is often energy-limited as a result of variations in snowpack depth (Peterson and Peterson 1994). Snow may control the timing of the start or end of the growing season and, therefore, total growing season length through its influence on soil temperatures, which warm rapidly after snowmelt (Graumlich and Brubaker 1986). This climate-radial tree growth relationship is well-documented in mountain hemlock trees (Graumlich and Brubaker 1986; Smith and Laroque 1998; Gedalof and Smith 2001a; Peterson and Peterson 2001; Marcinkowski *et al.* 2015) and field observations suggest amabilis fir trees typically initiate leaf and shoot expansion shortly after snowmelt (Hansen-Bristow 1986; Worrall 1983).

TR width data was compiled for one amabilis fir stand and eight mountain hemlock stands located on central and northern Vancouver Island (Figure 3.1; Table 3.1). These data were selected because they provided the longest potentially SWE-sensitive TR width records. Crossdated amabilis fir TR width measurements collected by R. Parish at Mt. Cain in 1999 were acquired from the International Tree-Ring Data Bank website (http://www.ncdc.noaa.gov /data-access/paleoclimatology-data/datasets/tree-ring). Mountain hemlock samples were collected between 1996 and 1998 by removing two cores with a 5.0 mm increment borer from trees at standard breast height. Ring widths were measured using WinDENDRO Ver 6.1b (WinDENDRO 1996; Laroque 2002). In 2014, the measurements were crossdated visually (list method) and statistically verified using the program COFECHA 3.0 (Holmes 1983; Grissino-Mayer 2001). In some cases physical samples were missing from the archived collections. Because crossdating was not possible without physical specimens, only a subset of the original samples could be used for each site. As a result, sample sizes per site were very low in some cases (Table 3.1).

TR chronologies were developed using the R package dplR (Bunn 2008). We removed long-term biological growth trend from the TR data by fitting a 100-year cubic smoothing spline with a frequency cutoff of 50 to each TR series (Cook and Peters 1981). Dimensionless growth indices were produced by dividing ring-width measurements by

the expected value of the spline. The majority of the TR data exhibited low-order autocorrelation as a result of the lagged influenced of environmental conditions in previous years (Fritts 1976). We fit an autoregressive model to the data to remove persistence, with the model order defined by minimization of the Akaike Information Criterion. Only residual chronologies estimated by this procedure were used in the subsequent analysis (Cook and Holmes 1986). Series were combined into single representative 'site-level' chronologies using a bi-weight robust mean estimation (Mosteller and Tukey 1977). Where two or more series were included from one tree, we averaged them prior to mean chronology estimation in order to weight individual trees equally. We determined the adequacy of the sample size for capturing the hypothetical population growth signal by calculating the expressed population signal (EPS; Wigley *et al.* 1984), and truncated the chronologies where EPS<0.80. Because of the low number of samples per site, we aggregated the records into regional chronologies where site-level chronologies were significantly intercorrelated. This significantly extended the lengths of our TR records by enhancing signal-to-noise ratios in the early part of the record. The methods used to estimate site-level chronologies were also used to estimate regional chronologies.

The Pearson correlation coefficient was used to summarize the strength of linear relationships between various time series in this study. All tests of association were conducted over the longest common interval between datasets. We used correlation tests to determine whether the site-level and regional TR chronologies were significantly linearly correlated with the gauged summer streamflow data, with Bonferroni corrections applied for repeated testing (Dunn 1961). The temporal stability of relationships in non-overlapping data subperiods was tested using a difference-of-correlations test that employs a Fisher's Z transformation of correlations (Snedecor and Cochrane 1989). Long chronologies that were significantly (p<0.01) correlated with summer streamflow over the full length of the streamflow record were retained as candidate model predictors.

3.6.3 Hydroclimate relationships

To determine the climatic variables controlling summer discharge in Tsable River, and to justify a SWE-based reconstruction model of the river, we tested

correlations of the gauged summer streamflow data with various monthly and seasonal climate data records. Effective sample sizes (Dawdy and Matalas 1964) were used as needed in testing the correlations for significance, to adjust for persistence in the individual time series.

Table 3.1: Tree-ring chronology information. Chronologies in bold font were entered as candidate predictors in the forward stepwise model.

Chronology	#	Lat/Long	Elev. (m asl)	RBAR[c]	Length (years)	Series (#)	Trees (#)	r_1[d]
Bulldog Ridge[a]	1	50.28 -127.24	1010	0.22	1845-1997	9	6	0.72
Castle Mountain[a]	2	50.45 -127.12	1150	0.32	1845-1997	10	7	0.75
Colonial Creek[a]	3	50.28 -127.46	990	0.29	1940-1997	7	5	0.76
Silver Spoon[a]	4	49.98 -126.67	1100	0.37	1955-1996	11	8	0.66
N. Isl. Regional[a]		-	-	**0.26**	**1630-1997**	**37**	**28**	**0.72**
Mt. Apps[a]	5	49.44 -124.96	1340	0.29	1795-1996	40	22	0.63
Mt. Arrowsmith[a]	6	49.24 -124.59	1460	0.33	1575-1997	11	8	0.72
Mt. Washington[a]	7	49.75 -125.30	1470	0.42	1795-1996	15	12	0.68
Cream Lake[a]	8	49.48 -125.53	1340	0.36	1525-1995	29	18	0.68
C. Isl. Regional[a]		-	-	**0.30**	**1510-1997**	**95**	**61**	**0.68**
Mt. Cain[b]	**9**	**50.22 -126.35**	**1005**	**0.31**	**1520-1999**	**64**	**34**	**0.83**

[a]Mountain hemlock
[b]Amabilis fir
[c]Mean correlation coefficient among TR series, calculated from the detrended residual chronology
[d]Mean first-order autocorrelation calculated using program COFECHA, prior to autoregressive modeling

To assess the influence of snow on runoff, we tested the correlation of gauged summer streamflow data with current and previous year May 1 SWE values. We applied the previously described difference-of-correlations test (Snedecor and Cochrane 1989) to determine if there is a significant change in the relationship between streamflow and SWE before and after the 1976/77 PDO shift (Mantua 2002). Because high summer streamflow is usually associated with enhanced snowmelt in hybrid streams (Eaton and Moore 2010), we checked that low summer streamflow years are also influenced by

meltwater by sorting the gauged summer streamflow data into lowest, middle, and highest terciles, and calculating Pearson's correlations between the summer streamflow and May 1 SWE values within each tercile.

Correlations of gauged summer runoff with monthly and seasonally aggregated temperature and precipitation data were calculated using the program Seascorr (Meko *et al.* 2011). Seascorr estimates confidence intervals on the sample correlations and partial correlations by a Monte Carlo simulation of the flow data by exact simulation (Meko *et al.* 2011). Correlations of the gauged summer streamflow data with maximum temperature data were tested in 1 to 6 month intervals, with intervals ending in each month of the 14-month period beginning in July of the previous year and ending in August of the current year. Partial correlations were then calculated to determine if annual, and especially summer, precipitation makes a significant contribution to summer runoff that is independent of the temperature influence. We also tested monthly and seasonal correlations between the temperature and precipitation data in the same seasonal and monthly groupings. Relationships to climate in the previous year were evaluated because we were curious whether they influence current-year summer runoff as a result of hydrological lag effects in the groundwater system.

3.6.4 Model estimation

The reconstruction model was estimated by forward stepwise multiple linear regression of the summer streamflow data in year *t* on the pool of candidate predictor variables in years *t*, *t*+1, and *t*+2. Lagged predictors were entered to allow TR information in subsequent years to inform on climate conditions in the given year (Cook and Kairiūkštis 1990). We evaluated regression models based on a suite of statistics widely used to evaluate TR based environmental reconstructions (Cook and Kairiūkštis 1990). The adjusted R^2 statistic provides a measure of the explanatory power of the models accounting for lost degrees of freedom. Analysis of the model residuals, and the Durbin-Watson (D-W) and variance inflation factor (VIF) statistics, were used to check the model fit and assumptions. The F-ratio gives an estimate of the statistical significance of the regression equation and the standard error of the estimate (SE) a measure of uncertainty of the predicted values of the model calibration. We used LOO cross-

validation (Michaelsen 1987) to validate the models against data that were not used in the calibration. This approach allowed us to use the full 37 years of corresponding streamflow and TR data for the validation procedure, which was important given the relatively short calibration interval. We calculated cross-validation statistics by comparing the predictand gauged summer streamflow data with the LOO-estimated values of the predictand. The reduction of error (RE; Fritts *et al.* 1990) provides a rigorous measure of model skill, with a positive value indicating that the LOO estimates better predict instrumental flow data than the mean of the instrumental data. The root mean squared error of cross-validation ($RMSE_{v)}$ gives a measure of the uncertainty of the predicted values over the verification period. The Pearson correlation (r) and R^2 of the observed and LOO-estimated values provide additional measures of accuracy (Cook and Karaiukstis 1990). The best model was calibrated over the full instrumental streamflow data record and used to reconstruct historical summer streamflow over the length of the shortest predictor dataset. We back-transformed the reconstructed values (modeled from TRs) to the original flow units for plotting and analysis, and checked that the selected model predictors are linearly correlated with the reconstructed flow data over the full instrumental data interval. To confirm that they operate as proxies for climate in our paleohydrological model we tested whether the model predictors are correlated with May 1 SWE and/or spring/summer maximum temperature. Correlations with temperature were calculated with Seascorr using the procedure described for hydroclimate correlations.

3.6.5 Analysis of the reconstruction

We compared statistical properties of the reconstructed record in the separate pre-instrumental (1520-1959) and instrumental (1960-1997) periods, with those of the gauged summer streamflow data. This comparison allowed us to determine if the pre-instrumental reconstructed record differs from reconstructed record during the instrumental era in any significant way, and also allowed us to assess the capacity of our model to approximate statistical characteristics of actual Tsable River summer streamflow. Extreme single-year droughts were defined based on a bottom fifth percentile threshold of summer streamflow, calculated based on the full reconstruction data period (1520-1997). Drought timing and magnitudes were then plotted as departures from the

reconstructed mean summer streamflow calculated from the instrumental period. Comparing reconstructed values in the pre-instrumental and instrumental periods puts extreme historical droughts in the context of recent conditions without making unequal comparisons between TR-modeled streamflow data and gauged streamflow data.

We calculated the return interval of extreme droughts in the reconstruction following the equation of Mays (2005) and used Chi-squared analysis to test if the frequency of these events in the gauged summer streamflow record (1960-2009) differed from an expected frequency of five events per 100 years (bottom fifth percentile). High year-to-year summer discharge variance is typical in hybrid watersheds and can make it difficult to identify multi-year stretches of generally low runoff, so we assessed the number of years of below median runoff over a sliding 21- year window. To determine whether reduced summer runoff corresponds with enhanced overall runoff variance, we visually compared extreme drought timing and intervals of generally low discharge with a sliding 21-year average of the standard deviations of the reconstructed summer streamflow values.

The gauged and reconstructed summer streamflow records were compared with instrumental ENSO and PDO records to investigate the influence of large-scale climate modes on droughts and wet episodes. A test of proportions (Newcombe 1998) was used to determine if the proportion of years with below-median (or above-median) runoff during El Niño years equals the proportion of years with below-median (or above-median) runoff during weak- and non-El Niño years. The strength of El Niño/La Niña in a given year was based on NOAA Multivariate ENSO Index ranks. The same difference-of-correlations test (Snedecor and Cochrane 1989) was used to determine if correlations of the winter PDO data with the gauged and reconstructed streamflow records are significantly different during cool versus warm PDO phases**.** Effective sample sizes (Dawdy and Matalas 1964) were used as needed to account for autocorrelation in the individual time series. A Morlet wavelet analysis (Torrence and Compo 1998) was performed on the full reconstructed record to highlight localized fluctuations of power over time that may be associated with climate modes.

3.7 Results

3.7.1 Tree-ring data

We developed eight site-level mountain hemlock chronologies and one site-level amabilis fir chronology for this study (Table 3.1). Four significantly intercorrelated (mean r=0.753, p<0.01) mountain hemlock chronologies were combined into a regional chronology representing northern Vancouver Island, and four significantly intercorrelated (mean r=0.841, p<0.01) mountain hemlock chronologies were combined into a regional chronology representing the central part of Vancouver Island. Consolidating short site-level chronologies enhanced chronology sample depths to the extent that the regional chronologies could be used for dendroclimatic reconstruction. Chronology lengths for the final chronologies ranged from 367 to 487 years and mean correlation coefficient among TR series (RBAR) ranged from r=0.26 to 0.31 (Table 3.1). All chronologies were significantly (p<0.01) correlated with the gauged summer streamflow data (r ranging from 0.466 to 0.867). The two regional chronologies and the Mount Cain amabilis fir chronology were retained as candidate model predictors.

3.7.2 Hydroclimate relationships

Of the monthly and seasonal climate data tested, the Tsable River gauged summer streamflow data are most strongly correlated with current-year May 1 SWE (Table 3.2), a positive relationship that is stable over the over the 1976/1977 PDO shift (Mantua 2002). This relationship is also significant (p<0.05) in the lower and upper, but not middle, terciles of the gauged data (lower tercile: n=17, r=0.529, upper tercile: n=17, r=0.552). The gauged data are also negatively correlated with maximum temperature in March through August of the current year (Table 3.2, Figure 3.3) and, independently, with winter precipitation but not summer precipitation (Figure 3.3). No relationships to climate in the previous year were significant. Panel B in Figure 3.3 indicates that temperature and precipitation data are significantly negatively correlated in prior July through current October and May through August.

Table 3.2: Hydroclimate correlations. Current year in capital letters. $p<0.01$

	Central Island mountain hemlock	Mt. Cain amabilis fir	SWE	Max T
Q (JA)	-0.75	-0.61	MAY 0.70	MAR-AUG -0.61
Central Island mountain hemlock	-	0.46	MAY -0.58	MAR-APR 0.41
Mt. Cain amabilis fir		-	MAY -0.53	Jul-Aug -0.36

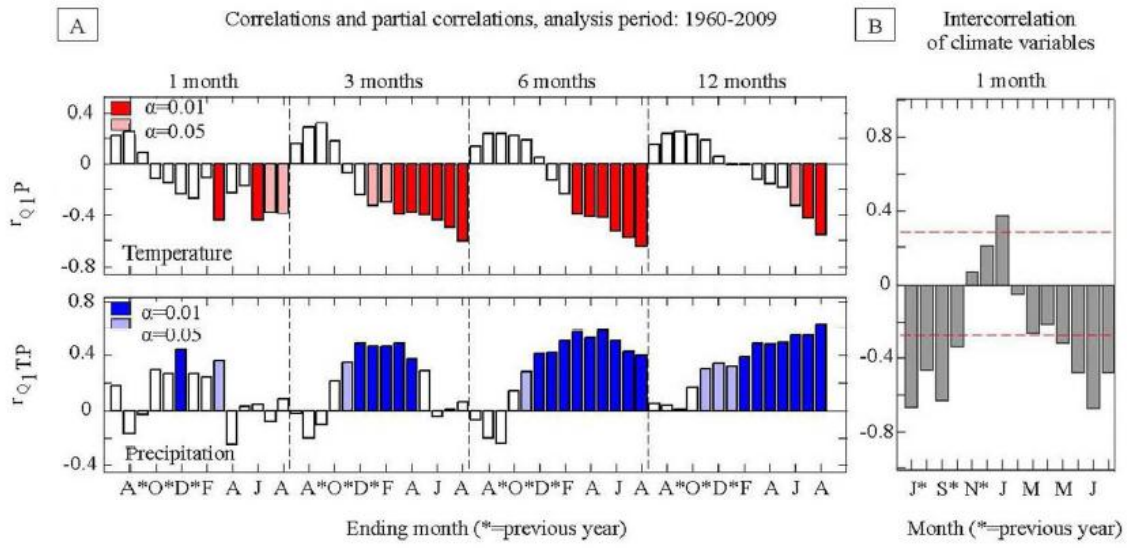

Figure 3.3: (A) Monthly and seasonal correlations between Tsable River July-August streamflow (Q) and maximum temperature, over 1-, 3-, 6-, and 12-month sliding windows beginning in the previous July through current August (top), and; monthly and seasonal partial correlations between Tsable River flows and precipitation, controlling for the influence of maximum temperature. (B) Monthly correlations between temperature and precipitation, beginning in the previous July through current August. Red-hatched bands represent 95% confidence intervals with the confidence interval set at 0+1.96/√N, where N is the sample size. All tests were calculated using Seascorr.

3.7.3 Model estimation and reconstruction

A reconstruction that used the central island regional chronology in time *t* and Mt. Cain amabilis fir chronology in time *t* was selected as the best model:

$$Q = 2.05 - (0.993*\text{Central Island TRs}) - (0.527*\text{Mt. Cain TRs}) \quad (2)$$

Time plots of the chronologies are presented in Figure 3.4. Despite similarities between the predictors, the standardized coefficients indicate that the amabilis fir chronology contributes significant additional explanatory power to the model (beta=-0.33) relative to the central island chronology (beta=-0.60). The reconstructed record spans 1520-1997 and explains 63% of the variance in the gauged Tsable River summer streamflow data (1960-2009) accounting for lost degrees of freedom. The reconstructed and the gauged streamflow data are compared in original streamflow units in Figure 3.5A. Regression and cross-validation statistics are summarized in Table 3.3 and a time plot of the cross validation is presented in Figure 3.5B. Collinearity diagnostics indicate that predictors are adequately independent and the F-ratio indicates a statistically significant regression equation. The positive RE value is very similar to the validation R^2, and the SE value approximates that of the $RMSE_v$, suggesting a well-validated model. The LOO-generated predicted values of the predictand are significantly and strongly (r=0.62, p<0.01) correlated with the gauged summer streamflow data. Analysis of regression residuals indicated that the models do not violate regression assumptions. The chronologies are significantly (p<0.01) correlated with the gauged summer streamflow data over the full period of that record (Figure 3.5C, Table 3.2).

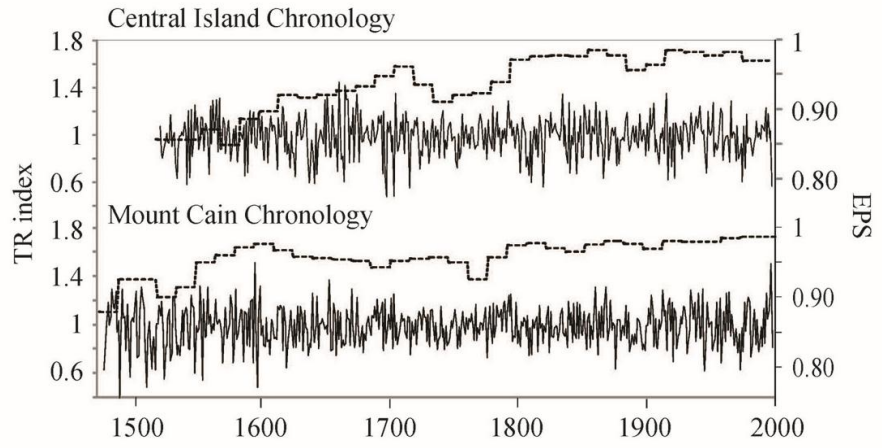

Figure 3.4: Time plot of TR chronologies used as model predictors. EPS values are plotted with a hatched line.

The central island regional chronology is most strongly negatively correlated with May 1 SWE, and is also weakly positively correlated with maximum temperature in

March through April (Table 3.2). The Mt. Cain amabilis fir chronology is most strongly negatively correlated with May 1 SWE, and also exhibits a weaker negative correlation with maximum temperature during July and August (Table 3.2; Figure 4).

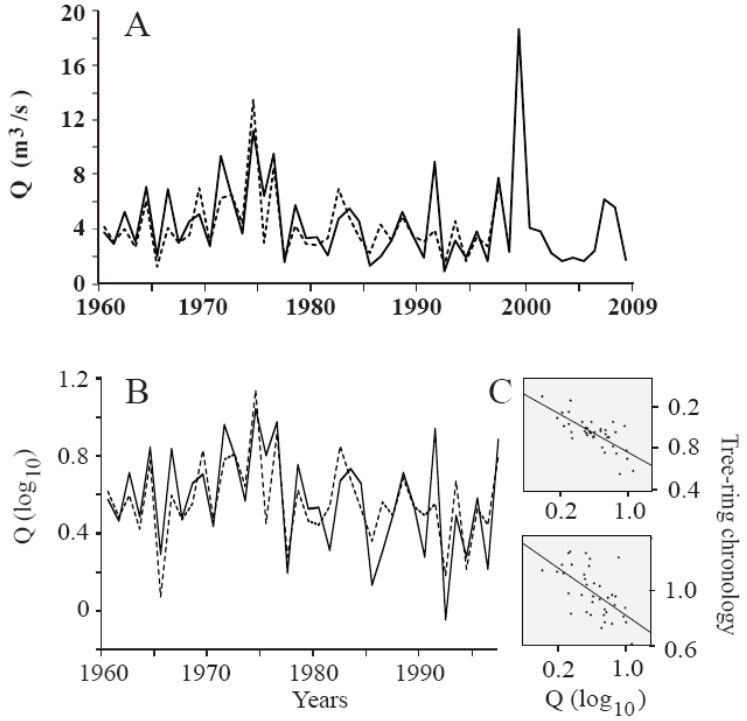

Figure 3.5: (A) Time plot of the reconstructed (hatched line) and gauged (solid line) summer streamflow data, backtransformed to original flow units, over the model calibration period. The instrumental data extend to 2009. (B) Time plot of the cross validation. The solid line represents the gauged (transformed) streamflow data and the hatched line represents the LOO estimates. (C) Scatterplots of the linear associations of the central island regional chronology (above: R^2=-0.565) and the Mount Cain chronology (below: R^2= -0.373) with the predictand streamflow data.

Table 3.3: Reconstruction and cross-validation statistics.

adj. R^2	D-W	VIF	SE	F-Ratio[a]	RE	$RMSE_v$[b]	r[c]	R^2[d]
0.63	2.08	1.27	0.16	32.86	0.62	0.16	0.79	0.62

[a]Significant at the 99% level
[b]Derived from transformed flow (unitless).
[c]Cross-validation r (p<0.01).
[d]Cross-validation R^2.

3.7.4 Analysis of the reconstruction

The cross-validation time plot exhibits strong coherence between the gauged summer streamflow data and the LOO-estimated values (Figure 3.5B). While the magnitudes of both high and low flows are over and underestimated at times (for example, the magnitudes of the three lowest flows are underestimated), the modeled data track the instrumental data well overall.

Generally, our reconstruction describes very high year-to-year variance typical of a small hybrid streamflow regime that shifts intermittently from more pluvial to more nival states, and where variance is not smoothed by hydrological lag over multiple years (Figure 3.6). Autocorrelation function plots indicate that neither the gauged or reconstructed summer streamflow data are significantly autocorrelated at lags <15 years. Generally symmetric high-to-low flow variance is punctuated by intervals of enhanced variance driven by high flows (Figure 3.6). While the mean summer streamflow values and standard variances are similar in the gauged and reconstructed records, the gauged minimum/maximum values are slightly lower/higher than the reconstructed values (Table 3.4). A scatterplot of the standardized residual values against the gauged summer streamflow data, as well as the width of the reconstruction confidence intervals (Figure 3.6) suggest that our model most accurately estimates summer streamflow values in low flow years and may underestimate them in high flow years.

The timing and magnitudes of bottom fifth percentile flow years ($Q<1.67$ m^3/s) are plotted in Figure 3.6. Twenty-two extreme droughts occurred prior to the instrumental record, with a 20 year return interval (Figure 3.6, Table 3.5). The most extreme droughts recorded occurred in 1651, 1660, and 1665, with an unusual cluster of seven drought years occurring between 1649 and 1667. Only once in the last 440 years have drought conditions persisted for three or more years (1665-1667). None of the reconstructed droughts was more severe than the worst instrumental drought in 1992, when summer streamflow was only 21% of the reconstructed instrumental period mean discharge (Table 3.5).

Gauged summer streamflow values also fell below the bottom fifth percentile threshold in five years (1977, 1985, 1992, 1996, and 2003) (Figure 3.6, Table 3.5). The Chi-squared analysis indicated that the frequency of extreme droughts in the gauged

record does not differ from the expected frequency (Chi-squared=4.69, p=0.10). We have reported the magnitudes of extreme instrumental droughts in terms of their departure from the reconstruction mean over the instrumental period which is a slightly unequal comparison since the instrumental period was omitted from the calculation of the bottom fifth percentile threshold.

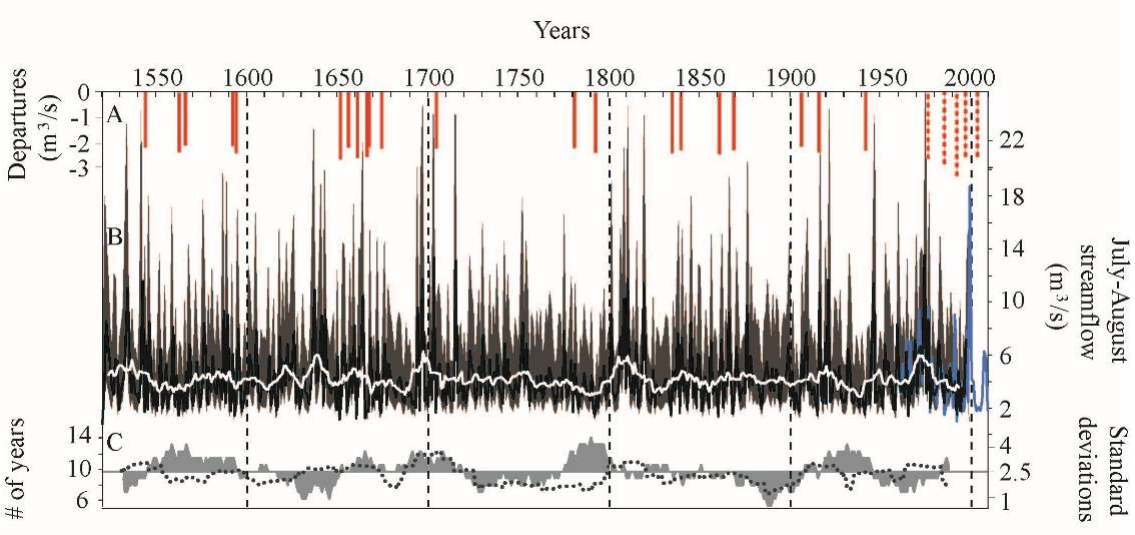

Figure 3.6: (A) Extreme droughts, plotted as departures from the reconstructed instrumental period mean. Reconstructed droughts are represented with red bars and gauged droughts with red hatched bars. The gauged drought magnitudes are calculated from a threshold derived from the reconstructed record. (B) Time plot of reconstructed Tsable River July-August streamflow (black line) with 5-year running mean (white line), gauged streamflow data (blue line), and 95% confidence intervals calculated from the RMSEv (Weisberg 1985; grey envelope). (C) Line graph of the number of years when July-August streamflow fell below the median value of the full-period reconstruction, plotted over a 21-year sliding window (grey fill) and a sliding 21-year average of the standard deviations of the reconstructed streamflow data (dotted line). For both the median departures and standard deviations, each plotted value represents the central value of the sliding window.

Table 3.4: Gauged and reconstructed streamflow statistics.

Streamflow data	min (m^3/s)	mean (m^3/s)	max (m^3/s)	cv[a]	r_1[b]
Gauged	0.9	4.4	18.6	0.53	-0.11
Reconstructed (instrumental period)	1.3	4.2	13.4	0.69	-0.12
Reconstructed (pre-instrumental period)	0.7	4.1	13.3	0.54	-0.11

[a]Coefficient of variation

[b]First-order autocorrelation coefficient. None significant (p<0.05) for lags 1-15.

Table 3.5: Pre-instrumental bottom fifth percentile low-flow timing and magnitudes (regular font), and gauged flows falling below the reconstructed bottom fifth percentile threshold (bold font). Presented in order of severity.

Year	Departure [a] (m^3/s)	Mean July-August flow (m^3/s)	% of reconstructed instrumental period mean Q
1992	**-3.33**	**0.91**	**21**
1651	-3.21	1.03	23
1660	-3.14	1.10	25
1665	-3.11	1.13	26
1860	-2.98	1.30	29
1593	-2.93	1.31	30
1792	-2.92	1.32	30
1834	-2.91	1.33	30
1915	-2.89	1.35	31
1985	**-2.86**	**1.38**	**31**
1562	-2.88	1.40	32
1941	-2.81	1.43	32
1868	-2.76	1.48	33
1839	-2.75	1.49	34
1704	-2.70	1.54	35
1674	-2.69	1.55	35
1780	-2.66	1.58	36
1543	-2.65	1.59	36
1655	-2.65	1.59	36
1977	**-2.65**	**1.59**	**36**
1666	-2.62	1.62	37
1667	-2.62	1.62	37
1905	-2.60	1.64	37
1565	-2.58	1.66	38
1591	-2.58	1.66	38
1996	**-2.58**	**1.66**	**38**
2003	**-2.58**	**1.66**	**38**

[a] Departure from the reconstructed instrumental period mean (4.24 m^3/s).

The number of years where reconstructed summer streamflow fell below the median value of the full-period reconstruction is plotted over a 21-year sliding window in Figure 3.6. Each value in Figure 3.6 represents the central value of the sliding window. The plot makes it possible to identify periods of time when summer streamflow was either high or low overall relative to the median, despite the very high year-to-year variance dominating the reconstruction. Periods of overall lower flows occurred from the mid-1560s to late 1500s, 1650-1720, 1770-1810, and 1905-1941. Visual comparison of these periods with intervals of higher year-to-year summer streamflow variance,

highlighted in Figure 3.6 by the sliding-mean standard deviations, does not suggest any relationship of generally higher/lower summer streamflow with higher overall variance.

Neither the gauged or reconstructed summer streamflow records exhibited differences in the number of below (above)-median flows during El Niño versus weak- and non-El Niño years (Table 3.6). Both records were significantly correlated with winter PDO over the full common data interval (r=-0.47 and r=-0.23 respectively, p<0.01), although the reconstructed record exhibited a weaker relationship. Relationships with winter PDO were stronger during the early/cool phase (1960-1976; r=-0.57 and r=-0.47 respectively, p<0.01) than the late/warm phase (1977-1997; r=-0.30 and r=-0.11 respectively, p<0.01), but the difference between correlations in these periods was not statistically significant for either record. The wavelet power spectrum identifies repeating, but not necessarily regular, fluctuations (energy) in the time series over time (Torrence and Compo 1998). The reconstructed streamflow data (Figure 3.7) exhibits significant (p<0.01) energy in the approximately 2, 4, and 8-year bands that is intermittent over time, and energy in the approximately 15-30 year band that is more persistent over time, including throughout the mid- 1600s, 1800-1850, and 1960-1980.

Table 3.6: Test of proportions determining associations of instrumental and reconstructed flow data to El Niño events, calculated over the period 1960-1997. Calculated using function *prop.test* in R. Proportions of years in each streamflow category noted in parentheses. The null hypothesis that both groups have the same true proportions was true for all tests, with p values ranging around 0.32 (average).

Streamflow category	# El Niño years	# non-El Niño years	# El Niño and non-El Niño years
Instrumental flow data			
Below median	9 (40.9%)	10 (62.5%)	19 (50%)
Above median	13 (59.1%)	6 (37.5%)	19 (50%)
Total	22 (100%)	16 (100%)	38 (100%)
Reconstructed flow data			
Below median	8 (36.4%)	11 (68.7%)	19 (50%)
Above median	14 (63.6%)	5 (31.3%)	19 (50%)
Total	22 (100%)	16 (100%)	38 (100%)

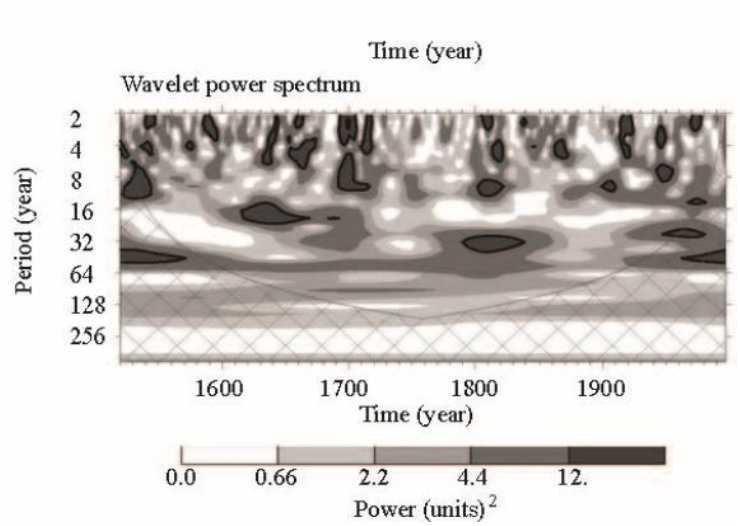

Figure 3.7: Morlet wavelet power spectrum on the full reconstructed streamflow record. The black contours represent the 95% confidence level based on a white-noise background spectrum. The hatched area represents areas of the spectrum susceptible to the effects of zero padding (Torrence and Compo 1998).

3.8 Discussion

3.8.1 Reconstruction model

Our reconstruction effectively estimates July-August streamflow in Tsable River based on two TR-derived proxy records sensitive to regional-scale SWE variability. Correlation analyses indicate that runoff during this season is driven principally by snowmelt, and that the selected TR predictors primarily operate as proxies for that streamflow component in our paleohydrological model. The sensitivity of gauged summer streamflow data to previous winter SWE and spring/summer maximum temperatures supports the interpretation that Tsable River is characterized by a hybrid hydrological regime. Tercile correlations confirm that low streamflow values, not just high streamflow values, are influenced by snowmelt. The gauged streamflow record is also influenced by summer temperature fluctuations which can impact runoff due to the large relative influence of evaporation on small basins (Margolis *et al.* 2011). Some temperature-related variability may be incorporated into the reconstruction since the two predictor TR chronologies are influenced by temperature in the spring and summer, respectively. The model residuals are correlated with maximum temperature during March (-0.42, $p<0.01$) but not during summer months, suggesting summer temperature

related variability from the Mount Cain TR chronology may influence the model estimates. The negative relationship between TRs and summer temperature means that summer temperature information within the TR chronology serves to weaken the relationship between TRs and streamflow, which may reduce model accuracy (although the TR-temperature relationship is notably weak; r=-0.36, p<0.01). Finally, the instrumental streamflow data are influenced by winter rainfall persisting in the groundwater system, and summer rainfall. Neither of these flow components is captured by our model but, because they contribute little to summer runoff, it is not likely this seriously reduces the accuracy of the reconstruction. A possible limitation of our reconstruction is that cross-validation statistics can be biased upward when the cross-validation period is short (Meko 2006), although the cross-validation time plot indicates a strong model validation.

Our reconstruction is primarily 'tuned' to SWE-driven runoff variations. However, we found that the gauged summer streamflow data are also influenced by spring/summer maximum temperature. The inability of our model to fully capture temperature-driven summer streamflow variability likely contributes to general underestimation of the severity of the lowest gauged flows (3/4 lowest instrumental flow values are underestimated), although low flows are still more precisely estimated than high flows. The incorporation of a summer temperature-sensitive proxy in a similar model may improve the accuracy of low-flow magnitude estimations and, given the non-independence of temperature and precipitation fluctuations during summer, might also enable a model to account for some portion of variability in summer precipitation.

As is typical in TR-based regression, our model does not capture the full range of instrumental streamflow variance (Table 3.4; Cook and Kairiūkštis 1990). We emphasize that as a result, the reconstruction likely underestimates the severity of historical lowest summer flows. For example, although the model residuals suggest low flows are generally more accurately estimated than high flows, the magnitudes of the three worst instrumental droughts are all underestimated in the cross-validated and reconstructed data (Figure 3.5A, 3.5B). We have also reconstructed mean, not minimum, July-August streamflow values; actual lowest streamflow values would be lower than those estimated by our model.

3.8.2 Extreme droughts

Twenty-two extreme droughts occurred over the 439-year pre-instrumental record. As a modern analogue, the low-flow magnitudes in all but one of these years were more severe than the gauged values in 2003 and 2009 when severe summer drought throughout southern and coastal B.C. seriously impacted community, irrigation, and hydroelectric water supplies in unglaciated catchments (B.C. Ministry of Environment 2010; Puska *et al.* 2011). Our reconstruction suggests that droughts of the severity of those in 2003 and 2009 are not anomalous relative to the last several hundred years and should be accounted for in water management strategies (in fact, 2009 was not flagged as an extreme drought year based on the long-term threshold). Further, worst-case scenario natural droughts based on hydrometric data records are likely underestimated since more severe events occurred outside the hydrometric data period. It is possible that extreme natural low flows, paired with pressures from land-use and climate change, could result in a drought that is more severe than any since 1520. It is important to consider that very low flows in unglaciated Vancouver Island streams since 2009, especially in 2014 and 2015 (B.C. Ministry of Forests, Lands and Natural Resource Operations 2014; B.C. River Forecast Centre 2015), may well have surpassed the severity of gauged droughts analyzed for this study but could not be accounted for due to unavailable hydrometric data. The instrumental drought in 1992 may be more extreme than any in the reconstructed record, but this should be interpreted conservatively since the reconstructed streamflow variance is somewhat suppressed relative to the gauged record; actual magnitudes of pre-instrumental low flows may be as or more extreme than in 1992.

Our results suggest that relative to the preceding 440 years, the magnitudes of extreme droughts in Tsable River did not generally worsen from 1960 to 2009. Frequencies of lowest flow events also did not increase. A large outlier (high-flow year) in 1999 obscures a significant long-term negative trend in the gauged data (tested using a *t*-test of the slope of a regression of the instrumental flow data on time with 1999 removed) indicating that, with the exception of one year, Tsable River summer runoff has declined overall between 1960-2009. Analysis of SWE and precipitation data shows the outlier is related to very high snowfall (July-August precipitation was equal to the long-term 1960-2009 average in that year, while SWE was 217% of the average). This trend is

not exceptional compared to the rest of the reconstruction, which suggests long-term streamflow declines of similar length and magnitude began around 1640, 1700, and 1800. Without data for the most extreme recent drought years, it is not possible to assess the unusualness of recent streamflow trends relative to the last few centuries.

Our findings highlight that consecutive years of very low flows have been extremely rare in the Tsable River system, which is consistent with minimal multi-year hydrological lag in small coastal watersheds and is an important hydrological feature for water management. Because the likelihood of extreme droughts is largely unrelated to conditions in the previous year, these events are highly unpredictable compared with large basins where persistent, multi-year drought is typical (Meko and Woodhouse 2011). From a model-development standpoint, mimicking the zero-autocorrelation structure of the gauged summer streamflow data was critical for developing an accurate reconstruction. The dendrohydrological approach risked introducing "artificial" persistence related to biological tree growth into our model, but use of residual chronologies guarded against this.

We found no evidence that the timing of below- or above- median streamflow in Tsable River corresponds with El Niño or weak- and non-El Niño years, in either the instrumental or reconstructed flow data. We evaluated El Niño years because they are typically associated with the low flows of interest to this study and which are most accurately estimated by our model. We did not evaluate associations with La Niña events that are typically more strongly associated with annual streamflow in hybrid watersheds, and correspond with enhanced winter precipitation and total runoff (Fleming *et al.* 2007). In contrast, both the reconstructed and gauged streamflow records are influenced by winter PDO during the common data interval, with the strongest (negative) relationships occurring during the cool phase of the oscillation. This suggests an influence of SWE on summer low flows, consistent with cool PDO phases promoting more snow and higher snowmelt-derived runoff than warm phases (Fleming *et al.* 2007). That the difference in correlations between the warm and cool phases was not statistically significant may have been due to small effective sample sizes (17 and 21 years). Intermittent ENSO-like power in the reconstructed record is evident in the approximately 2, 4, and 8-year bands of the wavelet power spectrum (Figure 3.7). PDO-like multidecadal power weakens between

1850 and 1910, as documented in other independent reconstructions of that oscillation (Gedalof and Smith 2001b, MacDonald and Case 2005).

Comparison with historical temperature, precipitation, and drought records is made difficult by a lack of relevant high-resolution records in Pacific Canada and the northwestern United States. The most pertinent records, which represent seasonal and/or spatial contexts distinct from those of this study, unsurprisingly yielded no notable similarities to historical Tsable River streamflow variability (Graumlich and Brubaker 1986; Larocque and Smith 2005; Luckman and Wilson 2005; Jarrett 2008; Wiles *et al.*, 2014). Neither does our reconstruction correspond with the few (non-hybrid) streamflow reconstructions developed in B.C. (Gedalof *et al.* 2004, Hart *et al.* 2010, Starheim *et al.* 2013), similar records from Canada's western interior (Case and MacDonald 2003; Axelson *et al.* 2009), or large-scale historical drought episodes such as the 1929-1940 Dust Dowl, the 1946-1956 drought in the southwestern United States (Fye *et al.* 2003), or the 16th century megadrought (Stahle *et al.* 2000). In the instrumental period, recent large-scale droughts in the Canadian Prairie provinces (e.g. 2002; 1999-2005; Canadian Foundation for Climate and Atmospheric Sciences 2010) are not expressed in the Tsable River gauged record, reinforcing the distinct hydroclimatological character of B.C.'s small coastal basins relative to surrounding regions.

3.9 Conclusion

Long-term perspectives on hydroclimate variability are critical for water management, with small temperate watersheds representing a frontier for paleohydrological modeling (Biondi and Strachan 2012). We demonstrate that a dendrohydrological approach focused on the SWE-driven streamflow component is appropriate for determining drought-season runoff in small hybrid watersheds in coastal B.C. Tree-ring records that are energy-limited by spring snowmelt timing were effective proxies for this streamflow component. Our reconstruction of Tsable River suggests that the severity of droughts in the 440 years preceding the instrumental record exceeded modern analogues such as the 2003 and 2009 droughts. The fact that recent 'extreme' events fall within a natural range of multi-century variability means that rather than being considered anomalies, extreme droughts should be expected and incorporated into

drought management strategies. Most importantly, our findings suggest that worst-case scenario natural drought estimates based on hydrometric data are likely underestimated. Given projected climate trends and pressures from land-use change and increasing human demand for water in the study area, exacerbation of natural droughts can be reasonably anticipated in hybrid basins in coming decades, potentially resulting in low flows that exceed any since 1520.

There has been a significant decline in Tsable River summer runoff from 1960-2009 with the exception of one year. The frequency of extreme droughts did not increase between 1960 and 2009, but we could not account for severe events after 2009 — including the major droughts that occurred in 2014 and 2015 — due to a lack of hydrometric data. Both the gauged and reconstructed streamflow records experienced significantly greater runoff during cool phases of the PDO, which favour deep snowpacks. There was no measurable influence of El Niño on the timing of below-median flows but ENSO-type variability is apparent in the wavelet analysis. This variability may be related to the influence of La Niña on high flows in hybrid systems in the study area. While our reconstruction is primarily 'tuned' to SWE-related flow variability, a model that could account for the influence of spring/summer temperature on summer streamflow may improve drought magnitude estimates.

Chapter 4 Is worst-case scenario streamflow drought underestimated in British Columbia? A multi-century perspective for the south coast, derived from tree-rings.

4.1 Article information

Chapter 4 consists of a manuscript accepted for publication in Journal of Hydrology (December 2015). The text and figures are taken directly from the published paper but have been renumbered and reformatted for consistency within this thesis. Citation style has also been reformatted for consistency.

4.1.1 Authors' names and affiliations

B. L. Coulthard[1]*, D. J. Smith[2], D. M. Meko[3]

[1] B. L. Coulthard, University of Victoria Tree-Ring Laboratory, Department of Geography, University of Victoria, PO Box 3060 STN CSC, Victoria, British Columbia, Canada, V8W 3R4

[2] D. J. Smith, University of Victoria Tree-Ring Laboratory, Department of Geography, University of Victoria, PO Box 3060 STN CSC, Victoria, British Columbia, Canada, V8W 3R4

*Corresponding author Email: coulthard.bethany@gmail.com, Telephone: +12504724733

4.1.2 Author's and coauthors' contributions

Coulthard developed the study and hypothesis, conducted fieldwork, laboratory work, and statistical testing, wrote the manuscript, and produced all of the tables and figures. Smith provided tree-ring samples and measurement data archived at the University of Victoria Tree-Ring Laboratory. Meko provided assistance with statistical analysis. Both Smith and Meko reviewed and edited the manuscript.

4.2 Abstract

Recent streamflow droughts in south coastal British Columbia have had major socioeconomic and ecological impacts. Increasing drought severity under projected climate change poses serious water management challenges, particularly in the small

coastal watersheds that serve as primary water sources for most communities in the region. A 332-year dendrohydrological record of regionalized mean summer streamflow for four watersheds is analyzed to place recent drought magnitudes in a long-term perspective. We present a novel approach for optimizing tree-ring based reconstructions in small watersheds in temperate environments, combining winter snow depth and summer drought sensitive proxies as model predictors. The reconstruction model, estimated by regression of observed flows on *Tsuga mertensiana* ring-width variables and a tree-ring derived paleorecord of the Palmer Drought Severity Index, explains 64% of the regionalized streamflow variance. The model is particularly accurate at estimating lowest flow events, and provides the strongest annually resolved paleohydrological record in British Columbia. The extended record suggests that since 1658 sixteen natural droughts have occurred that were more extreme than any within the instrumental period. Flow-duration curves show more severe worst-case scenario droughts and a higher probability of those droughts in the long-term reconstruction than in the hydrometric data. Such curves also highlight the value of dendrohydrology for probabilistic drought assessment. Consequently, current water management strategies based on worst-case scenarios from historical gauge data likely underestimate the potential magnitudes of natural droughts. If the low-flow magnitudes anticipated under climate change co-occur with lowest possible natural flows, streamflow drought severities in small watersheds in south coastal British Columbia could exceed any of those experienced in the past ~350 years.

4.3 Introduction

In 2014 and 2015 many British Columbia (B.C.) watersheds experienced streamflow droughts that were likely the most severe since streamflow monitoring began in the mid-20th century. Record-breaking low snowpacks and historic high summer temperatures took a particular toll on south coastal basins (Agriculture and Agri-Food Canada 2014; B.C. River Forecast Centre 2015). Despite very wet winters, these small watersheds can experience streamflow drought during late summer when snow has melted and weather is warm and dry.

Though they have relatively low storage capacity, small coastal watersheds serve as the primary water source for most communities in south coastal B.C. Many of the streams and rivers in these catchments are also used for hydroelectric power generation, support industry and agriculture, and are critical to the survival of local Pacific Salmon populations. Drought presents a major water management challenge, especially where there is high uncertainty around potential low flow severities (Lill 2002; Mishra and Coulibaly 2009; B.C. Ministry of Environment 2013).

In western Canada, few hydrometric records extend beyond the 1970s. These short instrumental records translate to less accurate estimates of potential low flow severities in a river, and less sound water management strategies (Rodenhuis *et al.* 2007). Short hydrometric records also make it difficult to determine if recent droughts are extreme relative to those that occurred in the past. Longer term proxy records of streamflow variability can be estimated from climate-sensitive TR records by capitalizing upon the influence of climate on both annual radial growth and seasonal runoff (Loaiciga *et al.* 1993). Dendrohydrological reconstructions can contextualize hydrological changes and inform on connections between modes of regional climatic variability and runoff that are not captured in the instrumental record (e.g. Earle 1993). The TR-based approach is particularly valuable since trees are often distributed over a large hydrological 'sample landscape' and, unlike many other paleoenvironmental proxies (*e.g.* lake cores, ice cores), information derived from them is annually to sub-annually resolved.

Dendrohydrological modeling has largely been accomplished in dry continental settings, where annual radial tree growth is limited by available soil moisture derived from the same rain and snow meltwater that supports streamflow (Meko and Woodhouse

2011). The approach is typically applied in large watersheds where errors related to evaporation and 'flashy' rainfall do not contribute to model error (Margolis *et al.* 2011). Long-term perspectives on hydrological phenomena such as low-flows, drought, and long-term runoff declines, have been incorporated into multi-scale and multi-agency watershed management strategies in the southwestern United States (Meko *et al.* 2001; Woodhouse and Lukas 2006), western interior Canada (Sauchyn *et al.* 2014), and internationally (Gou *et al.* 2010; Norton and Palmer 1992; Pederson *et al.* 2001).

Small, temperate watersheds represent a frontier in dendrohydrology due to small basin concentration times, flashy runoff, and an absence of moisture-sensitive tree species (Biondi and Strachan 2012). In coastal B.C. the approach is hindered further by complex hydroclimatology resulting from mountainous terrain and streamflow contributions from rainfall-runoff, snowmelt-runoff and glacier icemelt runoff. This heterogeneity can lead to differences in seasonal streamflow behaviour even in spatially adjacent watersheds (Eaton and Moore 2010). Previous efforts to establish dendrohydrological records in B.C. have focused on snow- and glacier-melt dominated runoff regimes in continental settings, using moisture-limited TRs (Gedalof *et al.* 2004; Watson and Luckman 2005; Hart *et al.* 2010; Starheim *et al.* 2013).

In this paper we develop a novel approach for dendrohydrological modeling in small, temperate watersheds in coastal B.C. Despite a lack of moisture-limited trees in this area, the radial growth of some high-elevation conifers is sensitive to annual maximum snow depth as a result of its influence on the length of the growing (energy) season (Peterson and Peterson 1994). This type of TR data has rarely been used for dendrohydrology. We combine TR width records from a snow depth-sensitive tree species (Mountain hemlock; *Tsuga mertensiana* (Bong.) Carrière; Smith and Laroque 1998; Gedalof and Smith 2001*a*; Peterson and Peterson 2001; Marcinkowski *et al.* 2015) with a paleoenvironmental record of seasonal drought as predictors in a dendrohydrological model. Our reconstruction targets regionalized summer streamflow in small, hybrid (rain- and snowmelt-driven) watersheds, where summer runoff is driven by a combination of snow meltwater from the previous winter, and summer air temperature and summer precipitation variations. We hypothesized that TR variability and summer discharge in these watersheds are determined by regional-scale climate fluctuations to the

extent that TR records can be used as proxies for climate in a model of historical streamflow. We apply the reconstruction to place droughts in long-term perspective, and relate streamflow anomalies to El Niño Southern Oscillation (ENSO; Holton *et al.* 1989) events and variations in the Pacific Decadal Oscillation (PDO; Mantua 2002). Our approach presents an opportunity to develop paleohydrological records for watersheds both smaller in scale and of a different hydrological regime type than those typically conducive to dendrohydrology.

4.4 Hydroclimatic Setting

The regional hydroclimatology of south coastal B.C. is affected by interannual and decadal climate variability driven by ocean-atmosphere interactions in the Pacific Basin, including synoptic-scale modes described by the PDO and ENSO, and to a lesser extent by the PNA pattern (Kiffney *et al.* 2002). Winter storms originating in the North Pacific Ocean deliver moisture to the B.C. coast where it is orographically released upon encountering the Vancouver Island Insular and Coast Mountain ranges, resulting in large quantities of snow and rain. Persistent high-pressure systems typically bring stable warm and dry conditions during the summer months (Stahl *et al.* 2006).

Atmospheric warming and changing rainfall, snowpack and snowmelt dynamics increasingly moderate these hydroclimate patterns (Barnett *et al.* 2004; Bonfils *et al.* 2008). Characteristically mild and wet winters have become milder and wetter over the past 100 years, while summers have become warmer and drier (Pike *et al.* 2010). Coast and Coast Mountain areas experienced a 1.4°C rise in mean winter temperature from 1895 to 1995 and winter precipitation (rain and snow) totals are expected to increase by 6% by 2050 (December-February; B.C. Ministry of Water, Land and Air Protection 2002; Pike *et al.* 2010). Milder winters and a larger proportion of cool-season precipitation falling as rain have caused widespread snowpack declines; snow water equivalent (SWE) totals diminished by 6% per decade from 1953 to 2000 (B.C. Ministry of Water, Land and Air Protection 2002; Rodenhuis *et al.* 2007).

Regional climate trends have altered the seasonal timing and magnitude of peak and low flows, and these changes are expected to intensify in all streamflow regime types (Stewart *et al.* 2005; Schnorbus *et al.* 2014). However, hybrid streams are probably most

susceptible to earlier, lower, longer, and more frequent low flows over the short term since they are strongly influenced by both warmer and drier summers, and shifting snowpack depth and snowmelt dynamics (Whitfield and Cannon 2000; Loukas *et al.* 2002; Déry *et al.* 2009; Eaton and Moore 2010). Our use of the term "drought" refers to streamflow drought, a sustained period of below-average stream discharge (Van Loon and Laaha 2015). Given the low storage capacity of the study catchments, and in keeping with B.C. government environmental management practices, below-average runoff over a period of >1 month is considered streamflow drought (B.C. Ministry of Environment 2013; Van Lanen *et al.* 2013).

4.4.1 Hybrid streams

Hybrid hydrological regimes predominate in south coastal B.C. and are typically found in mid- to low elevation coastal and near-coastal areas. Runoff in these streams is generally highest during winter (November, December, January) as a result of heavy rainfall. A secondary peak occurs in spring (April or May) as a result of snowmelt. Lowest flows occur during summer when inputs from snowmelt are exhausted and regional warm and dry high-pressure systems persist (Eaton and Moore 2010). Snowmelt can significantly recharge deep flow paths and contribute to summer baseflow, even where a basin contains only a small snow-fed headwater (Wade *et al.* 2001; Beaulieu *et al.* 2012). The quantity of discharge in the low-flow season is, therefore, determined by a combination of previous winter snowpack and snowmelt dynamics, summer season precipitation, and summer air temperature.

The proportion of snowmelt- and rainfall-derived runoff in hybrid streams varies year to year, so that the annual runoff pattern may fluctuate from a 'more rainfall-dominated' regime to a 'more snowmelt-dominated' regime (Moore *et al.* 2007). A high between-year range in flows from month to month is typical (Moore *et al.* 2007). While winter runoff is flashy in hybrid streams, summer flows are relatively due to few rainfall events. This makes them favourable for TR-based reconstruction since high-magnitude rains are not typically registered by annual tree growth increments (Meko and Woodhouse 2011). Summer streamflow in hybrid regimes usually increases during cool/wet La Niñas paired with negative phases of the PDO, while warm/dry El Niño

years and positive phases of the PDO usually coincide with a deepening of the Aleutian low, strengthening of the Pacific North America pattern, and reduced winter precipitation and summer runoff (Hamlet and Lettenmaier 1999; Fleming *et al.* 2007; Bonsal and Shabbar 2008). Cool PDO phases exert a strong influence on spring snowmelt dynamics, typically resulting in a later freshet, an increased persistence of meltwater into summer, and generally enhanced summer runoff (Pike and Spittlehouse 2008).

The climatic drivers of drought in hybrid streams are twofold: 1) less persistence of cool-season moisture into summer as a result of less snowfall, more rain-on-snow events, and earlier spring snowmelt; and, 2) an extension and intensification of the warm dry period between spring and fall rains (Eaton and Moore 2010). Annual minimum streamflow has decreased in these regimes over the last three decades especially during El Niño years, and low-flow magnitudes are projected to decline by up to 50% by the end of the century (Rodenhuis *et al.* 2007; Mantua *et al.* 2010). Profound impacts to stream ecosystem health, Pacific salmon habitat and survivorship (Young and Werring 2006; Nelitz *et al.* 2007) and human water use (Kay and Blecic 1996; Kiffney *et al.* 2002; Mote *et al.* 2003; Barnett *et al.* 2004; Nelitz *et al.* 2007; Mantua *et al.* 2010) are documented.

4.5 Study Area

The study area encompasses Vancouver Island and the southwestern slopes of the Pacific Ranges within the B.C. Coast Mountain and islands physiographic region (Valentine *et al.* 1978). High elevation areas experience short cool summers and long, cool and wet winters typical of a maritime montane climate. Pacific weather systems may deliver greater than 5000 mm of annual precipitation the majority of which falls as snow above 1000 m asl during winter (Pojar *et al.* 1991). Warm and dry high-pressure systems persist during summer (Valentine *et al.* 1978).

4.5.1 Study basins

Following the hydrological classification of Eaton and Moore (2010), we chose four streams susceptible to climate-induced low-flows to represent typical small, coastal hybrid flow regimes (Figure 4.1). Stream classification was based on analysis of the stream hydrographs (Figure 4.2), median and maximum basin elevation and mean annual discharge values (Table 4.1). We avoided watersheds characterized by major historical

land-use and vegetation change, and those containing natural storage features. Each basin exhibits unprecedented recent (Chemainus River: Craig 2004; Kanaka Creek Regional Park Management Plan 2004; Tsable River: Coulthard and Smith 2015) or predicted (Zeballos River: Déry *et al.* 2009) summer streamflow drought. Five species of wild Pacific salmon use the rivers for spawning and rearing and have been negatively affected by reduced summer flows (Gaboury and McCulloch 2002; Craig 2004; Poulin 2005; B.C. Conservation Foundation 2006).

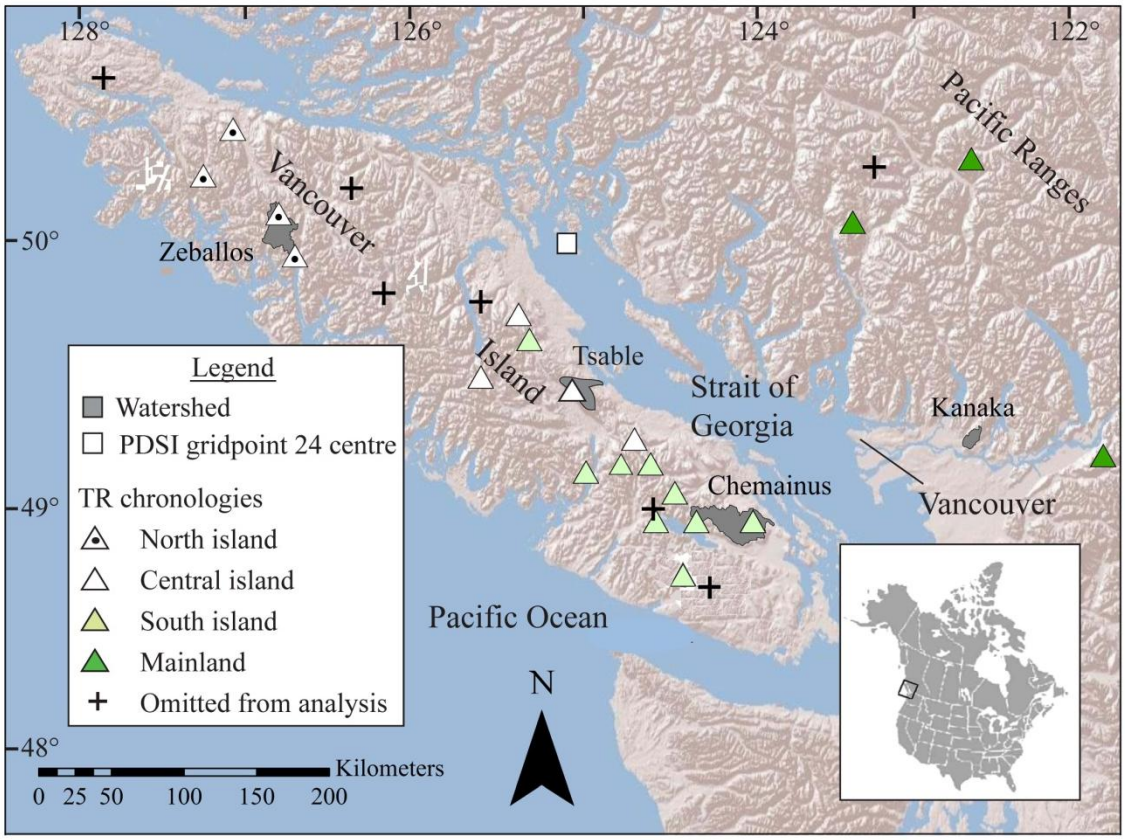

Figure 4.1: Map of the study area. Different symbols for TR site chronologies mark members of the four regionalized TR chronologies.

Kanaka Creek is located northeast of the city of Vancouver on the B.C. mainland, where it drains a small area of the Garibaldi Ranges on the northern margin of the Fraser Valley to the Fraser River and Strait of Georgia, (Figure 4.1; Table 4.1). The lowermost reaches of the basin are heavily urbanized. The Chemainus River watershed is located on

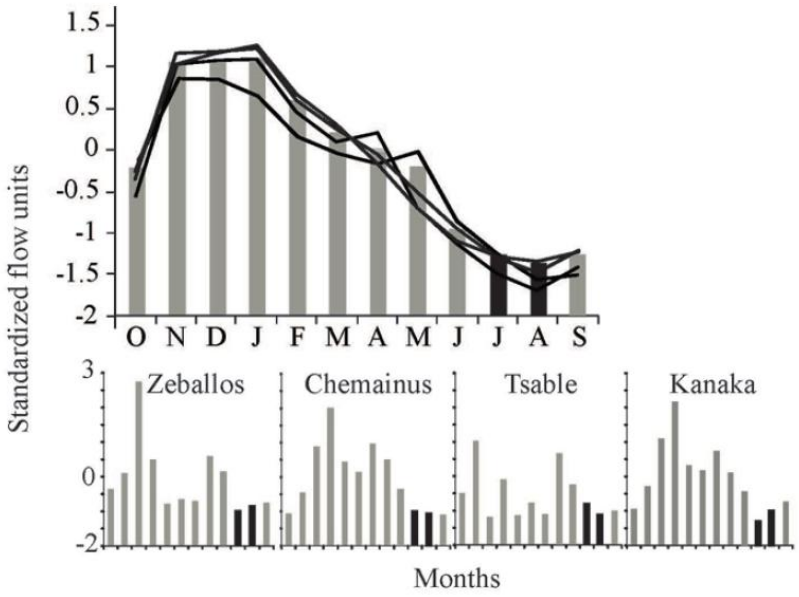

Figure 4.2: Above: Annual water-year hydrographs of gauged mean monthly discharge over the length of record used (Table 4.2) for each study basin, in standardized flow units (black lines). Grey bars represent standardized mean monthly discharge averaged across all basins, with the reconstruction highlighted with black bars. Below: Annual water-year hydrographs of the study streams in years with a strong springtime snowmelt-derived discharge component. The timing of this nival pulse is earlier (April) in the "more pluvial" Chemainus watershed, a lower-elevation basin where temperatures rise above zero and snowmelt occurs earlier in the season.

Table 4.1: Study basin information.

River	Station ID	Lat/ Long	Gross drainage area (km^2)	Mean annual Q[a] (m^3/s)	Median/maximum basin elevation (m asl)
Kanaka	08MH076	49.20 -122.53	48	2.7	230 / 1050
Chemainus	08HA001	48.87 -123.70	355	18.9	625 / 1539
Tsable	08HB024	49.517 -124.84	113	7.8	710 / 1500
Zeballos	08HE006	50.01 -126.84	178	25.9	740 / 1800

[a] Calculated over the length of record used (1960-1997).

the east coast of Vancouver Island where it drains high-elevation areas surrounding Mts Brenton and Whymper (Figure 4.1; Table 4.1). A band of urban development occupies a small portion of the watershed at the town of Chemainus, where the river flows eastward into the Strait of Georgia. The Tsable River watershed drains the northeastern portion of

Beaufort Range on central Vancouver Island, and contains several small lakes including Tsable Lake (~1 km^2) (Figure 4.1; Table 4.1). Both Chemainus and Tsable rivers experience relatively low mean annual discharge relative to basin size as they are located in the rain shadow of the Vancouver Island Ranges (Moore *et al.* 2007). Zeballos River is located on the northwest coast of Vancouver Island where it drains the steep western slopes of the Haihte Range to Zeballos Inlet and the Pacific Ocean (Figure 4.1; Table 4.1). The Zeballos watershed contains a small lake and run-of-river hydroelectric project.

Lowest mean monthly discharge in the four watersheds occurs in June and August (Figure 4.2). Winter precipitation falls predominantly as rain in the lower portions of the catchments, and as snow above 1000 m asl (Eaton and Moore 2010). Snow remains in storage until the onset of spring melt, often persisting well into summer at high elevations (Pojar *et al.* 1991). Industrial logging has occurred throughout all of the watersheds, and remains the dominant human land use in the three Vancouver Island basins.

4.5.2 Forest stands

The mountain hemlock trees sampled for this study were located between 900-1500 m asl within the Mountain Hemlock biogeoclimatic zone (Table 4.2; Klinka *et al.* 1991). At this elevation the annual radial growth of mountain hemlock is typically limited by growing season length, which is in turn controlled by snow depth and meltout timing (Gedalof and Smith 2001*a*; Peterson and Peterson 2001; Marcinkowski *et al.* 2015). Seventy percent of annual precipitation falls as snow and deep late-lying snowpacks maintain near-freezing soil temperatures that impede growth often as late as the end of July (Pojar 1991; Peterson and Peterson 2001). At lower elevations where snow melts earlier mountain hemlock trees may also be sensitive to summer temperature fluctuations, in either the year of or the year prior to growth (Marcinkowski *et al.* 2015). Climatic growth limitations may be periodically disturbed by fungal pests (e.g. *Heterobasidion annosum*) or hemlock dwarf mistletoe (*Arceuthobium tsugense*) (Means 1990).

Table 4.2: Tree-ring chronology information. Regional chronologies in italic font.

Chronology name	Inter-series r[a]	Latitude, longitude	Length (yrs)[b]	Trees, series (#)	Mean r_1[c]
		North Island Regional Chronology			
Bulldog Ridge[d]	0.53	50°17', -127°14'	1845-1997	6, 9	0.72
Castle Mtn.[d]	0.45	50°28', -127°03'	1845-1997	7, 10	0.75
Colonial Creek[d]	0.43	50°17', -127°33'	1940-1997	5, 7	0.76
Silver Spoon[d]	0.48	49°58', -126°40'	1955-1996	8, 11	0.66
N. Isl. Regional[d]	*0.51*		*1630-1997*	*37, 28*	*0.72*
		Central Island Regional Chronology			
Mt. Washington[d]	0.63	49°29', -125°17'	1795-1996	12, 15	0.68
Mt. Apps[d]	0.54	49°26', -124°57'	1795-1996	22, 40	0.63
Cream Lake[d]	0.61	49°29', -125°31'	1525-1995	18, 29	0.68
Mt. Arrowsmith[d]	0.63	49°14', -124°34'	1575-1997	8, 11	0.72
C. Isl. Regional[d]	*0.58*		*1510-1997*	*61, 95*	*0.68*
		South Island Regional Chronology			
Mt. Franklyn	0.50	48°54', -124°11'	1880-1996	16, 28	0.79
Mt. Becher	0.55	49°64', -125°22'	1668-1997	18, 32	0.76
Mt. Brenton	0.48	48°54', -123°50'	1726-1996	11, 17	0.77
Pirate Peak	0.54	49°06', -124°52'	1810-1997	20, 33	0.72
Gemini Mtn.	0.56	49°01', -124°19'	1850-1996	17, 26	0.64
Mt. Moriarity	0.61	49°08', -124°28'	1738-1996	20, 36	0.73
Douglas Peak	0.58	49°26', -124°57'	1750-1996	20, 37	0.82
Wapiti Ridge	0.62	48°54', -124°26'	1784-1996	21, 38	0.75
TAD Ridge	0.50	48°41', -124°16'	1720-1996	17, 28	0.75
S. Isl. Regional	*0.54*		*1680-1997*	*160, 275*	*0.74*
		Mainland Regional Chronology			
Joffre Lakes	0.61	50°21', -122°29'	1711-2012	15, 28	0.73
Mt. Cheam	0.70	49°10', -121°40'	1592-1999	22, 39	0.80
Brandywine	0.67	50°06', -123°13'	1740-1998	17, 30	0.69
Mainland Reg.	*0.57*		*1658-2012*	*34, 59*	*0.57*

[a]Calculated using the program ARSTAN.
[b]Length truncated where expressed population signal (EPS; Wigley *et al.* 1984) <0.80.
[c]Mean first-order autocorrelation of all TR series, calculated using the program COFECHA prior to a autoregressive modeling.
[d]Developed by Coulthard and Smith 2015.

4.6 Data and Methods

A network of mountain hemlock annual TR-width records (chronologies) potentially sensitive to annual maximum snow depth was constructed from TR records developed specifically for this study and additional TR chronologies developed by Coulthard and Smith (2015). These data were combined with an existing grid point-based

reconstruction of summer Palmer Drought Severity Index (PDSI; Cook *et al.* 1999; 2004) to reconstruct summer (July-August) regionalized streamflow for the target basins.

4.6.1 Tree-ring data

TR data were derived from tree cores collected in fall 2012 and from raw (un-crossdated) digital measurements of previously collected tree cores archived at the UVTRL (Table 4.2). The TR samples were not necessarily collected at sites within the study watersheds. Rather the primary criterion for site selection was maximization of the sensitivity of annual radial tree growth to regional-scale maximum snow depth variations (Smith and Laroque 1998; Laroque and Smith 2003). Two cores were removed from mature trees at standard breast height using a 5.0 mm increment borer, glued to slotted boards, and sanded to enhance annual ring boundaries. Ring widths were measured to an accuracy of 0.001 mm, using a Velmex measuring stage system, and crossdated (pattern-matched) using a visual list method that was verified statistically using the program COFECHA 3.0 (Holmes 1983; Grissino-Mayer 2001).

TR chronologies were developed using the R package dplR (Bunn 2008). A long-term age-related growth trend is typically a feature of TR data that must be removed to make inferences about climate-related growth variations (Fritts 1976). TR width series (measurements from one tree core) were detrended by fitting a cubic smoothing spline with a 50% frequency response at wavelength 100 years to each series and dividing the measured width by the corresponding value of the fitted line (Cook and Peters 1981). TR growth in the current year is often influenced by conditions in antecedent years (Fritts 1976). To remove this biological persistence we fit a low-order autoregressive model (Box and Jenkins 1976) to the TR series, with order identified by the Akaike Information Criterion (AIC). The "residual" TR series (Cook and Holmes 1986) produced by this procedure have a zero-autocorrelation structure matching that of the streamflow time series we reconstruct in this study. Series from individual cores were combined into single representative regional chronologies using a bi-weight robust mean (Mosteller and Tukey 1977). Adequacy of the sample size for capturing the hypothetical population growth signal was assessed with the expressed population signal (EPS; Wigley *et al.* 1984) and chronologies were truncated where EPS fell slightly below the below the

standard value of 0.80. The hypothetical growth signal is an estimate of the extent that a TR chronology based on a finite number of trees represents a hypothetically perfect TR chronology based on an infinite number of trees (Wigley *et al.* 1984).

4.6.2 PDSI data

The PDSI is a widely used regional drought index that incorporates temperature, precipitation, and soil moisture storage into a single measure of drought severity (Palmer 1965). Reconstructed annual values of the PDSI for grid cell 24 were downloaded from the NOAA National Climatic Data Center website (2.5° by 2.5° grid cell centered on 50°, -125°; data period used: 1600-1990; http://www.ncdc.noaa.gov/data-access/paleo climatology-data /datasets; Figure 4.1). The 46 drought-sensitive chronologies used by Cook *et al.* (2004) to generate the moderately strong (R^2=0.37), well-validated gridpoint-24 PDSI reconstruction are independent from the chronologies used in this study.

4.6.3 Hydroclimate data

Mean monthly discharge records were downloaded from the Water Survey of Canada website (http://www.wsc.ec.gc.ca/applications/H2O/index-eng.cfm). In addition to fulfilling criteria described previously the study basins were selected based on the length of continuous natural flow data, and a uniform absence of year-to-year statistical persistence during summer months, a statistical feature typical of small coastal basins (Table 4.3). We seasonalized (summed) the streamflow data (m^3) over July-August for each stream to target the drought season (Eaton and Moore 2010; Table 4.3). We calculated z-scores of summer streamflow for each stream over the common data period (1960-2012), created regionally-representative ("regionalized") data by averaging the records, and applied a log10 transformation where the regionalized data were significantly skewed (Table 4.3). Regression models were estimated on transformed flows, but are back-transformed and presented as z-scores for plotting and analysis.

We estimated records of precipitation-as-snow (PAS) anomalies on the coordinates of the TR sample sites, and maximum monthly temperature and total monthly precipitation anomalies on the coordinates of the streamflow gauge station sites, using the

Table 4.3: Summer streamflow statistics.

River	Period of record used	cv[a]	skew[b]	r_1[c]	% missing values
Kanaka	1960-2011	0.50	2.15*	-0.17	0.0
Chemainus	1960-2011	0.68	3.78*	0.05	1.9
Tsable	1960-2009	0.70	2.16*	0.07	1
Zeballos	1960-2011	0.33	2.38*	0.03	1.4

[a]Coefficient of variation
[b]Skewness coefficient; significance at $p<0.05$ (*) determined by D'Agostino normality test (D'Agostino and Pearson 1973)
[c]First-order autocorrelation coefficient (none significant ($p<0.05$) for lags 1-10; Venebles and Ripley 2002)

program ClimateWNA, ver. 4.83 (Wang *et al.* 2012), which downscales PRISM (Daly *et al.* 2002) monthly data (2.5 x 2.5 arc min) over the reference period 1961-1990. The PAS data calculated from average air temperature and total precipitation estimates at a given coordinate location and elevation (Wang *et al.* 2012). General statistical agreement between the monthly PAS data and snow depth and SWE data from manual snow survey sites, as well as the insufficient lengths of the instrumental snow records for comparison with the tree-ring data, prompted us to use PAS data for the subsequent analysis (stations 3B01, 3B02A, 3B23P, 1D16; http://bcrfc.env.gov.bc.ca/data/survey/). We seasonalized (summed) the PAS data over the period where values were >0 (October through April) as an estimate of the annual maximum snow depth, the parameter that most strongly influences tree growth. Climate data were regionalized by averaging, missing values in both the streamflow and climate data were filled using a long-term mean (<2% of each dataset), and records truncated where >2 consecutive yearly values were absent.

We used the NOAA Multivariate ENSO Index (MEI) ranks (http://www.esrl.noaa.gov/psd/enso/mei/) and standardized values of the PDO index, downloaded from the NOAA Earth System Research Laboratory website (http://www.esrl.noaa.gov/psd/data/climate indices/list/) to explore the influence of climate modes on streamflow within the instrumental period. We only analyzed values of the PDO index during winter (October through March) months since year-to-year variability in the index is most energetic during that season (Mantua 2002).

4.6.4 Diagnostic correlation analysis

As a verification of the assumptions underlying our model, the Pearson correlation coefficient was used to summarize the strength of linear relationships among the TR, streamflow, and climate data. An effective sample size (Dawdy and Matalas 1964) was used as needed to adjust for persistence in testing correlation for significance.

We first checked whether the individual stream and regionalized summer streamflow data are controlled by the expected climate parameters (annual maximum snow depth, and summer temperature and precipitation). We tested correlations of the streamflow data with previous winter PAS and same-year reconstructed values of the PDSI index, under the assumption that the PDSI operates primarily as a surrogate for summer temperature and precipitation variations. Temporal stability of correlations was tested using a difference-of-correlations test that includes a Fisher's Z transformation of correlations (Snedecor and Cochrane 1989).

Following this we verified that reconstructed PDSI is an appropriate proxy for summer-season temperature and precipitation fluctuations in the study basins. These correlation tests were calculated using the program Seascorr, which summarizes the strength of relationship of annually resolved time series (e.g. PDSI) with monthly and seasonally aggregated climate data and assesses significance of correlation by a Monte Carlo method (Meko *et al.* 2011). We tested monthly and seasonal correlations between reconstructed PDSI and maximum temperature data for periods ending in each month of the 14-month period beginning in July of the previous year and ending in August of the current year. Partial correlations calculated by Seascorr were then used to identify any influence of seasonal precipitation on the PDSI data independent of the temperature influence.

We also used Seascorr to eliminate from further analysis any of the TR chronologies without significant ($p<0.05$) linear, temporally stable relationships with previous winter PAS. The TR dataset was reduced further by computing regional TR chronologies from subsets of trees from highly correlated site chronologies. Aggregating chronologies in this way can extend the length of the TR records, and consequently the model prediction period, by enhancing the number of TR series, and the signal-to-noise ratio in the early portion of the data (Cook and Kairiūkštis 1990). As a final step,

Principal Components Analysis (PCA) was run on the regional chronologies to derive independent time series that emphasize common TR variability (Kachigan 1982). Only the eigenvectors with eigenvalues statistically greater than 1.0 were retained (North *et al.* 1982). The regional chronologies, PCs of the regional chronologies, and reconstructed PDSI data were evaluated as candidate predictors for the dendrohydrological model.

4.6.5 Reconstruction model

The reconstruction model was estimated by forward stepwise multiple linear regression of the regionalized July-August streamflow in year *t* on the pool of predictor variables model in years *t*, *t+1*, and *t+2*. Lags were included to allow TR information in ensuing years to inform on climate conditions in the current year (Cook and Kairiūkštis 1990). A suite of streamflow models were developed based on various predictor groupings, and evaluated based on explanatory power (adjusted R^2 statistic), model fit and assumptions (analysis of the model residuals, Durbin-Watson and variance inflation factor statistics: DW and VIF), a measure of uncertainty of the predicted values of the model calibration (standard error of the estimate: SE), and an estimate of the statistical significance of the regression equation (F-ratio). Due to the short length of the overall model calibration period we conducted two validation procedures, leave-one-out LOO cross-validation and split-period validation. Validation statistics were estimated by comparison of the observed and predicted values for each procedure (Michaelsen 1987; Snee 1977). These included the reduction of error (RE; Fritts 1990), a measure of uncertainty of the predicted values over the validation period (root mean square error of cross-validation; $RMSE_v$), and the Pearson correlation (r) and R^2 of the observed and estimated values. A sign test provided a measure of the number of times the direction of the departures of the annual values from the sample means agreed and disagreed (Cook and Kairiūkštis 1990). The best model was calibrated on the full period of July-August streamflow data and used to reconstruct regionalized streamflow over the length of the shortest predictor dataset. We used correlation analysis and a previously described difference-of-correlations test to confirm that the predictors selected for our model are linearly correlated with reconstruction-season discharge over the full period of the instrumental record.

4.6.7 Analysis of the reconstruction

We compared statistical properties of the gauged and reconstructed flows to assess their similarity within and outside the instrumental period. The 0.05 quantile, or fifth percentile, of single-year reconstructed flows was selected as a threshold defining a drought event. To put contemporary low-flows in the context of the instrumental period, we determined the timing and magnitudes of drought events relative to the reconstructed instrumental period mean discharge, and calculated a recurrence interval for these events following the equation of Mays (2005). We compare flow duration curves of the reconstructed and gauged streamflow records to determine if worst-case scenario drought magnitudes and probabilities would be similarly estimated from observed and modeled data. The regionalized flow data and the instrumental period reconstructed record were compared with instrumental records of ENSO and winter PDO over the common data period 1960-1990 to investigate large-scale climatological influences on droughts and wet episodes. A test of proportions (Newcombe 1998) was applied to determine whether the proportion of years with below- or above-median runoff during strong El Niño/La Niña years equals the proportion of years with below- or above-median runoff during weak- and non-El Niño/La Niña years. The strength of El Niño/La Niña events was based on MEI ranks. For winter PDO, the previously described test was used to test for significant difference of correlation (Snedecor and Cochrane 1989) of PDO with streamflow in the cool (1960-1976) versus warm (1976-1990) phases that occurred within our record (Mantua 2002); effective sample size (Dawdy and Matalas 1964) was used for this test, as needed, to adjust for autocorrelation in the individual series. A Morlet wavelet analysis on the full period of the reconstructed data highlights localized variations of power over time (Torrence and Compo 1998).

4.7 Results

4.7.1 Tree-ring data

We developed 19 new site-level mountain hemlock chronologies for this study, and also analyzed 10 mountain hemlock chronologies developed by Coulthard and Smith (2015 Table 4.2). Seven chronologies were omitted from further analysis as they did not meet minimum requirements (chronology information not presented). Interseries

correlation values of the detrended series used in the study ranged from r=0.43 to 0.67, indicating strong synchronicity among the records. Analysis of the cross-correlation matrix showed strong statistical agreement among groups of site-level chronologies developed for this study, providing justification for developing two regional mountain hemlock chronologies that represent south Vancouver Island and the south coastal mainland of B.C (Figure 4.1). We also used regional chronologies developed by Coulthard and Smith (2015) that represent northern and central Vancouver Island (Figure 4.1). The four regional chronologies have series intercorrelation values ranging from 0.50 to 0.57 and minimum (maximum) chronology lengths of 317 (487) years (Table 4.2). Correlation values among regional chronologies ranged from r=0.57 to 0.74 (p<0.01).

4.7.2 Diagnostic correlation analysis

Both the individual stream and regionalized summer streamflow records exhibit temporally stable significant positive linear correlations with previous winter PAS and reconstructed values of the PDSI (Table 4.4). None of the datasets, including PDSI, exhibited significant autocorrelation at lags <10 years. Results of the Seascorr analyses indicate that the reconstructed PDSI record is primarily sensitive to variability in summer temperature and precipitation, and is also weakly associated with precipitation in the previous autumn (Figures 4.3A and 4.3B). The index exhibits strongest time-stable monthly and seasonal negative correlations with maximum temperature during June-July. A positive correlation with precipitation during June-August is evident (Figure 4.3B) from partial correlations that adjust for the strong negative inter-correlation between precipitation and temperature during warm-season months (Figure 4.3C). The partial correlations also indicate a strong seasonal pattern in the inter-correlation of monthly precipitation and temperature in the study area, with positive correlation in winter and negative correlation in other months (Figure 4.3C). Taken together, these hydroclimate relationships support the interpretation that the study watersheds and the regionalized data derived from them represent hybrid annual flow regimes.

Table 4.4: Hydroclimate correlations and their temporal stability. Analysis period 1960-1990.

Streamflow data (July-August)	Winter PAS[a]	p[b]	PDSI[c]	p[b]
Regionalized	0.54	0.31	0.59	0.93
Kanaka	0.34	0.74	0.61	0.85
Chemainus	0.59	0.87	0.65	0.37
Tsable	0.60	0.40	0.42	0.97
Zeballos	0.49	0.06	0.36	0.70

[a]Correlation of regionalized streamflow with winter PAS; all correlations significant at 0.01 level
[b]*p*-value for a test of the null hypothesis that the population sample correlations in preceding column for the first and second halves of the 1960-1990 period are the same (those split-sample correlations not listed)
[c]Correlation of regionalized summer streamflow with summer reconstructed PDSI at gridpoint 24; all correlations significant at 0.01 level

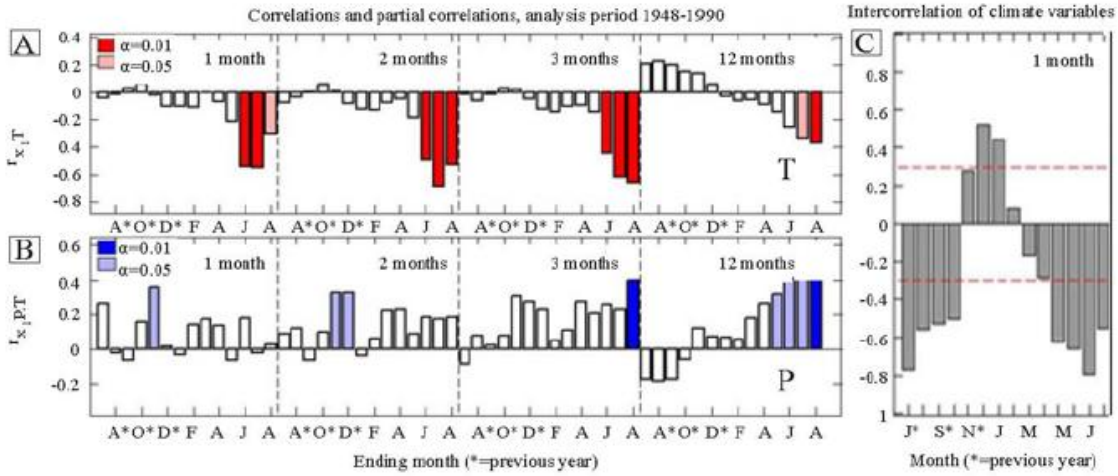

Figure 4.3: (A) Monthly and seasonal correlations between reconstructed PDSI and regional maximum temperature (T) data, over 1-, 2-, 3-, and 12-month sliding windows beginning in the previous July through current August. The strongest correlation is during June-July (r=-0.68, p<0.01). (B) Monthly and seasonal partial correlations between reconstructed PDSI and regional total precipitation (P) data, controlling for the influence of T. The strongest independent correlation of reconstructed PDSI with P is during June-July-August (r=0.65, p<0.01). (C) Monthly intercorrelations of T and P. Red-hatched lines represent 95% confidence interval. All correlations were calculated using Seascorr.

4.7.3 Reconstruction model

Stepwise regression identified reconstructed PDSI and the first principal component (PC1) of the regional TR chronologies as the best predictors of regionalized summer streamflow. PC1, with same-sign weights (0.92 to 0.73) on the four regional

chronologies, explained 73% of the regional-chronology variance. The final reconstruction model is shown in Equation 1:

$$Q = 0.235-(0.100*PC1) + (0.041*PDSI) \quad (3)$$

The model explains 64% of the variance (adjusted R^2=0.64) of regionalized summer streamflow, Q, in the 31-year (1960-1990) calibration period. Each model predictor is significantly (p<0.01) linearly correlated with the regionalized streamflow data over the full period of the common record, without the influence of statistical outliers (Figure 4.4). The reconstruction spans the period 1658-1990. Values of the standardized regression coefficients indicate that PC1 (-0.602) has a larger effect in determining the dependent regionalized flow values than reconstructed PDSI (0.370). We checked that PC1 was significantly linearly correlated with winter PAS (r=-0.66, p<0.01) and that this relationship was stable over time (p=0.62 for the previously described difference-of-correlations test).

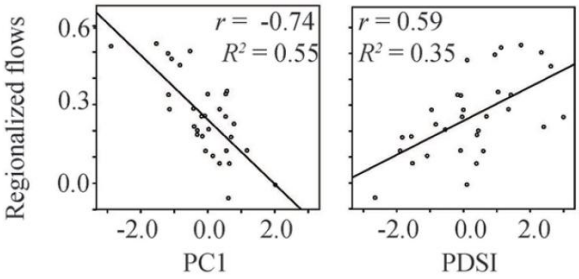

Figure 4.4: Scatterplots of the regionalized flow data and PC1 (left) and reconstructed PDSI (right). Correlations significant at the 99% level.

Reconstruction, cross-validation, and split-period validation statistics are summarized in Table 4.5 and the reconstruction is plotted in Figure 4.5. Collinearity diagnostics indicate that the model predictors are adequately independent (Table 4.5), the F-ratio suggests that the regression equation is statistically significant, and positive RE values close to the calibration R^2 values, similar SE and $RMSE_v$ values, and strong relationships between the observed and predicted values of the validation periods indicate a well-validated model (Table 4.5; Figure 4.5). The results of the sign tests indicate the

direction of observed and expected departures from the sample means agree significantly more often than would be expected by chance (Table 4.5).

Table 4.5: Reconstruction, cross-validation, split-period validation, and sign-test statistics. * $p<0.05$, ** $p<0.01$.

Reconstruction	R^2	adj. R^2	D-W[a]	VIF	SE	F-Ratio[b]
	0.66	0.64	1.70	1.16	0.09	27.86
LOO validation	RE	$RMSE_v$[c]	r[d]	R^2_v[e]	Sign test (agree/disagree)	
	0.60	0.096	0.78	0.60	27/31[b]	
Split-period Validation	RE	$RMSE_v$[c]	R^2_c		Sign test (agree/disagree)	
1960-1974	0.77	0.101	0.76		14/15[b]	
1975-1990	0.55	0.106	0.53		11/16[b]	

[a] Durbin-Watson statistic.
[b] significant at the 99% level
[c] derived from transformed z-scores of Q.
[d] Cross-validation r ($p<0.01$).
[e] Cross-validation R^2.

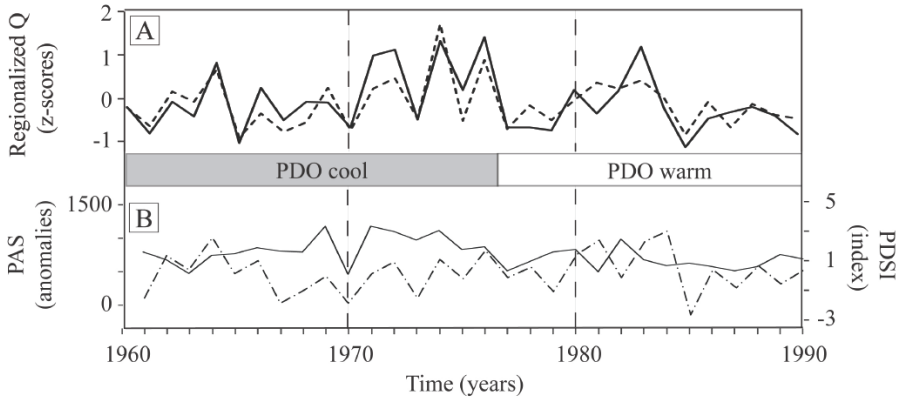

Figure 4.5: (A) Time plot of the gauged (black line) and estimated (hatched line) records from the model calibration, and (B) time plot of previous December through March PAS (black line) and reconstructed PDSI (hatched line).

Analysis of regression residuals revealed no violation of regression assumptions, and suggested generally symmetric error in the estimation of high and low instrumental flows. Visual inspection of the calibration period time plot confirms this, showing over- and under-predictions throughout the record for both high- and low- flow years (Figure 4.5). The model is unusually effective for estimating the magnitudes of extreme events, with little compression of the reconstruction variance relative to the instrumental data despite an expectation of compressed variance in TR based regression analysis (Figure

4.5; Meko and Graybill 1995). The magnitudes of lowest instrumental flow years are particularly accurately estimated; no major discrepancies between gauged and reconstructed records occur during those years.

4.7.4 Analysis of the reconstruction

The basic statistical properties of the regionalized flow data are preserved in the reconstructed instrumental and pre-instrumental records (common instrumental data interval only); autocorrelation is absent at lags <10 years and mean, minimum, and maximum flows are similar (Table 4.6). The greatest discrepancy is larger maximum flows in the pre-instrumental period. The instrumental period reconstruction exhibits a similar range variance to that of the gauged data, while the coefficient of variation (CV) for instrumental portion of reconstruction is smaller (Table 4.6). A 5-year running mean elucidates generally regularized interdecadal variability in the full-period reconstruction (Figure 4.6).

Table 4.6: Descriptive statistics of gauged and reconstructed flow data, as z-scores.

Flow data type (back-transformed)	cv[a]	mean	max	min	r_1[b]
Regionalized gauged	6.4	-0.11	1.41	-1.12	-0.045
Instrumental period reconstructed	5.3	-0.11	1.72	-0.91	-0.160
Pre-instrumental period reconstructed	3.4	-0.19	2.37	-1.18	-0.110

[a]Coefficient of variation

[b]First-order autocorrelation coefficient (none significant (p<0.05) for lags 1-10; Venebles and Ripley 2002).

Seventeen bottom fifth percentile flows occurred within the reconstructed record. with a return interval of 21 years. Remarkably, none of these events occurred during the instrumental period. The reconstruction suggests droughts of this magnitude have a 21-year recurrence interval. The timing and magnitudes of bottom fifth percentile flow years are plotted in Figure 4.6 and listed in Table 4.7, and the flow threshold (z-score<-0.93) is delineated with a black-hatched line on the reconstruction time plot (Figure 4.6). Note that for context the hatched line extends beyond the interval of reconstruction into the

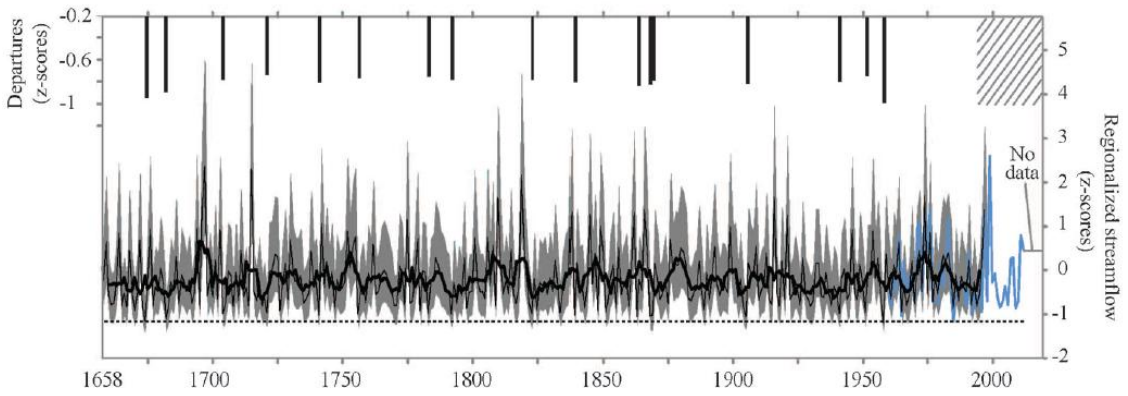

Figure 4.6: Time plot of reconstructed regionalized summer streamflow plotted as z-scores (black line) with a five-year running mean (heavy black line), and gauged data (blue line). The grey envelope represents 95% confidence intervals calculated from the $RMSE_v$ following the equation of Weisberg (1985). The vertical black bars represent bottom fifth percentile flows relative to the reconstructed instrumental period mean discharge. The bottom fifth percentile flow threshold (z-score<-0.92) is delineated on the time plot with a black-hatched line.

Table 4.7: Lowest reconstructed and gauged flows, listed in order of severity. A) Pre-instrumental period bottom fifth percentile low flows; B) Lowest gauged flows, with departures calculated from the 1960-1990 gauged mean.

	Year	Departure from mean z-score	Score
(A)	1958	-0.99	-1.17
	1674	-0.93	-1.11
	1682	-0.89	-1.08
	1905	-0.84	-1.02
	1863	-0.83	-1.02
	1868	-0.83	-1.01
	1839	-0.82	-1.00
	1741	-0.81	-0.99
	1869	-0.80	-0.99
	1792	-0.78	-0.97
	1941	-0.78	-0.97
	1704	-0.78	-0.97
	1756	-0.78	-0.96
	1783	-0.77	-0.96
	1823	-0.77	-0.95
	1951	-0.75	-0.93
	1721	-0.74	-0.93
(B)	1985	-1.01	-1.12
	1965	-0.90	-1.01
	1992	-0.87	-0.98
	1996	-0.80	-0.91
	2009	-0.73	-0.84
	2003	-0.71	-0.82

contemporary period, although these data were not included in the percentile or recurrence interval calculations. Our reconstruction indicates that bottom fifth percentile flows occurred in two consecutive years in 1868 and 1869, and that they did not persist for more than two years at any time. The most extreme single-year departures occurred in 1674, 1682, and 1958, and the magnitudes of these departures exceed any within the gauged record, with the exception of 1985. Flow duration curves (low flow region only, p>0.50) are plotted in Figure 4.7. Whether compared with the shorter gauged streamflow record from the calibration period (1960-1990) or the full gauged streamflow record 1960-2012), the reconstruction curve (1658-1990) suggests a higher probability of more severe droughts than the gauge data suggests.

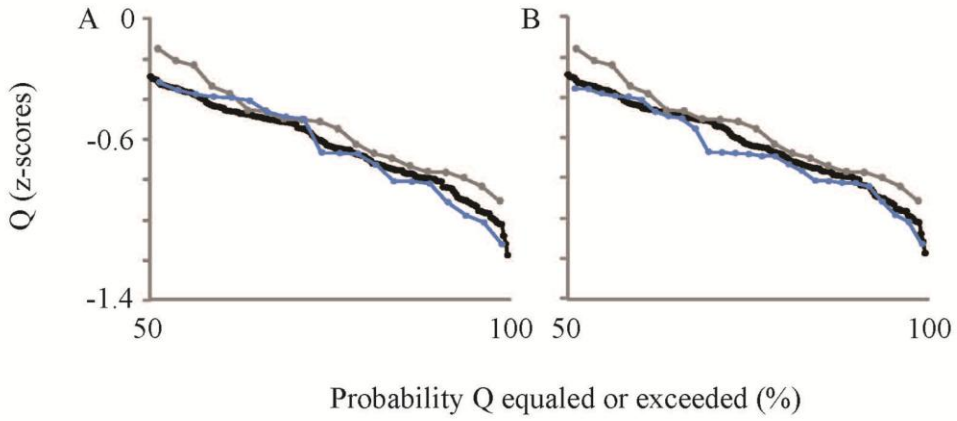

Figure 4.7: Flow duration curves of the low flow region only (p>0.50). In panel A the curve from the calibration period hydrometric data (1960-1990; blue line) is compared with curves from the calibration period reconstruction (grey line) and the full-period reconstruction (black line). In panel B hydrometric data from the full available data record (1960-2012; blue line) are compared with the reconstruction curves from panel A.

Neither the regionalized or reconstructed flows exhibited a significantly different proportion of below- or above-median flows during strong El Niño/La Niña years relative to weak and non-El Niño/La Niña years (Table 4.8). Both regionalized and reconstructed instrumental period flows were significantly negatively correlated with values of the PDO index during winter (Table 4.9). Analysis of subperiods revealed that, for both records, the influence of the PDO is stronger during the cool phase of the oscillation, although a test of the difference in correlations between subperiods was only significant

for the gauged data. The wavelet power spectrum of the reconstructed flow data identifies significant but intermittent power in the approximately 4- to 10- year bandwidths, energy at approximately 16-year periods in the early part of the record, and an absence of multidecadel variability except in the early 1800s (Figure 4.8).

Table 4.8: Test of proportions assessing the association of regionalized summer runoff (Q) with strongest El Niño and La Niña events over the period 1960-1990. Calculated using R function *prop.test*. Proportions of years in each streamflow category in parentheses. The null hypothesis that groups have the same true proportions was true for all tests, *p*- values ranged from 0.31-0.73.

Streamflow category	*# El Niño years*	*# weak/non-El Niño years*
Regionalized Q (gauged)		
Below median	5 (38.5%)	14 (56.0%)
Above median	8 (61.5%)	11 (44.0%)
Total	13 (100%)	25 (100%)
Reconstructed Q		
Below median	6 (46.2%)	13 (52.0%)
Above median	7 (53.8%)	12 (48.0%)
Total	13 (100%)	25 (100%)
Streamflow category	*# La Niña years*	*# weak/non-La Niña years*
Regionalized Q (gauged)		
Below median	5 (41.7%)	17 (65.4%)
Above median	7 (58.3%)	9 (34.6%)
Total	12 (100%)	26 (100%)
Reconstructed Q		
Below median	7 (58.3%)	12 (46.2%)
Above median	5 (41.7%)	14 (53.8%)
Total	12 (100%)	26 (100%)

Table 4.9: Associations of regionalized and reconstructed flows with PDO variability over the instrumental period.

	Full period	Cool phase	Warm phase	N_1, N_2[a]	p[b]
Regionalized streamflow	r=-0.37 (p<0.05)	-0.67 (p<0.05)	0.08 (p<0.05)	17, 21	0.012
Reconstructed streamflow	-0.35 (p<0.05)	-0.60 (p<0.05)	-0.14 (p<0.05)	17, 21	0.124

[a]Effective sample sizes for early and late periods.
[b] p-value for a test of the null hypothesis that the population sample correlations for the cool and warm phases are the same. Significant where p<0.05.

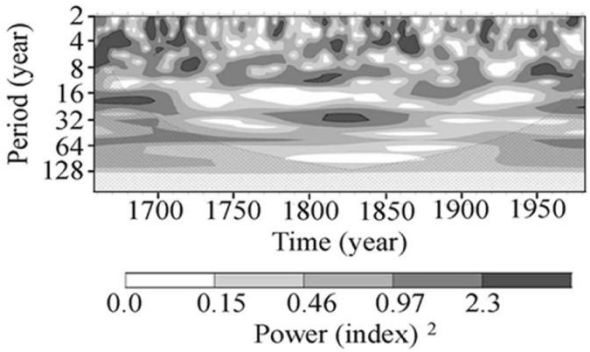

Figure 4.8: Morlet wavelet power spectrum on the full-period reconstructed streamflow record. Black contours represent 95% confidence level based on a white-noise background spectrum. The hatched area represents areas of the spectrum susceptible to the effects of zero padding (Torrence and Compo 1998).

4.8 Discussion

4.8.1 Predictor selection and model estimation

Our model effectively estimates variability in regionally-synchronous low-flow season stream discharge for the hybrid watersheds examined in this study. Correlation analyses indicate that: 1) the flow data are driven by variations in previous winter PAS, and summer air temperature and total summer precipitation; and, 2) the selected model predictors serve as proxies for those climate variables.

TR width variability as captured by PC1 operates as a proxy for winter PAS; increased PAS results in a shorter growing season and smaller ring widths, and also promotes greater summer-season runoff. Marcinkowski *et al.* (2015) found that prior to 2000, energy limitation by late-lying snow was the only time-stable control on the annual growth of mountain hemlock trees in the nearby Cascade Mountains, which is encouraging for the use of this species as a proxy for snowmelt-dominated streams. The authors also report that some post-2000 mountain hemlock trees exhibit a weakened relationship to winter precipitation, possibly due to the increasingly growth-limiting role of climbing spring temperatures, however our reconstruction omits data from that period.

Reconstructed PDSI for gridpoint 24 is sensitive to regional-scale fluctuations in maximum temperature and total precipitation during summer (Figure 4.3). In years where values of the PDSI are lower, summer conditions are warmer, evaporation is greater, and precipitation and streamflow are reduced. The results of the correlation analyses are

consistent with the assumption that the reconstructed annual values of the PDSI serve as a proxy for summer air temperature and to a lesser extent summer precipitation in our reconstruction. Although warmer conditions could theoretically increase flow inputs from snowmelt, most snow meltwater is likely in the groundwater system by July-August (Beaulieu *et al.* 2012).

Because year-to-year streamflow in the small study watersheds is not autocorrelated, we were able to estimate a paleohydrological model based on predictors that inform only on single-year flows, without risking underestimation of an autocorrelated discharge component. In contrast, dendrohydrological models in large basins with slow concentration times can rely on complicated regression models including time-lagged TR variables to capture the dependence of flows in a given year on climatic conditions in previous years (Loaiciga *et al.* 1993). Where flashy discharge does not preclude the dendrohydrological approach, small watersheds may lend themselves to simpler TR-derived streamflow models based on a smaller number of predictors, as well as a lower probability of model over fitting. For this study, targeting the low-flow season enabled us to avoid the flashy winter high-flow period.

4.8.2 Reconstructed record and drought events

Generally, our reconstruction describes an historical pattern of intra-decadal high- and low-flow oscillations, with few sustained periods of very high or very low discharge. This lack of persistence is typical of a hybrid flow regime, and an important feature of the flow data for water management. It was critical that the zero-autocorrelation structure in our small study basins not be distorted by using TR data that contain biological persistence as model predictors, in this case through the use of residual chronologies (Meko and Woodhouse 2011).

All of the seventeen reconstructed bottom fifth percentile flow years occurred prior to the hydrometric data period. With the exception of very low instrumental flows in 1985, sixteen of these events were more extreme than any in the gauged record (Figure 4.6; Table 4.6). Our reconstruction suggests that pre-instrumental droughts were more severe than those in 1992, 1996, 2003, and 2009, when water scarcity throughout south coastal B.C. severely impacted municipal, hydroelectric, and agricultural water supplies

(B.C. Ministry of Environment 2010; Puska *et al.* 2011). The reconstructed record suggests both more severe worst-case scenario droughts, and a slightly higher probability of those droughts, than do the hydrometric data (Figure 4.7). An important point in interpreting these results is that there is unexplained variance in the reconstruction, and a confidence interval around the low reconstructed flows, such that the true flows may have been lower. Further, reconstructed estimates of extremes are conservative due to expected variance compression, so that a reconstruction flow duration curve could typically show only less extreme values than a flow duration curve of observed streamflow values. It is therefore significant that the reconstruction curve suggests more likely, more severe droughts than the hydrometric curve. Especially given the accuracy of our model in estimating lowest flow magnitudes, our results suggest that: 1) extreme events cannot be reliably predicted based on the existing hydrometric flow record for hybrid watersheds in south coastal B.C.; and, 2) water management strategies based on these data are likely to underestimate worst-case scenario naturally occurring droughts.

Both mean winter and summer temperatures and projected to increase by 1.7°C by 2050, while total summer precipitation is predicted to decrease by 13% (December-February; B.C. Ministry of Water, Land and Air Protection 2002; Pike *et al.* 2010). It is not unreasonable to expect that future bottom fifth percentile-type natural low flows exacerbated by projected climate change-induced flow reductions could result in drought episodes of a severity unprecedented in the last ~350 years. We could not account for the extreme 2014 and 2015 droughts due to the unavailability of hydrometric data (B.C. Ministry of Forests, Lands and Natural Resource Operations 2014).

Diagnostic correlation analyses supported the interpretation that lowest flows generally correspond with diminished snowpack and/or unusually warm and dry summer conditions. Depending on the fluctuating seasonal hydrology of hybrid regimes, hydrological drought may be caused by reduced winter snowpacks, increased summer temperature and aridity, or both. For example, inspection of the model predictor values in lowest flow years shows that the conspicuous droughts in 1682 and 1958 are coincident with large negative values of the PDSI, while 1674 and 1905 had very large TR index values expected during a year of reduced PAS.

4.8.3 Influences of ocean-atmosphere climate variability

The lack of relationship between the timing of high or low runoff with strong El Niño/La Niña events is surprising since, in the study region, warm dry El Niños typically reduce snowmelt-derived summer runoff while La Niñas enhance it (Fleming *et al.* 2007). ENSO fluctuations may not strongly determine regionally-synchronous runoff in the study streams, but it is more likely that either: 1) the sample size was too small for capturing real long-term relationships between ENSO and streamflow; or, 2) the influence of summer climate conditions, expressed by the PDSI, periodically 'overrides' that of winter conditions in determining summer runoff quantities. Visual inspection of time plots in Figure 4.5 provides some indication of an overriding effect of summer conditions particularly during the warm PDO phase. The year-to-year association of gauged and estimated flows with PDSI during that phase is stronger than with PAS, including in years of enhanced snowpack followed by a warm/dry summer (e.g. 1985-1989). In contrast, the PAS and PDSI records generally "agree" during the cool phase; warm/dry conditions and cool/wet conditions persist from winter to summer (e.g. 1968-1971) so that streamflow is more strongly linked with PAS fluctuations during this phase. Although we could not assess these relationships quantitatively, they are consistent with the stronger — and in the case of the gauged record, significantly different — correlation of streamflow with winter PDO during the cool versus the warm phase, and with the role of PDO cool phases in enhancing snowmelt-derived runoff. The wavelet power spectrum exhibits some ENSO-type interannual variability intermittently throughout the reconstructed record, with loss of energy across all bandwidths 1730-1760 and 1880-1910, while multi-decadal PDO-type variability is significant only during 1800-1850 (Figure 4.8). Lower frequency variability may be absent as a result of detrending applied to the TR data.

4.8.4 Comparison with other paleorecords

The distinctly coastal nature of our study basins is reinforced by the general disagreement of our reconstruction with relevant paleoenvironmental records from continental western Canada and the United States, including a large number of streamflow reconstructions of continental, glacierized basins using precipitation-limited

TRs (Case and MacDonald 2003; Gedalof *et al.* 2004; Beriault and Sauchyn 2006; Axelson *et al.* 2009; Sauchyn *et al.* 2014). Those records generally correspond with modes of ocean-atmosphere variability affecting continental environments and are consistent with historical North American-scale drought episodes (Cook *et al.* 2004; Stahle *et al.* 2007). Nor does our record resemble two streamflow reconstructions of non-hybrid basins in central-western B.C. (Hart *et al.* 2010; Starheim *et al.* 2013). A TR derived reconstruction of May-July precipitation from the south coast of Vancouver Island presented by Jarett (2008) bears little resemblance to the streamflow record developed for this study, likely due to the limited influence of precipitation during that season on July-August streamflow in the watersheds analyzed here.

4.8.5 Sources of unexplained variance

Choices relating to chronology development and regression model estimation, quality of the streamflow data, length of the calibration period, the inability of TRs to perfectly record climate fluctuations, and periodic decoupling of TR-climate relationships, may be responsible for a proportion of unexplained model variance. Uncertainty in the low-frequency component of streamflow variability is likely due to the detrending that we applied to the TR measurements. Sources of uncertainty not captured by the regression error variance include changes in watershed characteristics, undetected flow inputs lagged over years due to storage, and undetectable historical changes in the relationship between TR widths and climate. The model error of the reconstructed PDSI data is not explicitly accounted for in our regression modeling.

4.9 Conclusion

Our reconstruction indicates that recent droughts in hybrid watersheds in south coastal B.C. were not as severe as those that occurred naturally in the pre-instrumental period. Sixteen droughts occurred since 1658 that were more extreme than any in the gauged record. A frequency analysis of the reconstructed record suggests more severe worst-case scenario droughts and a slightly higher probability of those droughts than does a frequency analysis of the hydrometric data. This emphasizes both the usefulness of long-term records for probabilistic drought assessment, and the value of dendrohydrology as a source of long-term records.We suggest that water management strategies based on

lowest observed flows determined from hydrometric data will underestimate the potential magnitudes of natural drought scenarios in these watersheds. In addition, if low-flow conditions anticipated under climate change exacerbate lowest possible natural flows, drought severities could exceed those in the past ~350 years. We reconstructed mean not minimum discharge values; actual low flow magnitudes would depart even further from mean flow values. We could not compare the extreme 2014 and 2015 droughts with preceding events due to a lack of hydrometric data.

Both gauged and reconstructed regionalized flows were negatively associated with fluctuations in winter PDO, most strongly during the PDO cool phase. The correlation of the gauged record with the PDO index was, in fact, significantly different during the cool versus warm phases, corroborating that summer discharge in hybrid streams is more strongly influenced by cool- than warm-phase PDO conditions as a result of increased snowmelt-derived runoff during cool phases (Fleming *et al.* 2007). We found no evidence of a statistical relationship between the timing of high or low runoff years with strong El Niño/La Niña events. This may have been due to an inability of the short comparable datasets to capture extant hydroclimate relationships. Alternatively, visual comparison of the streamflow data with PAS and PDSI records suggested an overriding influence of summer climate conditions over snowmelt quantities during the PDO warm phase, which could account for weak runoff-PDO linkages during that phase. Our reconstruction is distinctly coastal in flavor. It is incongruous with paleohydrological records from continental environments or records of spring precipitation and snowmelt-dominated streamflow as a result of the inconsistent year-to-year influence of snowmelt on hybrid stream discharge.

From a model-development standpoint, we demonstrate that TR-based reconstruction of small hybrid basins in temperate environments can be optimized using a combination of PAS and summer drought sensitive proxies as model predictors. Our model hindcasts synchronous variability in summer discharge among the four study streams over the interval 1658-1990, and explains 64% of the discharge variance over the 1960-1990 model calibration period. Targeting the low-flow season enabled us to avoid high and flashy winter flows that cannot not be modeled using TRs in the study environment, while the lack of year-to-year persistence in the flow data made these

watersheds amenable to a simple paleohydrological model based on a smaller number of predictors and minimized the probability of model over fitting. This study represents the first attempt to develop a paleohydrological model of regionally-synchronous streamflow in B.C., and to our knowledge provides the strongest annually resolved paleoenvironmental record of streamflow in the province.

Chapter 5 Comparison of reconstructions

5.1 Introduction

The three proxy hydroclimatic records presented in the dissertation are related to annual variations in the regional snowpack. The records are not independent, since each is based in full or in part on similar sets of mountain hemlock and/or amabilis fir TR chronologies from south coastal B.C. Nonetheless, the predictor-predictand relationships vary among models in such a way that comparing the reconstructions sheds light on linkages between regional snow and streamflow variability over the past several hundred years. To appraise the quality of the reconstructions, three comparisons are made. First, the instrumental (predictand) data records are compared to provide a baseline for describing what relationships 'actually' exist among the modeled systems. Second, the reconstructions are compared. Third, reconstructed and instrumental records are compared within the instrumental period, to give an indication of how well the models capture observed extremes.

5.2 Comparison of the instrumental data

It is important to know how the measured snow and streamflow data are associated, since this gives an indication of what 'real' relationships exist among the modeled systems. Time plots of the instrumental data records are presented in Figure 5.1. All data in Figure 5.1 are z-scores, but scores for the instrumental records were calculated from the means and standard deviations of the corresponding full-period reconstruction scores. This approach allows the instrumental period data variance to be interpreted relative to the long-term record.

The instrumental records span 1960-2015 (SWE), 1960-2009 (Tsable River streamflow), and 1960-2012 (regionalized streamflow). Both the SWE and streamflow records reflect the very high snowpack year in 1999, confirming a strong association between high snow and high summer runoff. Both streamflow records have bottom fifth percentile values in 1985 and1992, even though SWE values were not low in those years. In fact, very low snow and low summer runoff (drought) years do not coincide during the 49 common years of record. This finding is consistent with summer droughts occurring in

hybrid watersheds independent of the influence of snowmelt, likely as a result of hot, dry summer conditions (Eaton and Moore 2010). The stronger association between runoff and snowmelt in high SWE years versus low SWE years is obvious from correlations among the records over the full SWE data period, the highest half of the SWE values, and the lowest half of the SWE values (Table 5.1).

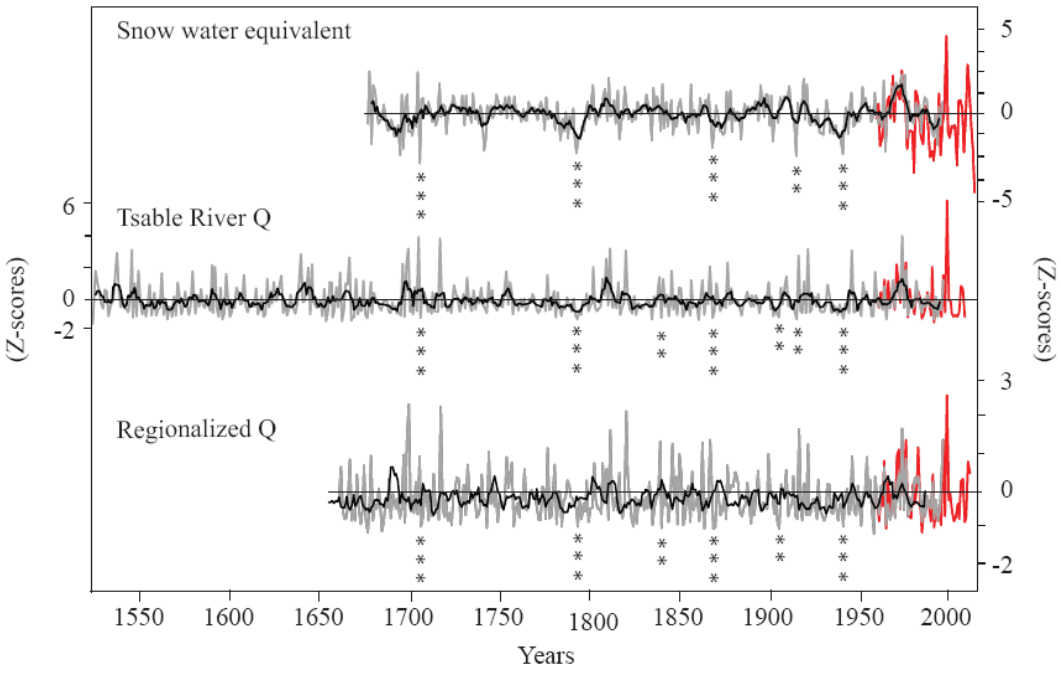

Figure 5.1: Time plot of dendrohydrological reconstructions (grey lines) for south coastal B.C. shown with 5-year running means (black lines). Z-scores of the instrumental records (red lines) were calculated from the means and standard deviations of the associated full-period reconstruction z-scores. Note the axes have different scales. Corresponding bottom fifth percentile years among records are noted with asterisks (corresponds among 2(3) records = 2(3) asterisks).

Table 5.1: Correlations of streamflow records with SWE. **=p<0.01

	SWE	Upper half of SWE values	Lower half of SWE values
Tsable	0.692**	0.783**	0.23
Regionalized	0.641**	0.667**	0.20

5.3 Comparison of the reconstructions

Time plots of the three reconstructions are presented in Figure 5.1. It is easiest to identify similarities among highest SWE and runoff years, because the streamflow time plots are dominated by large positive values. The highest fifth percentile reconstructed values correspond among all three records in 1715, 1810, 1921, and 1974, and among two of three records in 1696, 1697, 1703, 1819, 1866, and 1916. A strong relationship between high SWE and streamflow is consistent with the streamflow reconstructions being 'tuned' to snowmelt-derived summer runoff, and consistent with observational data from 1999.

In the time plots of the streamflow reconstructions, high positive values associated with enhanced runoff obscure lower-magnitude variance in the lower flows (Figure 5.1). Bottom fifth percentile values among the reconstructions are therefore noted with asterisks. These occurred almost as frequently at the high SWE-high runoff matches, including in 1704, 1792, 1868, 1941 (all records), 1839, 1905 (both streamflow reconstructions) and 1915 (Tsable River streamflow reconstruction and SWE).

Figure 5.2A allows closer inspection of the relative magnitudes of bottom fifth percentile years among records, plotted as departures from the mean (zero). Note that the SWE data have the largest extremes and the regionalized streamflow reconstruction the smallest. Of the nine reconstructed years when snow was very low, streamflow drought occurred in eight. Coherence between the low SWE and Tsable River drought is reasonable since both reconstructions are based entirely on snow-sensitive TR records. Agreement between low SWE and regionalized streamflow droughts also reflects the abiding influence of the snow-sensitive model predictor(s) in those years, since the additional model predictor, the reconstructed PDSI, is insensitive to moisture from snow meltwater (Hayes *et al.* 2005).

There are also many years when only the regionalized reconstruction documents extreme low values. In fact, over the common data period extreme droughts in the regionalized record occurred as often on their own as they did in tandem with very low values of the other two reconstructions (8 years each). Droughts only documented in the regionalized reconstruction were likely driven by warm and dry summer conditions and

were incorporated by the PDSI predictor. Inspection of the instrumental data demonstrated that this kind of drought occurred in hybrid watersheds in 1985 and1992.

Given that the Tsable River reconstruction is based on snow-sensitive TRs, it is surprising that many reconstructed droughts in that river occurred in years without a particularly low snowpack. A possible explanation for this is that, due to the shorter length of the SWE reconstruction compared with the Tsable River reconstruction, a smaller number of bottom fifth percentile values are flagged for SWE. If bottom fifth percentiles were calculated from a longer SWE record, or if a 10th or 15th percentile threshold were used with the shorter record, more very low SWE years would be identified and would likely align with Tsable River droughts.

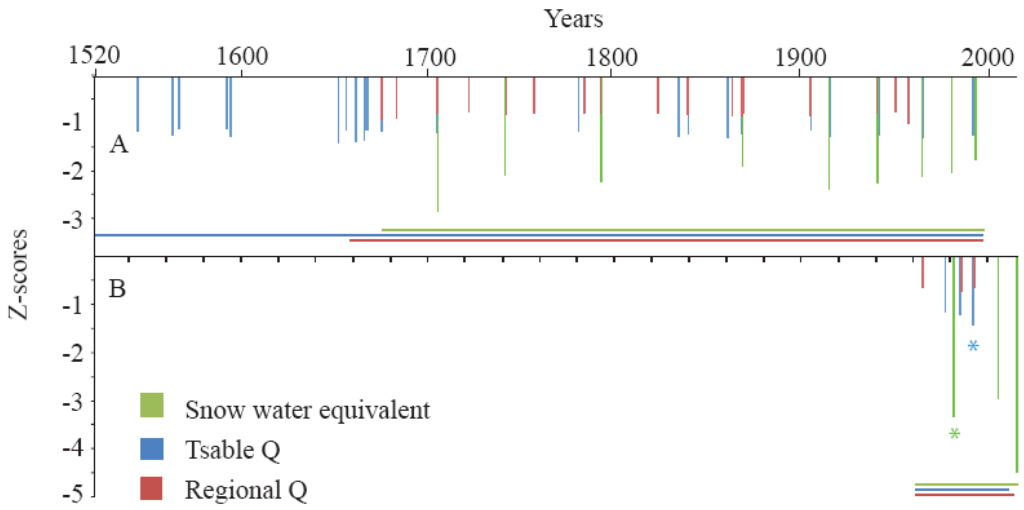

Figure 5.2: Comparison of reconstructed and instrumental bottom fifth percentile values of the reconstructions. (A) Reconstructed bottom fifth percentile years, as z-scores calculated from the full period reconstructed record and plotted as departures from the mean (zero). (B) Instrumental record bottom fifth percentile years, as z-scores calculated from the full period reconstructed record and plotted as departures from zero. Scores for the instrumental data were calculated from the reconstructed mean and standard deviation so that they may be interpreted presented relative to the long-term reconstruction variance. Asterisks identify years when bottom fifth percentile reconstructed values are corroborated by observation data. Horizontal coloured bars delineate data periods.

5.4 Comparison within the instrumental period

The ability of each reconstruction to capture extreme values in the corresponding instrumental record can inform on model accuracy. Bottom fifth percentile values for the observational records are plotted as departures from the mean (zero) in Figure 5.2B. Comparison of Figures 5.2A and 5.2B shows that lowest reconstructed and observed years only match in 1992 and in 1981 (Tsable River and SWE respectively, noted with asterisks). None of the lowest values in the regionalized streamflow reconstruction and instrumental data correspond.

In other words, only very extreme low values 'synch up' among records within the instrumental data period. The lowest instrumental values for the regionalized record were less extreme than any in the reconstructed record, and they were likely not tracked by the regionalized streamflow reconstruction for that reason. Both 1992 and 1981 were the lowest instrumental data values for the SWE and Tsable River streamflow data, respectively, and both were registered as extreme by their respective reconstructions. Unfortunately, data limitations prevented a comparison of the reconstruction models and/or instrumental streamflow data in the most extreme SWE year, 2015, which would likely have shown strong cohesion among records.

A final point of interest is that the low snowpack in 1981 did not correspond with low summer runoff in either the reconstructed or observed records. Inspection of regionalized summer precipitation data (see Chapter 4 for data description) suggests that high summer rainfall in that year likely buffered low snow meltwater quantities to prevent summer drought. While this scenario does not occur at any other time in the reconstruction histories, it may suggest that in years where low SWE and drought correspond there was likely limited summer rainfall.

5.5 Conclusion

Separate comparisons of the observational and reconstructed data demonstrate that there is a strong association between high SWE and high streamflow years in both sets of records. There is also strong agreement between low SWE and drought years; almost all of the low SWE years were accompanied by streamflow drought. What is more interesting is that many streamflow droughts were not accompanied by low SWE. In the

case of the Tsable River reconstruction this is probably due to more bottom fifth percentile years being flagged in the longer Tsable River record than in the shorter SWE record. However, the regionalized streamflow reconstruction is a similar length to the SWE reconstruction and a similar number of low values are flagged, yet they do not correspond with low snow years. This observation supports the argument that incorporation of PDSI as a model predictor allowed the regionalized streamflow reconstruction to 'tune in' to both streamflow droughts caused by low snow meltwater, and streamflow droughts caused by hot and dry summer conditions. An important finding of this analysis is that reconstructions of summer runoff in hybrid streams based solely on snowmelt proxies might 'miss' drought years, since droughts can be provoked by hot and dry summer conditions even if snowmelt is normal (as seen in the observation data in 1985 and 1992).

Comparison of the reconstructed and instrumental datasets within the common period of record highlights that the reconstructions are most effective at tracking extreme high and low SWE and streamflow years; only the lowest instrumental values are also very low in the reconstructions. The long-term reconstructed records also demonstrated strongest synchronicity, in the most extreme years. This finding is promising since historical extremes are critical for informing and improving water management strategies.

Chapter 6 Conclusion

6.1 Introduction

This dissertation presents three dendrohydrological reconstructions developed using networks of energy-limited TR data that are sensitive to annual snowpack fluctuations and, in the regional runoff model, a PDSI reconstruction. The reconstructions are for the south coastal B.C. region, and include a 322-year record of annual SWE, a 477-record of summer streamflow in a small hybrid-regime river (Tsable River), and a 332-year record of 'regionalized' summer streamflow among four hybrid watersheds. The reconstructions were developed to provide a long-term context for understanding recent snowpack declines and summer streamflow drought, and to inform more accurate water management strategies.

6.2 Main research results

1. TR records that are energy-limited by spring snowpacks have been little used in dendroclimatology. I demonstrated that large networks of this type of tree-ring data could be developed for south coastal B.C. Successful crossdating among the TR chronologies and time-stable relationships with various snow records suggest large-scale synchronicity both in regional snowpack variations and their influence on the growth of high-elevation conifer trees. The TR-snow relationship is strong enough to form a basis for paleohydrological models of snow and snow-influenced processes. See Chapter 2.

2. Evidence from a small number of TR chronologies suggests the correlation between TRs and snow becomes non-significant from around the mid-1990s to present. This loss of association may be due to less snow and earlier, warmer, springs leading to snowpack depth being replaced by spring temperature as the main control on growing season length. I advise that future studies using TRs with a similar growth limitation carefully evaluate the stability of the TR-snow relationship over the last 15 years. This limitation may prevent model calibration

on the most interesting (extreme) years and prevent comparison of extreme years with past conditions, as was the case for this research. See Chapter 2.

3. The reconstruction of Vancouver Island SWE (56% explanatory power) demonstrated that record low spring snow measurements in 2015 were likely lower than in any year since 1675. The reconstruction is remarkably effective at approximating the full range of instrumental SWE variance, especially extreme years. See Chapter 2.

4. I demonstrate that by targeting specific runoff regimes and seasons (*e.g.* influenced by snowmelt during summer), energy-limited snow-sensitive TR records can be powerful for reconstructing streamflow and summer streamflow drought. Despite the complex hydrological setting and small sizes of the watersheds that were modeled, my streamflow reconstructions are of comparable quality to those developed using the traditional approach based on moisture-limited trees in arid settings. See Chapters 3 and 4.

5. Both the single-stream and regionalized streamflow reconstructions suggest droughts occurred in the past that were more extreme than any documented within hydrometric data records. Recent droughts are therefore not anomalous relative to the past several hundred years, and should be anticipated within water management strategies. Worst-case scenario natural droughts compounded by land use change and climate change could cause droughts more severe than any in the past ~300-400 years. See Chapters 3 and 4.

6. Combining proxies for both total annual snowpack and summer temperature and aridity as model predictors was the most successful approach for estimating summer streamflow droughts. The suite of dendrohydrological reconstructions developed for this research document synchronous very high and very low snow

and streamflow years, making them particularly valuable for estimating more accurate extreme event probabilities. See Chapter 5.

6.3 Conclusion

The paleohydrological records developed for this dissertation suggest that: 1) low SWE in 2015 was likely unprecedented over several centuries; and, 2) streamflow droughts, at both stream- and regional-scales, have been more severe in the past than during the instrumental period. These results underscore both the magnitude of hydroclimatic change in recent decades, and the critical need for long-term estimates of hydroclimatic variability for informing accurate water management strategies, including water supply forecasting and water storage planning, in south coastal B.C.

The reconstruction models are based on networks of annual TR width data from energy-limited, snowpack-sensitive conifer trees. One of the models incorporates a TR-derived reconstruction of PDSI, which serves as a proxy for summer temperature and aridity, as a model predictor (Cook *et al.* 1999). When specific runoff regimes and seasons were targeted, these snow-sensitive records were powerful for reconstructing snowpack and runoff in a highly complex hydrological setting, and for small watersheds. To the author's knowledge these are the first paleohydrological reconstructions of their kind, and they provide the longest, most statistically robust, annually-resolved record of historical snow and streamflow in B.C.

The reconstruction of Vancouver Island May 1 SWE suggests that spring snowpacks in 2015 were lower than in any year since 1675. Snowpack meltwater is the primary source of summer surface and groundwater on Vancouver Island, thus snowpack declines are closely linked to streamflow and hydrological drought. The reconstruction of summer streamflow for Tsable River suggests since 1520, twenty-one droughts occurred that were more extreme than recent "severe" events like those in 2003 and 2009. At a regional scale, sixteen reconstructed natural droughts were more extreme than any within the instrumental period. Unfortunately, the impact of record-low snowpacks in 2015 on streamflow, and the anomalousness of the extreme streamflow drought experienced throughout coastal B.C. in that year, could not be evaluated due to a lack of hydrometric data. Given the unprecedented nature of the low snowpack in 2015 within a multi-century

context, and record-high summer temperatures in that year, it would be reasonable to surmise that regional streamflow drought severities in 2015 exceeded those that have occurred in the last several hundred years.

Both snowpack and streamflow appear to be associated with variability in the PDO over multiple centuries, especially during cool phases of the oscillation that promote deep snowpacks and enhanced summer runoff. It is important to note that while climate oscillations like the PDO and ENSO may play a part in recent snowpack declines and streamflow droughts, this does not preclude the role of global climate warming in triggering these events. For example, while climate change has caused snowpack and streamflow declines by bringing about warmer winters and warmer and drier summers, it may also have amplified the PDO and ENSO (Diaz *et al.* 2001; D'Arrigo *et al.* 2005; Collins *et al.* 2010).

Combining proxies for both total annual snowpack and summer temperature and aridity as model predictors was the most successful approach for estimating summer streamflow droughts. This approach was taken with the regional summer streamflow reconstruction, which had the best model explanatory power, the strongest calibration statistics, and the ability to document droughts in years that did not have low SWE. Taken together, the reconstructions are most accurate at documenting extreme high and low snow and streamflow years. This is encouraging since quantifying historical extremes is most important for developing more water management strategies in south coastal B.C. The environmental reconstructions and methods developed for this research can be used by water managers to: 1) extend the lengths of datasets used for assessing drought probabilities; and, 2) minimize the likelihood of underestimating worst-case scenario natural droughts.

6.4 Future research

1. There is excellent potential for expanding the use of energy-limited TR data for dendrohydrological reconstruction in non-arid environments, within B.C. and globally. This will most likely be possible in settings with very deep annual snowpacks, and efforts should focus on places where snowmelt and snow-influenced streamflow are important for human water use, industry and

agriculture, and stream ecology. This type of TR record would likely be an effective predictor of summer runoff in snowmelt-dominated watersheds.

2. Phenological studies should be conducted to provide concrete evidence that the cambial growth of energy-limited TRs that are sensitive to snow initiates at a threshold low snowpack depth. A similar analysis was conducted by Vaganov *et al.* (1999) to show that snowpack depths in subarctic Eurasia overcame the influence of growing season temperature in limiting annual radial growth in some trees.

3. Based on the TR chronologies developed and analyzed for this research, it is still unclear why some sites promote snowpack-related energy-limitation and some do not. Previous studies on this type of annual growth limitation report that mountain hemlock trees growing above 1000 m asl are typically sensitive to snow, and that the influence of snow overwhelms the role of aspect in enhancing or minimizing the climate-growth signal (Marcinkowski *et al.* 2015). I found that many mountain hemlock chronologies located above 1000 m asl were insensitive to snowpack depth. Further study of tree-level site and snow characteristics is required to focus sampling efforts on snow-limited forest stands.

4. I found that combining total annual snowpack and summer temperature and aridity proxies optimized summer streamflow drought reconstructions. Future studies might capitalize on local moisture-limited records from Douglas fir (*Pseudotsuga menzeisii* (Mirb.) Franco) or other moisture-limited TR records as summer temperature and aridity proxies, rather than using a reconstructed dataset like the PDSI reconstruction. The use of widely distributed Douglas fir could expand the application of this modeling approach beyond the range of existing PDSI reconstructions.

Bibliography

Agriculture and Agri-Food Canada. (2014). *2014 Annual Review of Agroclimate Conditions Across Canada*. Retrieved May 1, 2015, from http://www.agr.gc.ca/eng/?id=13995 80648022

Axelson, J., Sauchyn, D. J., & Barichivich, J. (2009). New reconstructions of streamflow variability in the South Saskatchewan River basin from a network of tree ring chronologies, Alberta, Canada. *Water Resources Research, 45*(W09422), doi:10.1029/2008WR007639.

Barnett, T., Malone, R., Pennell, W., Stammer, D., Semter, B., & Washington, W. (2004). The effects of climate change on water resources in the West: introduction and overview. *Climatic Change, 62*(1), 1–11.

B.C. Conservation Foundation. (2006). *Vancouver Island Focus Watersheds: Trent and Tsable rivers*. Retrieved September 25, 2013, from http://www.bccf.com/steelhead /focus5.htm

B.C. Ministry of Environment. (2010). *Preparing for Climate Change: British Columbia's Adaptation Strategy*. Retrieved September 25, 2013, from http://www2.gov.bc.ca/gov/ Download Asset?assetId=29CDF35B126E483A966 B0D5DAE2E3E38& filename=adaptation_strategy .pdf

B.C. Ministry of Environment, Water Protection and Sustainability Branch. (2013) *A Water Sustainability Act for B.C.: legislative proposal overview.* Retrieved October 14, 2014, from http://engage.gov.bc.ca/watersustainabilityact/files/2013/10/WSA_ overview_web.pdf

B.C. Ministry of Forests, Lands and Natural Resource Operations. (2014, Jul. 17). Water Supply and Streamflow Conditions Bulletin. Retrieved July 19, 2014, from http://bcrfc.env.gov.bc.ca/bulletins/watersupply/index-watersupply.htm

B.C. Ministry of Forests, Lands, and Natural Resource Operations (2015) Water Supply and Streamflow Conditions Bulletin. Retrieved August 15, 2015, from http://bcrfc.env.gov.bc.ca/bulletins/watersupply/index-watersupply.htm

B.C. Ministry of Water, Land and Air Protection. (2002). *Indicators of Climate Change for British Columbia, 2002.* Retrieved September 25, 2013, from http://www. env.gov.bc.ca/cas/pdfs/indcc .pdf

B.C. River Forecast Centre. (2015). *Snow Survey and Water Supply Bulletin*. Retrieved June 20, 2015, from http://bcrfc.env.gov.bc.ca/bulletins/watersupply/current.htm

B.C. Water Sustainability Act. (2015). *Water Sustainability Act: ensuring our water stays healthy and secure.* Retrieved Oct 1, 2015, from http://engage.gov.bc.ca/watersustainabilityact/the-proposal/

B.C. Wildfire Service (2015). *Summary of Previous Fire Seasons.* Retrieved Oct 1, 2015, from http://bcwildfire.ca/history/summaryarchive.htm

Beaulieu, M., Schreier, H., & Jost, G. (2012). A shifting hydrological regime: a field investigation of snowmelt runoff processes and their connection to summer base flow, Sunshine Coast, British Columbia. *Hydrological Processes*, *26*(17), 2672–2682.

Belmecheri, S., Babst, F., Wahl, E. R., Stahle, D. W., & Trouet, V. (2015). Multi-century evaluation of Sierra Nevada snowpack. *Nature Climate Change*. doi:10.1038/nclimate2809

Beriault, A. L., & Sauchyn, D. J. (2006). Tree-ring reconstructions of streamflow in the Churchill River Basin, northern Saskatchewan. *Canadian Water Resources Journal*, *31*(4), 249–262.

Biondi, F., Gershunov, A., & Cayan, D. R. (2001). North Pacific decadal climate variability since 1661. *Journal of Climate*, *14*(1), 5-10.

Biondi, F., & Strachan, S. (2012). Dendrohydrology in 2050: Challenges and opportunities. In Grayman W., Loucks, D., and Saito, L. (Eds.) *Toward a Sustainable Water Future: Visions for 2050 (*pp. 355-362). Reston, VA: American Society of Civil Engineers.

Bonfils, C., Santer, B., Pierce, D., Hidalgo, H., Bala, G., Das, T., Barnett, T., Cayan, D., Doutriaux, C., Wood, A., Mirin, A., & Nozawa, T. (2008). Detection and attribution of temperature changes in the mountainous western United States. *Journal of Climate, 21*(23), 6404–6424.

Boninsegna, A., Argolla, J., Aravena, J-C, Barichivich, J., Christie, D., Ferrera, M. E., Lara, A., Le Quesne, C., Luckman, B. H., Masiokas, M. H., Morales, M. S., Oliviera, J. M., Roig, F., Srur, A., Villalba, R. (2009). Dendroclimatological reconstructions in South America: a review. *Palaeogeography, Palaeoclimatology, Palaeoecology, 281*(3-4), 210-228.

Bonsal, B., & Shabbar, A. (2008). Impacts of large-scale circulation variability on low streamflows over Canada: a review. *Canadian Water Resources Journal*, *33*(2), 137-154.

Box, G., & Jenkins, G. (1976). *Time Series Analysis: Forecasting and Control, Revised Edition*. Oakland CA: Holden-Day.

Bunn, A. G. (2008). A dendrochronology program library in R (dplR). *Dendrochronologia*, *26*(2), 115–124.

Canadian Foundation for Climate and Atmospheric Sciences. (2010, Mar.). *Annual Progress Report for the Drought Research Initiative (DRI)*. Retrieved from http://www.drinetwork.ca /pdf/2009_DRI_Annual_Report.pdf

Case, R. A., & MacDonald, G. M. (2003). Tree ring reconstructions of streamflow for three Canadian prairie rivers. *JAWRA Journal of the American Water Resources Association*, *39*(3), 703–716.

Case, M. J., & Peterson, D. L. (2007). Growth-climate relations of lodgepole pine in the North Cascades National Park, Washington. *Northwest Science*, *81*(1), 62-75.

Collins, M., An, S. I., Cai, W., Ganachaud, A., Guilyardi, E., Jin, F. F., ... & Wittenberg, A. (2010). The impact of global warming on the tropical Pacific Ocean and El Niño. *Nature Geoscience*, *3*(6), 391-397.

Cook, E. R., & Holmes, R. L. (1986). Users manual for program ARSTAN. *Laboratory of Tree-Ring Research, University of Arizona, Tucson, USA*.

Cook, E., & Kairiūkštis, L. (Eds.) (1990). *Methods of Dendrochronology: Applications in the Environmental Sciences.* Netherlands: Kluwer Aacademic Publishers.

Cook, E. R., Meko, D. M., Stahle, D. W., & Cleaveland, M. K. (1999). Drought Reconstructions for the Continental United States. *Journal of Climate*, *12*(4), 1145–1162.

Cook, E. R., & Peters, K. (1981). The smoothing spline: a new approach to standardizing forest interior tree-ring width series for dendroclimatic studies. *Tree-Ring Bulletin*, *41*(1), 45-53.

Cook, E. R., Woodhouse, C., Eakin, C. M., Meko, D. M., & Stahle, D. W. (2004). Long-term aridity changes in the western United States. *Science*, *306*(5698), 1015–1018.

Coppola, A., Leonelli, G., Salvatore, M. C., Pelfini, M., & Baroni, C. (2012). Weakening climatic signal since mid-20th century in European larch tree-ring chronologies at different altitudes from the Adamello-Presanella Massif (Italian Alps). *Quaternary Research*, *77*(3), 344-354.

Coulthard, B. & Smith, D. J. (in press). A 477-year dendrohydrologcial assessment of drought severity for Tsable River, Vancouver Island, British Columbia, Canada. *Hydrological Processes.*

Cowichan Watershed Board. (2015). Cowichan Watershed Board: supply and demand. Retrieved September 22, 2015, http://www.cowichanwatershedboard.ca/content/supply-and-demand

CVRD. (2015). Cowichan Valley Regional District: living the new normal. Retrieved September 22, 2015, from http://cvrdnewnormalcowichan.ca/

Craig, J. D. C. (2004, December). Construction of artificial fish habitat in the Chemainus River, 2004. *Report prepared for BC Conservation Foundation: Greater Georgia Basin Steelhead Recovery Plan, Nanaimo, BC.* Retrieved September 25, 2013, from http://www.bccf.com/ steelhead /pdf/Chemainus_R _artificial_fish_habitat_2004%20new.pdf

D'Agostino, R. B., & Pearson, E. S. (1973). Tests for Departure from Normality. *Biometrika* 60, 613–22.

Daly, C., Gibson, W. P., Taylor, G. H., Johnson, G. L., & Pasteris, P. (2002). A knowledge-based approach to the statistical mapping of climate. *Climate Research*, *22*(2), 99-113.

D'Arrigo, R., Wilson, R., Deser, C., Wiles, G., Cook, E., Villalba, R., Tudhope, A., Cole, J., & Linsley, B. (2005). Tropical-north Pacific climate linkages over the past four centuries. *Journal of Climate*, *18*(24), 5253-5265.

D'Arrigo, R., Wilson, R., Liepert, B., & Cherubini, P. (2008). On the 'divergence problem'in northern forests: a review of the tree-ring evidence and possible causes. *Global and Planetary Change*, *60*(3), 289-305.

Dawdy, D., & Matalas, N. (1964). Statistical and probability analysis of hydrologic data, part III: Analysis of variance, covariance and time series. In V. T. Chow (Ed.), *Handbook of Applied Hydrology, A Compendium of Water-Resources Technology* (pp. 8.68-8.90). New York, NY: McGraw-Hill.

Déry, S. J., Stahl, K., Moore, R. D., Whitfield, P. H., Menounos, B., & Burford, J. E. (2009). Detection of runoff timing changes in pluvial, nival, and glacial rivers of western Canada. *Water Resources Research*, *45*(W06701), doi:10.1029/2009WR008244.

Diaz, H. F., Hoerling, M. P., & Eischeid, J. K. (2001). ENSO variability, teleconnections and climate change. *International Journal of Climatology*, *21*(15), 1845-1862.

Duffy, A. (2015). Drought hits Vancouver Island cattle producers. *The Times Colonist*. Retrieved Oct 1, 2015, from http://www.timescolonist.com/business/drought-hits-vancouver-island-cattle-producers-1.2031592

Dunn, O. J. (1961). Multiple comparisons among means. *Journal of the American Statistical Association*, *56*(293), 52-64.

Earle, C. (1993). Asynchronous droughts in California streamflow as reconstructed from tree rings. *Quaternary Research*. *39*(3), 290-299.

Eaton, B., & Moore, R. (2010). Regional hydrology. In R. G. Pike, T. E. Redding, R. D. Moore, R. D Winkler, & K. D. Bladon (Eds.), *Compendium of Forest Hydrology and Geomorphology in British Columbia* (pp. 85-110). Victoria, BC: Ministry of Forests and Range Research Branch / FORREX Forest Research Extension Partnership.

Engeland, K., Hisdal, H., & Frigessi, A. (2004). Practical extreme value modelling of hydrological floods and droughts: a case study. *Extremes*, *7*(1), 5-30.

Esper, J., & Frank, D. (2009). Divergence pitfalls in tree-ring research. *Climatic Change*, *94*(3), 261-266.

Ettl, G. J., & Peterson, D. L. (1995*a*). Growth response of subalpine fir (*Abies lasiocarpa*) to climate in the Olympic Mountains, Washington, USA. *Global Change Biology*, *1*(3), 213-230.

Ettl, G. J., & Peterson, D. L. (1995*b*). Extreme climate and variation in tree growth: individualistic response in subalpine fir (*Abies lasiocarpa*). *Global Change Biology*, *1*(3), 231-241.

Fleming, S. W., & Sauchyn, D. J. (2013). Availability, volatility, stability, and teleconnectivity changes in prairie water supply from Canadian Rocky Mountain sources over the last millennium. *Water Resources Research*, *49*(1), 64-74.

Fleming, S. W., Whitfield, P. H., Moore, R. D., & Quilty, E. J. (2007). Regime-dependent streamflow sensitivities to Pacific climate modes cross the Georgia–Puget transboundary ecoregion. *Hydrological Processes*, *21*(24), 3264–3287.

Fritts, H. C. (1976). *Tree Rings and Climate*. London: UK. Academic Press.

Fritts, H. C. (1990). Modeling tree-ring and environmental relationships for dendrochronological analysis. In R. Dixon, R. Meldahl, G. Ruark, & W. Warren (Eds.), *Process Modeling of Forest Growth Responses to Environmental Stress* (pp. 368-382). Portland, OR: Timber Press.

Fritts, H. C., Guiot, J., & Gordon, G. A. (1990). Verification. In E. R. Cook & L. Kairiūkštis (Eds.), *Methods of Dendrochronology: Applications in the Environmental Sciences.* (pp. 178-184). Netherlands: Kluwer Aacademic Publishers.

Fye, F. K., Stahle, D. W., & Cook, E. R. (2003). Paleoclimatic analogs to twentieth-century moisture regimes across the United States. *Bulletin of the American Meteorological Society*, *84*(7), 901-909.

Gaboury, M., & McCulloch, M. (2002, September). Fish habitat restoration designs for five east Vancouver Island watersheds. *Report prepared for BC Conservation Foundation, Nanaimo, BC*. Retrieved September 25, 2013, from http://a100.gov.bc.ca/appsdata/acat/ documents/r5855/FishHabitatRestoration Designsfor5ECVIWatersheds_1143409089471_d65067ddb3744fadbb2db077cc5c960e.pdf

Gedalof, Z., Peterson, D., & Mantua, N. (2004). Columbia river flow and drought since 1750. *JAWRA Journal of the American Water Resources Association, 40*(6), 1579–1592.

Gedalof, Z., & Smith, D. J. (2001a). Dendroclimatic response of mountain hemlock (*Tsuga mertensiana*) in Pacific North America. *Canadian Journal of Forest Research*, *31*(2), 322–332.

Gedalof, Z., & Smith, D. J. (2001b). Interdecadal climate variability and regime-scale shifts in Pacific North America. *Geophysical Research Letters, 28*(8), 1515-1518.

Gou, X., Deng, Y., Chen, F., Yang, M., Fang, K., Gao, L., Yang, T., & Zhang, F. (2010). Tree ring based streamflow reconstruction for the Upper Yellow River over the past 1234 years. *Chinese Science Bulletin*, *55*(36), 4179–4186.

Granger, C. W. (1966). On the typical shape of an econometric variable. *Econometrica, 34*(1):150-161.

Graumlich, L., & Brubaker, L. (1986). Reconstruction of annual temperature (1590–1979) for Longmire, Washington, derived from tree rings. *Quaternary Research*, *25*(2), 223-234.

Griffin, D., & Anchukaitis, K. J. (2014). How unusual is the 2012–2014 California drought? *Geophysical Research Letters*, *41*(24), 9017-9023.

Grissino-Mayer, H. D. (2001). Research report evaluating crossdating accuracy: a manual and tutorial for the computer program COFECHA. *Tree-Ring Research, 57*(1), 115–124.

Hamlet, A. F., & Lettenmaier, D. P. (1999). Columbia River Streamflow Forecasting Based on ENSO and PDO Climate Signals. *Journal of Water Resources Planning and Management*, *125*(6), 333–341.

Hansen-Bristow, K. (1986). Influence of increasing elevation on growth characteristics at timberline. *Canadian Journal of Botany*, *64*(11), 2517-2523.

Hart, S. J., Smith, D. J., & Clague, J. J. (2010). A multi-species dendroclimatic reconstruction of Chilko River streamflow, British Columbia, Canada. *Hydrological Processes*, *24*(19), 2752–2761.

Hayes, M., Svoboda, M., Le Comte, D., Redmond, K. T., & Pasteris, P. (2005). Drought monitoring: New tools for the 21st century. In D. Wilhite (Ed.) *Drought and Water Crises*: *Science, Technology, and Management Issues.* Boca Raton, FL: Taylor and Francis.

Holmes, R. L. (1983). Computer-assisted quality control in tree-ring dating and measurement. *Tree-Ring Bulletin*, *43*(1), 69-78.

Holton, J. R., & Dmowska, R. (1989). *El Niño, La Niña, and the Southern Oscillation* (Vol. 46). S. G. Philander (Ed.). Academic Press.

Hume, S. (2015). Drought conditions threaten fish habitat, pulp mill jobs. *The Vancouver Sun*. Retrieved Oct 1, 2015, from http://www.vancouversun.com/Stephen+Hume+ Drought+ conditions+threaten+fish+habitat+pulp+mill+jobs/11160839/story.html?__ lsa=6e17-b4f4

Huntington, T. G. (2006). Evidence for intensification of the global water cycle: review and synthesis. *Journal of Hydrology*, *319*(1), 83-95.

Field, C. B. (Ed.). (2014). *Climate change 2014: impacts, adaptation, and vulnerability* (Vol. 1). IPCC.

Jarrett, P. (2008). *A dendroclimatic investigation of moisture variability and drought in the Greater Victoria water supply area, Vancouver Island, British Columbia*. Unpublished MSc. thesis, University of Victoria, Victoria B.C., Canada. Retrieved March 4, 2015, from https://dspace.library.uvic.ca//handle/1828/883

Jonas, T., Marty, C., & Magnusson, J. (2009). Estimating the snow water equivalent from snow depth measurements in the Swiss Alps. *Journal of Hydrology*, *378*(1), 161-167.

Kachigan, S. (1982). *Multivariate Statistical Analysis: a Conceptual Introduction*. New York, NY: Radius Press.

Kay, J., & Blecic, B. (1996, April). *Chemainus River Water Allocation Plan.* Nanaimo, BC: Province of British Columbia Ministry of Environment, Lands, and Parks.

Kiffney, P., Bull, J., & Feller, M. (2002). Climatic and hydrologic variability in a coastal watershed of southwestern British Columbia. *JAWRA Journal of the American Water Resources Association*, *38*(5), 1437-1451.

Klinka, K., Pojar, J., & Meidinger, D. (1991). Revision of biogeoclimatic units of coastal British Columbia. *Northwest Science, 65*(1), 32-47.

Larocque, S. J., & Smith, D. J. (2005). A dendroclimatological reconstruction of climate since AD 1700 in the Mt. Waddington area, British Columbia Coast Mountains, Canada. *Dendrochronologia, 22*(2), 93-106.

Laroque, C. P (2002). *Dendroclimatic response of high-elevation conifers, Vancouver Island, British Columbia*. Unpublished Ph.D. thesis, University of Victoria, Victoria B.C., Canada.

Laroque, C. P., & Smith, D. J., (1999). Tree-ring analysis of yellow cedar (*Chamaecyparis nootkatensis*) on Vancouver Island British Columbia. *Canadian Journal of Forest Research, 29*(1), 115–123.

Laroque, C. P., & Smith, D. J. (2003). Radial-growth forecasts for five high-elevation conifer species on Vancouver Island, British Columbia. *Forest Ecology and Management, 183*(1), 313-325.

Li, J., Chen, F., Cook, E. R., Gou, X., & Zhang, Y. (2007). Drought reconstruction for north central China from tree rings: the value of the Palmer drought severity index. *International Journal of Climatology, 27*(7), 903-909.

Lill, A. (2002, September). Greater Georgia Basin steelhead recovery action plan. *Report prepared for BC Conservation Foundation: Greater Georgia Basin Steelhead Recovery Plan, Nanaimo, BC.* Retrieved September 25, 2013, from http://www.bccf.com/steelhead /pdf/Steelheadreport092702.pdf

Loaiciga H., Haston, A., & Michaelsen, J. (1993). Dendrohydrology and long-term hydrologic phenomena. *Reviews of Geophysics, 31*(2), 151-171.

Loukas, A., Vasiliades, L., & Dalezios, N. (2002). Climatic impacts on the runoff generation processes in British Columbia, Canada. *Hydrology and Earth System Sciences Discussions, 6*(2), 211-228.

Luckman, B. H., & Wilson, R. J. S. (2005). Summer temperatures in the Canadian Rockies during the last millennium: a revised record. *Climate Dynamics, 24*(2-3), 131-144.

MacDonald, G. M., & Case, R. A. (2005). Variations in the Pacific Decadal Oscillation over the past millennium. *Geophysical Research Letters*, L08 703. doi:10.1029/2005GL022478

Mantua, N. (2002). Pacific-Decadal Oscillation. In M. MacCracken and J. S. Perry (Eds.), *Encyclopedia of Global Environmental Change*. (Vol. 1. pp. 592-594). Chichester: UK. John Wiley and Sons.

Mantua N., Tohver, I., & Hamlet, A. (2010). Climate change impacts on streamflow extremes and summertime stream temperature and their possible consequences for freshwater salmon habitat in Washington State. *Climatic Change, 102*(1-2), 187-223.

Marcinkowski, K., Peterson, D. L., & Ettl, G. J. (2015). Nonstationary temporal response of mountain hemlock growth to climatic variability in the North Cascade Range, Washington, USA. *Canadian Journal of Forest Research, 45*(999), 676-688.

Margolis, E., Meko, D., & Touchan, R. (2011). A tree-ring reconstruction of streamflow in the Santa Fe River, New Mexico. *Journal of Hydrology, 397*(1), 118-127.

Mays, L. M. (2005). *Water Resources Engineering*. New York, NY: Wiley & Sons.

McGregor, S., Timmermann, A., & Timm, O. (2010). A unified proxy for ENSO and PDO variability since 1650. *Climate of the Past, 6*(1), 1-17.

Means, J. E. (1990). Tsuga mertensiana (Bong.) Carr. mountain hemlock. *Silvics of North America, 1*, 623-631.

Meko, D. M. (2006). Tree-ring inferences on water-level fluctuations of Lake Athabasca. *Canadian Water Resources Journal, 31*(4), 229-248.

Meko, D. M., & Graybill, D. (1995). Tree-ring reconstruction of upper Gila River discharge. *JAWRA Journal of the American Water Resources Association, 31*(4), 605-616.

Meko, D. M., Therrell, M., Baisan, C., & Hughes, M. K. (2001). Sacramento River flow reconstructed to AD. 869 from tree rings. *Journal of the American Water Resources Association, 37*(4), 1029–1039.

Meko, D. M, Touchan, R., & Anchukaitis, K. (2011). Seascorr: a MATLAB program for identifying the seasonal climate signal in an annual tree-ring time series. *Computers & Geosciences, 37*(9), 1234-1241.

Meko, D. M., & Woodhouse, C. A. (2005). Tree-ring footprint of joint hydrologic drought in Sacramento and Upper Colorado river basins, western USA. *Journal of Hydrology, 308*(1), 196-213.

Meko, D. M., & Woodhouse, C. A. (2011). Application of streamflow reconstruction to water resources management. In M. K. Hughes, T. W. Swetnam, & H. F. Diaz (Eds.), *Dendroclimatology* (pp. 231-261). Netherlands: Springer.

Michaelsen, J. (1987). Cross-validation in statistical climate forecast models. *Journal of Climate and Applied Meteorology, 26*(11), 1589-1600.

Mishra, A., & Coulibaly, P. (2009). Developments in hydrometric network design: A review. *Reviews of Geophysics*, 47(RG2001), doi:10.1029/2007RG000243.

Moore, R. D., Allen, D. M. & Stahl, K. (2007, August). Climate change and low flows: influences of groundwater and glaciers. *Final report prepared for Climate Change Action Fund, Natural Resources Canada, Vancouver, BC.* Retrieved September 25, 2013, from https://www.sfu.ca/personal/ dallen/ CCAF_ A875-FinalReport.pdf

Mosteller, F., & Tukey, J. (1977). *Data Analysis and Regression: a Second Course in Statistics.* Reading, MA: Addison-Wesley Publishing Company.

Mote, P. W., Parson, E. A., Hamlet, A. F., Keeton, W. S., Lettenmaier, D., Mantua, N., Miles, E. L., Peterson, D. W., Peterson, D. L., Slaughter, R., & Snover, A. K. (2003). Preparing for climatic change: the water, salmon, and forests of the Pacific northwest. *Climatic Change*, *61*(1-2), 45–88.

Nelitz, M., Alexander, C. A., Wieckowski, K., & Council, P. F. R. C. (2007, September). Helping Pacific salmon survive the impact of climate change on freshwater habitats: Case Studies. *Final report prepared for Pacific Fisheries Resource Conservation Council, Vancouver, BC.* Retrieved from https://www.sfu.ca/personal/dallen/ CCAF_ A875-FinalReport.pdf

Newcombe, R. G. (1998). Interval Estimation for the difference between independent proportions: comparison of eleven methods. *Statistics in Medicine 17*(8), 873–890.

North, G. R., Bell, T. L., Cahalan, R. F., & Moeng, F. J. (1982). Sampling errors in the estimation of empirical orthogonal functions. *Monthly Weather Review*, *110*(7), 699-706.

Norton, D. A., & Palmer, J. G. (1992). Dendroclimatic evidence from Australasia. In R. S. Bradley, & P. D. Jones (Eds.) *Climate Since AD 1500* (pp. 463-481). New York, NY: Routledge.

Pachauri, R. K., Allen, M. R., Barros, V. R., Broome, J., Cramer, W., Christ, R., ... & van Vuuren, D. (2014). Climate Change 2014: Synthesis Report. Contribution of Working Groups I, II and III to the Fifth Assessment Report of the Intergovernmental Panel on Climate Change.

Palmer, W. (1965). *Meteorological Drought*. Washington, DC: US Department of Commerce, Weather Bureau.

Pederson, G. T., Gray, S. T., Woodhouse, C. A., Betancourt, J. L., Fagre, D. B., Littell, J. S., Watson, E., Luckman, B. H., & Graumlich, L. J. (2011). The unusual nature of recent snowpack declines in the North American Cordillera. *Science, 333*(6040), 332-335.

Pederson, N., Jacoby, G. C., D'Arrigo, R. D., Cook, E. R., Buckley, B. M., Dugarjav, C., & Mijiddorj, R. (2001). Hydrometeorological reconstructions for Northeastern Mongolia derived from tree rings: 1651-1995. *Journal of Climate, 14*(5), 872-881.

Peng, C., Ma, Z., Lei, X., Zhu, Q., Chen, H., Wang, W., Liu, S., Li, W., Fang., X., & Zhou, X. (2011). A drought-induced pervasive increase in tree mortality across Canada's boreal forests. *Nature Climate Change, 1*(9), 467-471.

Peterson, D. W., & Peterson, D. L. (1994). Effects of climate on radial growth of subalpine conifers in the North Cascade Mountains. *Canadian Journal of Forest Research, 24*(9), 1921-1932.

Peterson, D. W., & Peterson, D. L. (2001). Mountain hemlock growth responds to climatic variability at annual and decadal time scales. *Ecology, 82*(12), 3330–3345.

Peterson, D. W., Peterson, D. L., & Ettl, G. J. (2002). Growth responses of subalpine fir to climatic variability in the Pacific Northwest. *Canadian Journal of Forest Research, 32*(9), 1503-1517.

Pike, R. G., Spittlehouse, D. L., Bennett, K. E., Egginton, V. N., Tschaplinski, P. J., Murdock, T. Q., & Werner, A. T. (2008). Climate change and watershed hydrology: Part I–Recent and projected changes in British Columbia. *Streamline Watershed Management Bulletin, 11*(2), 1-8.

Pike, R., Bennett, K., Redding, T., Werner, A. T., Spittlehouse, D. L., Moore, R. D., Murdock, T. Q., Beckers, J., Smerdon, B. D., Bladon, K. D., Foord, V. N., Campbell, D. A., Tschaplinski, P. J. (2010). Climate change effects on watershed processes in British Columbia. In R. G. Pike, T. E. Redding, R. D. Moore, R. D. Winkler, & K. D. Bladon (Eds.), *Compendium of Forest Hydrology and Geomorphology in British Columbia* (pp. 699-747). Victoria, BC: Ministry of Forests and Range Research Branch / FORREX Forest Research Extension Partnership.

Pojar, J., Klinka, K., & Demarchi, D. A. (1991). Mountain hemlock zone. In Meidinger, D. and Pojar, J. (Eds.) *Ecosystems of British Columbia* (pp. 113-124). Victoria, BC: Ministry of Forests.

Politis, D. N., Romano, J. P., & Wolf, M. (2004). Inference for autocorrelations in the possible presence of a unit root. *Journal of Time Series Analysis, 25*(2), 251-263.

Poulin, V. (2005, January). Vancouver Island riparian restoration recommendation and prescriptions–Quinsam, Chemainus, Englishman, Little Qualicum, and Oyster Rivers. *Report prepared for BC Conservation Foundation: Greater Georgia Basin Steelhead Recovery Plan, Nanaimo, BC.* Retrieved September 25, 2013, from http://www.bccf.com/ steel head/pdf/vi_riparian_prescription_report_final_2005.pdf

Puska, L., Clements, L., & Chandler, K. (2011). Climate change and food security on Vancouver Island: discussion paper. *Report prepared by Vancouver Island Local Food Project, Victoria, BC.* Retrieved March 4, 2015, from http://www.uvic.ca/ research/centres/ cue/assets/docs /Climate%20Change%20and%20Food %20Report.pdf

Rodenhuis D. R., Bennett, K. E., Werner, A. T., Murdock, T. Q., & Bronaugh, D. (2007, December). Climate overview 2007: Hydro-climatology and future climate impacts in British Columbia. *Report prepared by the Pacific Climate Impacts Consortium, Victoria, BC.* Retrieved September 25, 2013, from http://www.pacificclimate.org/ sites/default/files/ publications/Rodenhuis.ClimateOverview.Mar2009.pdf

Sauchyn, D. J., Vanstone, J., St. Jacques, J.-M., & Sauchyn, R. (2014). Dendrohydrology in Canada's western interior and applications to water resource management. *Journal of Hydrology*, 592 (2), 548-558.

Schnorbus, M., Werner, A., & Bennett, K. (2014). Impacts of climate change in three hydrologic regimes in British Columbia, Canada. *Hydrological Processes, 28*(3), 1170-1189.

Silvestri, S. (2004). Stock Assessment of winter steelhead trout in Goldstream, Sooke, Trent and Tsable Rivers, 2004. *Report prepared by BC Conservation Foundation: Greater Georgia Basin Steelhead Recovery Plan, Nanaimo, BC.* Retrieved from http://a100.gov.bc.ca/apps data/ acat/documents/r5850/StockAssessmentReportFinal-NonPrintingCopy_1143403749 784_bb9844 0f95634e108ba9ff1269fd7f72.pdf

Smith, D. J., & Laroque, C. P. (1998). High-elevation dendroclimatic records from Vancouver Island. In D. MacIver & R. E. Meyer (Eds.), *Proceedings of the Workshop on Decoding Canada's Environmental Past: Climate Variations and Biodiversity Change during the Last Millennium* (pp. 33-44). Downsview, Ont: Atmospheric Service, Environment Canada.

Smith, T. M., Reynolds, R. W., Peterson, T. C., & Lawrimore, J. (2008). Improvements to NOAA's historical merged land-ocean surface temperature analysis (1880-2006). *Journal of Climate, 21*(10), 2283-2296.

Snedecor, G. W. & Cochran, W. G. (1989). *Statistical Methods.* Ames: IA. Iowa State University Press.

Snee, R. D. (1977). Validation of regression models: methods and examples. *Technometrics, 19*(4), 415-428.

Snover, A. K., Mauger, G. S., Whitely Binder, L. C., Krosby, M, & Tohver, I. (2013). Climate Change Impacts and Adaptation in Washington State: Technical Summaries

for Decision Makers. State of Knowledge Report prepared for the Washington State Department of Ecology. Climate Impacts Group, University of Washington, Seattle.

Stahl, K., Moore, R. D., & Mckendry, I. G. (2006). The role of synoptic-scale circulation in the linkage between large-scale ocean–atmosphere indices and winter surface climate in British Columbia, Canada. *International Journal of Climatology*, *26*(4), 541–560.

Stahle, D. W., Fye, F., Cook, E., & Griffin, R. D. (2007). Tree-ring reconstructed megadroughts over North America since AD 1300. *Climatic Change*, *83*(1-2), 133-149.

Stahle, D. W., Cook, E. R., Cleaveland, M. K., Therrell, M. D., Meko, D. M., Grissino-Mayer, H. D., Watson, E., & Luckman, B. H. (2000). Tree-ring data document 16th century megadrought over North America. *Eos, Transactions American Geophysical Union*, *81*(12), 121-125.

Starheim, C. C. A., Smith, D. J., & Prowse, T. D. (2013). Dendrohydroclimate reconstructions of July–August runoff for two nival-regime rivers in west central British Columbia. *Hydrological Processes*, *27*(3), 405-420.

Stephens, K., Ven der Gulik, T., & Heath, T. (1992). Water, water everywhere: does British Columbia really need a water conservation strategy? *The BC Professional Engineer*, *43*(8), 3-7.

Stewart, I., Cayan, D., & Dettinger, M. (2005). Changes toward earlier streamflow timing across western North America. *Journal of Climate*, *18*(8), 1136-1155.

Stokes, M. A., & Smiley, T. L. (1968). *Tree-Ring Dating*. Chicago: IL. University of Chicago Press.

Timilsena, J., & Piechota, T. (2008). Regionalization and reconstruction of snow water equivalent in the upper Colorado River basin. *Journal of Hydrology*, *352*(1), 94-106.

Torrence, C., & Compo, G. (1998). A practical guide to wavelet analysis. *Bulletin of the American Meteorological Society*, *79*(1), 61-78.

Touchan, R., Anchukaitis, K. J., Meko, D. M., Sabir, M., Attalah, S., & Aloui, A. (2011). Spatiotemporal drought variability in northwestern Africa over the last nine centuries. *Climate Dynamics*, *37*(1-2), 237-252.

Trenberth, K., Overpeck, J., & Solomon, S. (2004). Exploring drought and its implications for the future. *Eos, Transactions American Geophysical Union*, *85*(3), 27-27.

Vaganov, E. A., Hughes, M. K., Kirdyanov, A. V., Schweingruber, F. H., & Silkin, P. P. (1999). Influence of snowfall and melt timing on tree growth in subarctic Eurasia. *Nature*, *400*(6740), 149-151.

Valentine, K. W. G., Sprout, P. N., Baker, T. E., & Lawkulich, L. M. (Eds.) (1978). *The Soil Landscapes of British Columbia*. BC Ministry of Environment, Resource Analysis Branch. 197 p.

van der Kamp, D., Bürger, G., & Murdock, T. Q. (2011). Projections of future drought and fire weather severity in southeast British Columbia using statistical downscaling. *Pacific Climate Impacts Consortium, University of Victoria*.

Van Lanen, H. A. J., Wanders, N., Tallaksen, L. M., & Van Loon, A. F. (2013). Hydrological drought across the world: impact of climate and physical catchment structure. *Hydrology and Earth System Sciences*, *17*, 1715-1732.

Van Loon, A. F., & Laaha, G. (2015). Hydrological drought severity explained by climate and catchment characteristics. *Journal of Hydrology*, 256(1), 3-14.

Venables, W., & Ripley, B. (2002). Modern Applied Statistics Using S. Springer-Verlag.

Wade, N., Martin, J., & Whitfield, P. (2001). Hydrologic and climatic zonation of Georgia basin, British Columbia. *Canadian Water Resources Journal*, *26*(1), 43-70.

Walker, S. (2000). The value of hydrometric information in water resources management and flood control. *Meteorological Applications*, *7*(4), 387-397.

Wang, T., Hamann, A., Spittlehouse, D., and Aitken, S. N. (2006). Development of scale-free climate data for western Canada for use in resource management. *International Journal of Climatology*, *26*(3): 383-397.

Wang, T., Hamann, A., Spittlehouse, D. L., & Murdock, T. Q. (2012). ClimateWNA-high-resolution spatial climate data for western North America. *Journal of Applied Meteorology and Climatology*, *51*(1), 16-29.

Ware, D. M., & Thomson, R. E. (1991). Link between long-term variability in upwelling and fish production in the northeast Pacific Ocean. *Canadian Journal of Fisheries and Aquatic Sciences*, *48*(12), 2296-2306.

Watson, E., & Luckman, B. H. (2004). Tree-ring based reconstructions of precipitation for the southern Canadian Cordillera. *Climatic Change*, *65*(1-2), 209-241.

Watson, E., & Luckman, B. H. (2005). Spatial patterns of preinstrumental moisture variability. *Journal of Climate*, *18(15)*, 2847-2863.

Weisberg, S. (1985). Applied Linear Regression, 2nd Ed. New York, NY: John Wiley.

Whitfield, P. H., & Cannon, A. (2000). Recent variations in climate and hydrology in Canada. *Canadian Water Resources Journal*, *25*(1), 19-65.

Whitfield, P. H., Wang, J. Y., & Cannon, A. J. (2003). Modelling future streamflow extremes—floods and low flows in Georgia basin, British Columbia. *Canadian Water Resources Journal*, *28*(4), 633-656.

Wigley, T. M. L., Briffa, K. R., & Jones, P. D. (1984). On the average value of correlated time series, with applications in dendroclimatology and hydrometeorology. *Journal of Applied Meteorology*, *23*(2), 201–213.

Wiles, G. C., D'Arrigo, R., Barclay, D., Wilson, R. S., Jarvis, S. K., Vargo, L., & Frank, D. (2014). Surface air temperature variability reconstructed with tree rings for the Gulf of Alaska over the past 1200 years. *The Holocene*, *24*(2), 198-208.

Willson, M. F., & Halupka, K. C. (1995). Anadromous fish as keystone species in vertebrate communities. *Conservation Biology*, *9*(3), 489-497.

Wolter, K., & Timlin, M. S. (1993, March). Monitoring ENSO in COADS with a seasonally adjusted principal component index. In *Proceedings of the 17th Climate Diagnostics Workshop* (pp. 52-7).

WinDENDRO, 1996. WinDENDRO reference manual V. 6.1b, February 1996. Regent Instruments, Québec.

WinDENDRO, 2012. WinDENDRO reference manual V. 2012b, June 2012. Regent Instruments, Québec.

Woodhouse, C. A., Gray, S. T., & Meko, D. M. (2006). Updated streamflow reconstructions for the Upper Colorado River basin. *Water Resources Research*, *42*(5).

Woodhouse, C. A., & Lukas, J. J. (2006). Drought, tree rings and water resource management in Colorado. *Canadian Water Resources Journal*, *31*(4), 297-310.

Woodhouse, C. A., Meko, D. M., MacDonald, G. M., Stahle, D. W., & Cook, E. R. (2010). A 1,200-year perspective of 21st century drought in southwestern North America. *Proceedings of the National Academy of Sciences*, *107*(50), 21283-21288.

Worrall, J. (1983). Temperature–bud-burst relationships in amabilis and subalpine fir provenance tests replicated at different elevations. *Silvae Genetica*, *32*(5/6), 203-209.

Yang, Y. K., Huang, Q., Liu, Y., Wang, W. K., & Wang, Y. M. (2010). Advances in streamflow reconstruction using tree-ring data. *Advances in Water Science*, *21*(3), 430-434.

Young, J., & Werring, J. (2006, October). The Will to Protect: Preserving BC's Wild Salmon Habitat. *Report prepared for the David Suzuki Foundation.* Retrieved September 25, 2013, from http://www.davidsuzuki.org/publications/downloads /2006/DSF-Will_to_Protect-72.pdf

Zhang, Q., & Hebda, R. (2004). Variation in radial growth patterns of *Pseudotsuga menziesii* on the central coast of British Columbia, Canada. *Canadian Journal of Forest Research, 34*(9), 1946-1954.

Zubel, M., & Eng, P. (2000). Groundwater Conditions of the Columbia Valley Aquifer Cultus Lake, British Columbia. *Report prepared for the Ministry of Environments, Lands, and Parks Water Management.* Retrieved October 1, 2015, from http://www. env.gov.bc.ca/wsd/plan_protect_sustain/groundwater/library/cvreport.pdf.